SVERIGES GEOLOGISKA UNDERSÖKNING

SERIE C NR 786 AVHANDLINGAR OCH UPPSATSER ÅRSBOK 75 NR 7

MICHAEL B. STEPHENS

FIELD RELATIONSHIPS PETROCHEMISTRY AND PETROGENESIS OF THE STEKENJOKK VOLCANITES CENTRAL SWEDISH CALEDONIDES

UPPSALA 1982

SVERIGES GEOLOGISKA UNDERSÖKNING

SERIE C NR 786 AVHANDLINGAR OCH UPPSATSER ÅRSBOK 75 NR 7

MICHAEL B. STEPHENS

FIELD RELATIONSHIPS PETROCHEMISTRY AND PETROGENESIS OF THE STEKENJOKK VOLCANITES CENTRAL SWEDISH CALEDONIDES

UPPSALA 1982

ISBN 91-7158-240-1
ISSN 0082-0024

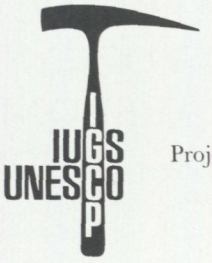

Project No. 60: Correlation of Caledonian Stratabound Sulphides

Address:
Michael B. Stephens
Geological Survey of Sweden
Box 670
S-751 28 Uppsala

Schmidts Boktryckeri AB
Helsingborg 1982

CONTENTS

SUMMARY

Stephens, M.B., 1981-06-15: Field relationships, petrochemistry and petrogenesis of the Stekenjokk volcanites, central Swedish Caledonides. Sveriges geologiska undersökning, Ser. C, No. 786, pp. 1–111. Uppsala 1982.

The mixed, yet felsic-dominated volcanic and subvolcanic rocks of the Stekenjokk volcanite-bearing formation (Skogsbäcken Volcanite Formation, Basalt—quartz keratophyre formation, Stekenjokk Quartz-Keratophyre, Lasterfjäll Quartz-Keratophyre-bearing Formation) have been examined in their type area in the Caledonides of northern Jämtland and southern Västerbotten, Sweden. In this area, the Stekenjokk volcanites vary up to c. 1 km in thickness and extend c. 90 km along strike. The normally lower part (c. 50—100 m) of the Stekenjokk volcanites is dominated by various proportions of layered tuffite, graphitic and limey phyllite, and minor limestone. Minor sedimentary intercalations within the overlying volcanites proper include reworked volcanic material, fine-grained, often graphitic phyllite and limestone. Such intercalations are thought to represent less violent phases or real pauses in the volcanic activity and, being interpreted as marine, indicate the submarine nature of the ongoing volcanism. The Stekenjokk volcanites are host to a number of Zn-Cu-dominated stratabound sulphide mineralizations including the major Stekenjokk-Levi ore deposit. These deposits occur within the lower tuffite-phyllite unit as well as along the contact between graphitic phyllite and felsic volcanites (Stekenjokk-Levi) and within the volcanites themselves, usually towards the normal structural base of the formation.

The Stekenjokk volcanites occur within two separate thrust slices, referred to as the Gelvenåkko (Gellvernokko) and Stikke Nappes, within the upper (Köli) part of the Seve-Köli Nappe Complex. On the basis of the distribution of gabbro intrusions and the local recognition of a thrust contact (presence of regional-scale discordant relationships and/or phyllonitic rocks), it is suggested that the lower of these nappes, the Stikke Nappe, is separated from the lowest Köli tectonic unit (Björkvattnet Nappe), containing diagnostic Ordovician and Silurian fossils, by an important tectonic break. The Stekenjokk volcanites are affected by a polyphase (D_{1-4}) deformation sequence and chlorite to biotite grade regional metamorphism. Published geobarometric results, based on the composition of sphalerite encapsulated in pyrite, suggest metamorphic pressures of c. 5 kbar. An earlier proposal suggesting that the Stekenjokk volcanites (Stikke Nappe) lie in an inverted stratigraphy is supported by recent metal zonation and wall-rock alteration studies in sulphide deposits as well as the distribution of sulphide deposits associated with the volcanites. Lithostratigraphic correlation, available fossil evidence and the inversion hypothesis suggest an Ordovician age for the Stekenjokk volcanites.

Study of selected profiles exhibits the complex, internal lithological variation within the Stekenjokk volcanites and the difficulties of along strike correlation even over short distances. A cyclic alternation of dominating felsic and subordinate mafic units occurs, for example, in the Björkvattnet area (Stikke Nappe), while a distinct polarity in the composition of the volcanites is apparent in the Gauste area (Gelvenåkko Nappe), mafic-dominated passing upwards into felsic-dominated units. The volcanite packet appears to be thicker (500—1000 m) where more varied — including particularly coarser pyroclastics and subvolcanic felsic intrusions — sequences occur. On this basis, the successions near Björkvattnet and Stekenjokk, for example, are thought to represent accumulations closer to major eruptive centres. Finely layered, thin (<200 m) units with occasional sedimentary intercalations are interpreted as a more distal pyroclastic facies (*e.g.* Stor-Blåsjön area).

Field and microscope studies suggest division of the mafic rocks into two groups. Group 1 greenstones and greenschists are composed of the mineral assemblages chlorite-albite±amphibole±epidote±calcite±Ti-rich minerals. Textural variation suggests the pre-

sence of both volcanic and high-level intrusive rocks, while coarser pyroclastic products, lapilli tuff and volcanic breccia, have been recognized locally. Group 2 greenstones and dolerite to gabbro sheets are darker and consist of the mineral assemblages amphibole-albite-chlorite-epidote-Ti-rich minerals±calcite as well as chlorite-albite-calcite-Ti-rich minerals±biotite±epidote±apatite±white mica. Texture and presence of chilled margins attest to the intrusive origin of these rocks. Based on their occurrence in other rock-types, including felsic high-level intrusions, they are thought to define the latest phase of magmatic activity in the Stekenjokk volcanites.

Inspection of the petrochemical data, supported by Q-mode cluster analysis, suggests breakdown of each of the field/microscope-distinguishable mafic rock groups into two subgroups (1A and 1B, 2A and 2B). The breakdown of the darker Group 2 rocks corresponds to amphibole-bearing (Group 2A) and amphibole-free (Group 2B) mineralogical types. Contents of relatively more incompatible (Ti, P, Zr, Y) and more compatible (Ni, Cr) elements as well as the varying behaviour of the elements Ti, total Fe, P, and Zr with increasing differentiation suggest three separate mafic fractionation series composed respectively of Group 1A, Groups 1B+2A and Group 2B mafic rocks. Previous study of the variable alteration in the Group 1B mafic rocks suggests that all these elements except Cr behaved in a more or less immobile fashion during spilitization.

The Group 1A basalts and basaltic andesites are strongly spilitic and show a mildly tholeiitic differentiation trend. They are both highly fractionated and, relative to mid-ocean ridge basalt (MORB), highly depleted in the more incompatible elements and Zr/Y ratio, *i.e.* show a strong affinity to island arc tholeiites. The Groups 1B+2A basaltic rocks are variably spilitic and show a strongly tholeiitic differentiation trend. Allowing for the broad range in degree of fractionation (1B rocks showing more primitive and 2A rocks showing more differentiated characteristics) as well as Cr and minor Zr losses during spilitization of 1B basalts, an affinity to MORB is indicated. The Group 2B basaltic rocks are apparently little altered and mildly alkalic and highly differentiated in character. They show a firm within-plate basalt (WPB) affinity, being enriched in P, K and probably Zr and Y in more parental magmas compared with the other mafic rock series. The variable petrochemical composition of the mafic rocks can be largely explained by secondary alteration processes combined with fractional crystallization of Mg/Ni/Cr-bearing phases (all series), plagioclase (Group 2) and a Ti-rich phase (Group 2B only) *within* the three separate fractionation series. Partial melting of a mantle source under varying P_{H_2O} (1A>1B+2A and 2B) and P_{load} (1A>2B>1B+2A) conditions, controlling both varying degrees of partial melting and Mg/Ni/Cr-bearing phase fractionation, together with mantle source heterogeneity (mantle source for the 2B series enriched in, at least, P, K, Zr, and Y relative to that for the other series) are thought to be dictating the chemical variation *between* the different mafic series.

The felsic rocks consist of the mineral assemblages albite-quartz-chlorite±epidote±mica±calcite±Fe-Ti oxides. Textural considerations suggest the presence of both phyric vitric-crystal tuffs and subvolcanic intrusions. The thicker, more homogeneous volcanites are thought to represent ash-flows, while the finely layered sequences intimately intermixed with more tuffitic or even phyllitic material are more tentatively interpreted as ash-fall and reworked ash-fall deposits.

The bulk of the felsic rocks investigated petrochemically represent original, variably differentiated dacite—rhyodacite compositions, probably of the low-Al_2O_3, low-K type. However, similar to the basalt and basaltic andesite to spilite alteration, the felsic rocks have suffered substantial alteration to quartz keratophyre. On the basis of the contents of the more incompatible elements P, Zr and Y, the presence of SiO_2, Zr and MgO 'gaps' and the form of Zr-Y, P_2O_5-Zr and P_2O_5-Y variation trends, it appears that the main group of felsic rocks does not belong to any of the three mafic fractionation series which have been

recognized. In particular, a bimodal distribution based on SiO_2 content is apparent for the Stekenjokk volcanites, silicic andesite compositions being absent. The felsic rocks within the main group are suggested to have formed by partial melting of a basaltic parent with amphibole as a residual product and subsequent separation of plagioclase from the resultant liquid. Bearing in mind the magmatic history of the Stekenjokk volcanites and the island arc setting indicated by the 1A mafic rocks, alternative models involving partial melting of either the subducting slab of basaltic oceanic crust along the postulated Benioff Zone or low-K_2O basaltic material at the root of the island arc are suggested. Two felsic rock samples showing low Zr, Y and Zr/Y values lie along the Group 1A Zr-Y variation trend together with basaltic andesites. They possibly represent altered fractionation products of the Group 1A island arc tholeiite series.

A two-stage working model is suggested for generation of the Stekenjokk volcanites involving firstly build-up of an island arc in a probably ensimatic setting (generation of felsic rocks and 1A mafic series) passing progressively over to a rifted arc situation (generation of largely intrusive 1B+2A and 2B mafic series).

INTRODUCTION

The Stekenjokk volcanites, an alternating series of metamorphosed mafic and dominating felsic volcanic and subvolcanic rocks, belong to the low-grade Köli part of the Seve-Köli Nappe Complex (Zachrisson 1973) and occur within the Western Synform (Zachrisson 1969) of northern Jämtland and southern Västerbotten, Sweden (Plate I). They are thought to have been deposited prior to a packet of phyllites and mafic volcanites (Remdalen Group) and after deposition of a gabbro-intruded, calcareous phyllite sequence (Blåsjö Phyllite, Lasterfjäll Calcareous Phyllite) of presumed Silurian age (Zachrisson 1964, 1969; Nilsson 1964 and Fig. 1). The volcanites occur within two thrust nappe units within the Western Synform (Zachrisson 1969). The lower one has been loosely referred to as the Lower Köli unit and includes minor nappes and repetitions (*e.g.* Remdalen "repetition"); the upper one has been recognized south of Stekenjokk and is referred to as the Gelvenåkko (Gellvernokko) Nappe. The relative amount of translation between these units is unknown but, since a similar stratigraphy occurs within each unit, it is considered to be considerably less than, for instance, the transport distance of the whole Seve-Köli Nappe Complex over the underlying allochthon and autochthon.

The present contribution is divided into two parts. Part I deals with field relationships in five critical areas and includes remarks on mineralogy and petrography; Part II is concerned with petrochemistry and also presents speculative remarks on the petrogenesis of the Stekenjokk volcanites. Complementary papers on the general setting of the volcanites in relation to other volcanic and subvolcanic units within the Köli Nappes (Stephens 1980a), and the spilitization of the Stekenjokk volcanites and its relationship to massive sulphide genesis (Stephens 1980b) have already been presented. It is necessary at the outset to emphasize the

intense deformation and low-grade regional metamorphism that the Stekenjokk volcanites have suffered; the immediately following section concerning deformation, thus, completes these introductory remarks.

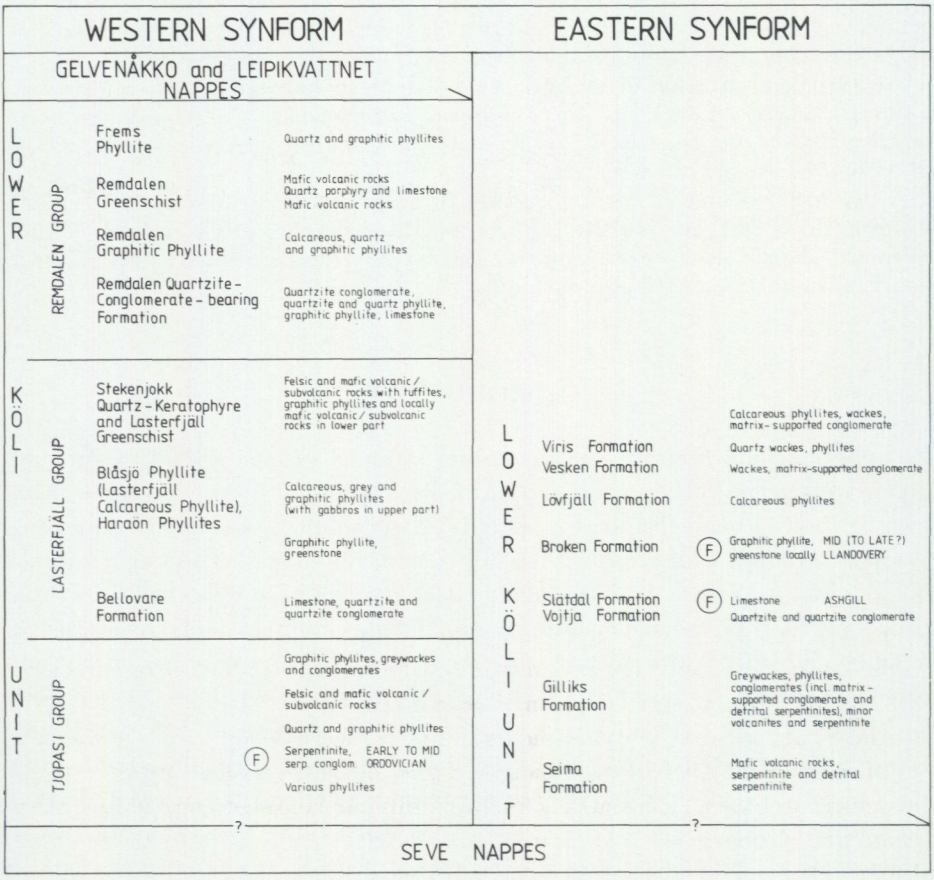

Fig. 1. Present status regarding the tectonostratigraphy of the Köli Nappes in northern Jämtland and southern Västerbotten. The Lower Köli unit includes minor repetitions such as the Remdalen "repetition" (Western Synform). The Gelvenåkko (Gellvernokko) Nappe includes lithologies belonging to the Lasterfjäll and Remdalen Groups, and the Leipikvattnet (Leipik) Nappe lithologies correlatable possibly with the Lasterfjäll and Remdalen Groups. The figure is modified after Fig. 7 in Gee and Zachrisson (1979) based in turn on data in Zachrisson (1964, 1969) for the Western Synform and Kulling (1933, *in* Strand and Kulling 1972) and Stephens (1977) for the Eastern Synform. F indicates diagnostic fossil occurrence.

DEFORMATION

The Stekenjokk volcanites have suffered chlorite to biotite grade regional metamorphism and a complex deformation history, similar to the remainder of the Köli (Gee 1968; Zachrisson 1969; Trouw 1973; Stephens 1977; Sjöstrand 1978; Beckholmen 1980). Geobarometric results (Hutchison and Scott 1980), based on the composition of sphalerite encapsulated in pyrite at the Stekenjokk ore deposit, suggest metamorphic pressures of 5.0 ± 0.6 kbar.

The earliest recognizable mesoscopic structure is a penetrative schistosity (S_1) which occasionally occurs as an axial surface structure to tight or isoclinal, mesoscopic folds (F_1). Sjöstrand (1978) suggested that such folds initiated prior to formation of the regional foliation and were modified subsequently during foliation development (Sjöstrands D_1 and D_2 phases of deformation). In several areas the early foliation and associated linear structures are tightly folded by reclined to plunging inclined folds (F_2) on variable axes, and a new crenulate-style foliation (S_2) is developed as an axial surface structure. The latter, locally penetrative, is often a metamorphic layering (differentiated crenulation cleavage) parallel to the axial surfaces of the F_2 mesoscopic folds. Where these structures are well developed, the main foliation is often a composite S_{1-2} surface.

All the structures mentioned above, as well as the thrusts, are deformed by NNE- to NE-trending, normal (upright) folds (F_3). These folds are particularly intense within the Western Synform — itself a macroscopic F_3 fold — where a new crenulation cleavage (S_3) is commonly found parallel to the axial surfaces of the F_3 folds. Locally, an even later set of mesoscopic folds (F_4), with kink-like characteristics and down-dip sense of overturn, is developed.

The F_1 and F_2 structures are thought to be related to the progressive emplacement of the metamorphic allochthon on top of the Baltoscandian platform, the F_3 structures to basement instability following this emplacement and the F_4 structures to gravitational collapse of earlier steeply dipping surfaces (see also Stephens 1977).

The metamorphism and complex deformation which the Stekenjokk volcanites have suffered inhibit confident interpretation of their primary nature and estimation of their original thickness; thickness values given are almost certainly minimum values. Assessment of the degree of deformation also focuses attention on the difficulty in interpreting what is indeed only a structural succession as a stratigraphic one.

Part I: FIELD RELATIONSHIPS

GENERAL REMARKS

Brief description of the field relationships in five critical areas are presented below. In all areas except Gauste (Leipikvattnet), the volcanite-bearing unit has been accorded names of formation status. These include for Björkvattnet, the Skogsbäcken Volcanite Formation (Sjöstrand 1978); for Stor-Blåsjön, the Basalt—quartz keratophyre formation (Nilsson 1964); for Duoranåjje (Stekenjokk), the Stekenjokk Quartz-Keratophyre (Zachrisson 1964) and for Remdalen, the Lasterfjäll Quartz-Keratophyre-bearing Formation (Zachrisson 1964). Petrographic descriptions of the volcanites within these formations may be found in the works of Sjöstrand and Nilsson (Björkvattnet and Stor-Blåsjön respectively), in Högbom (1925) and Juve (1974) for Stekenjokk and in Högbom (1925) and Du Rietz (1941) for Remdalen. Although the volcanites are metamorphosed, the prefix 'meta' is not employed for purposes of brevity.

DESCRIPTION OF INDIVIDUAL AREAS AND REMARKS ON PETROGRAPHY

BJÖRKVATTNET

The Stekenjokk volcanites generally overlie gabbro-intruded calcareous phyllite (Blåsjö Phyllite) and interlayered calcareous and graphitic phyllite (Haraön Phyl-

Fig. 2. F_2 reclined folds in quartz keratophyre. View looking NNE on a road section approximately 500 m west of the lake Björkvattnet.

lites) and underlie a limestone unit and a well-developed sequence of quartzite conglomerate and interbedded grey to graphitic phyllite (Portfjället Conglomerate). The critical contacts, exposed at the western end of Kvarnbergsvattnet, are interpreted as being primary. The structures within the volcanites are dominated by the penetrative S_1 foliation and close to tight, north-plunging reclined folds (F_2), (see Fig. 2), which possess a well-developed, variably differentiated crenulation cleavage (S_2) as an axial surface structure in the 'less competent' lithologies. Locally, the sequence is overturned in the F_2 folds such that the volcanites underlie the calcareous phyllites (Fig. 3a). The thickness of the volcanites is thought to be in the range 500 m (F_2 limb area) to 950 m (F_2 hinge area).

The lower part of the volcanites (approx. 70—90 m) is composed mostly of

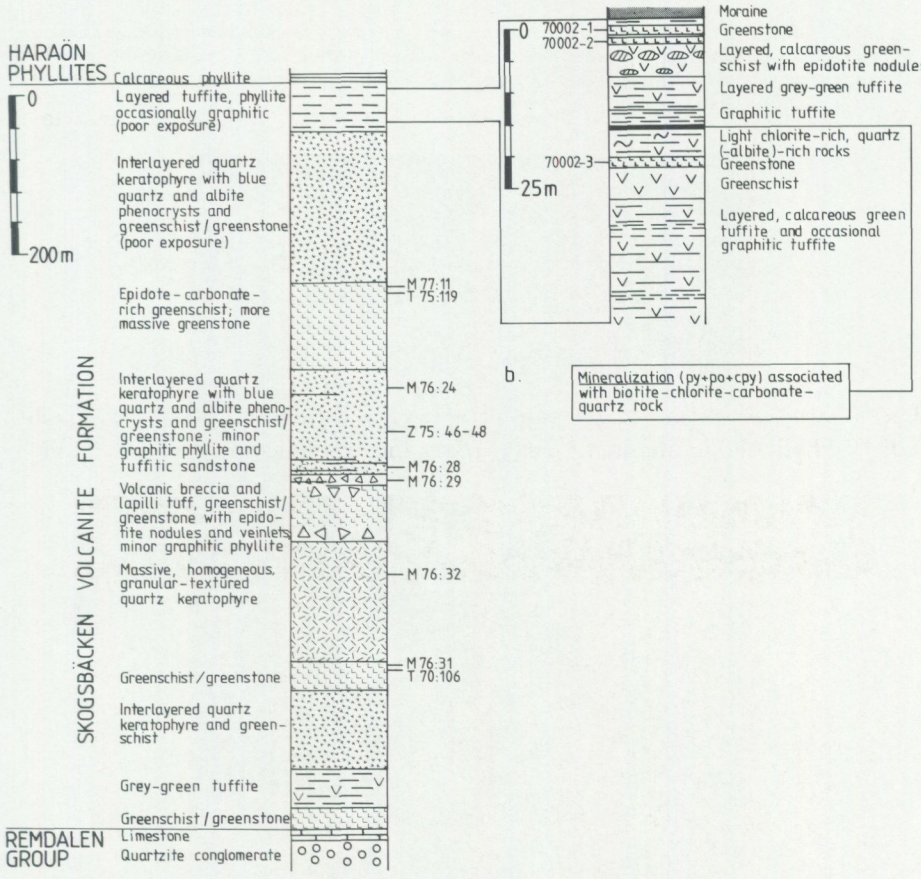

Fig. 3. a. Schematic section through the Stekenjokk volcanites (Skogsbäcken Volcanite Formation) in the Björkvattnet area. b. Borehole section (70002) through part of the layered tuffite sequence showing the position of the Björkvattnet Cu-Zn massive sulphide deposit. Note that the strata in these sections lie on the locally overturned limb of a major F_2 fold. Locations of analyzed samples in these sections are indicated.

layered tuffite[1] (dark and graphitic to grey-green and green in colour) with subordinate intercalations of graphitic phyllite. It is within this sequence that the massive Cu-Zn sulphide deposit at Björkvattnet is situated (Tegengren *et al.* 1924; Zachrisson 1977, 1980; Stephens *et al.* 1979). Two levels of homogeneous, schistose greenstone lying on either side of the mineralization interrupt this sequence (Fig. 3b). The 'upper' (note F_2 complication in this area) greenstone contains a chlorite-albite-biotite-calcite-epidote-sphene (leucoxene) mineral assemblage, while the 'lower' greenstone is composed of the minerals amphibole-albite-chlorite-epidote-calcite-sphene (leucoxene). In better preserved parts an intergranular texture with grain size approximately 1 mm is preserved. The greenstones are between 1—2 m in thickness and possess sharp, chilled margins (approx. 3—5 cm) to the sur-

[1] The term tuffite refers to a mixed volcano — sedimentary rock. Processes involved in its formation may include simple mingling of a water-lain ash-fall tuff with sedimentary detritus or the reworking and redeposition of a pyroclastic deposit with or without mingling with ordinary sedimentary detritus.

Fig. 4. Rubbly massive greenstone (flow?) with epidotite nodules and veinlets overlying greenschist with sharp contact. Approximately 1 km west of the lake Björkvattnet.

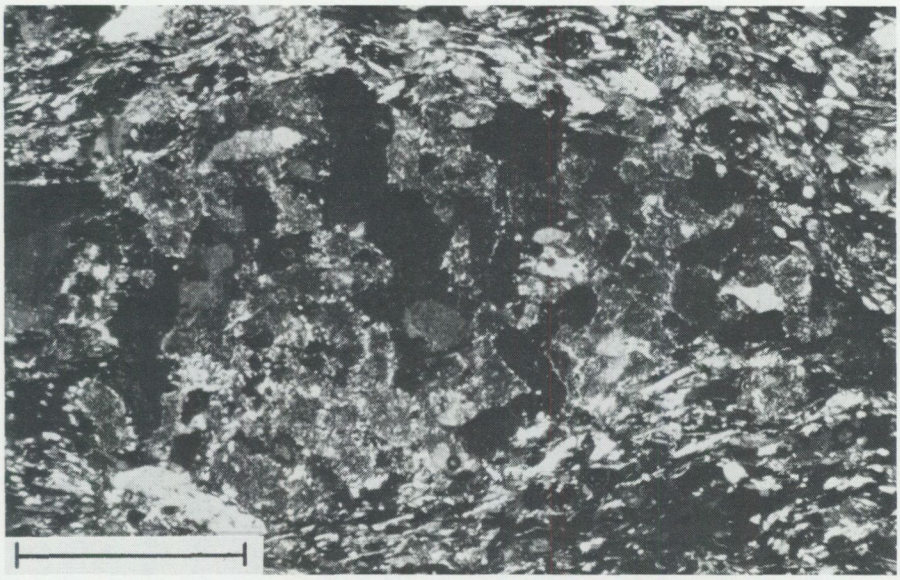

Fig. 5. Epidote-rich knot in fine-grained, aphyric greenschist with mineral assemblage chlorite-albite-amphibole-epidote-calcite. The knot is aligned in and wrapped around by the foliation. An extrusive origin is inferred for this rock. T75:119, crossed nicols. Bar length = 1 mm.

Fig. 6. Volcanic breccia. Approximately 800 m northwest of the lake Björkvattnet.

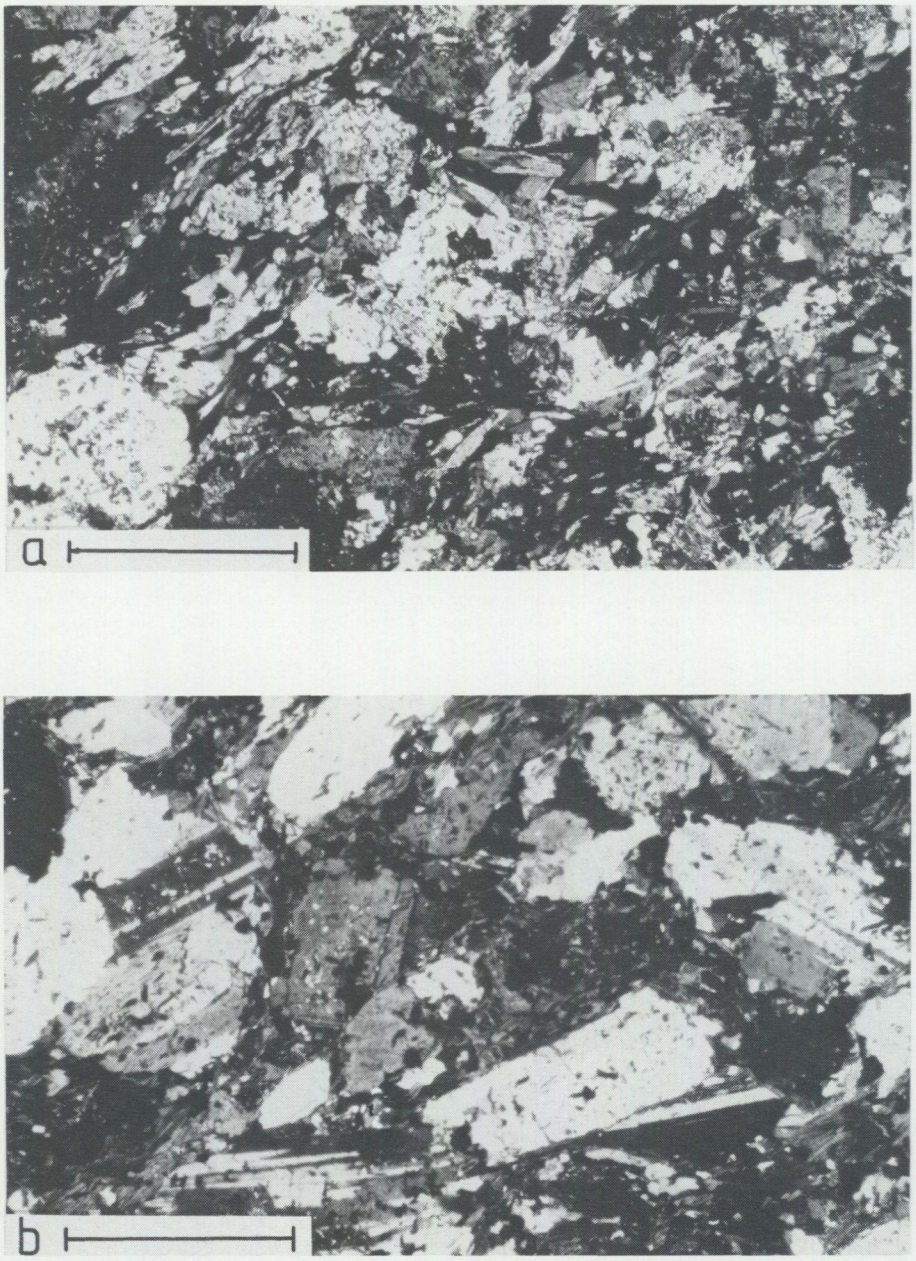

Fig. 7. Coarse greenstones with intergranular texture interpreted as being high-level intrusive in origin.

a. Paler type with mineralogy chlorite-albite-amphibole-epidote-calcite-(Ti-rich minerals); albite grain size c. 1 mm. M76:31, crossed nicols. Bar length = 1 mm.

b. Darker type with mineralogy chlorite-albite-calcite-biotite-Ti-rich minerals-apatite; albite grain size c. 1—1.5 mm. T75:122, crossed nicols. Bar length = 1 mm.

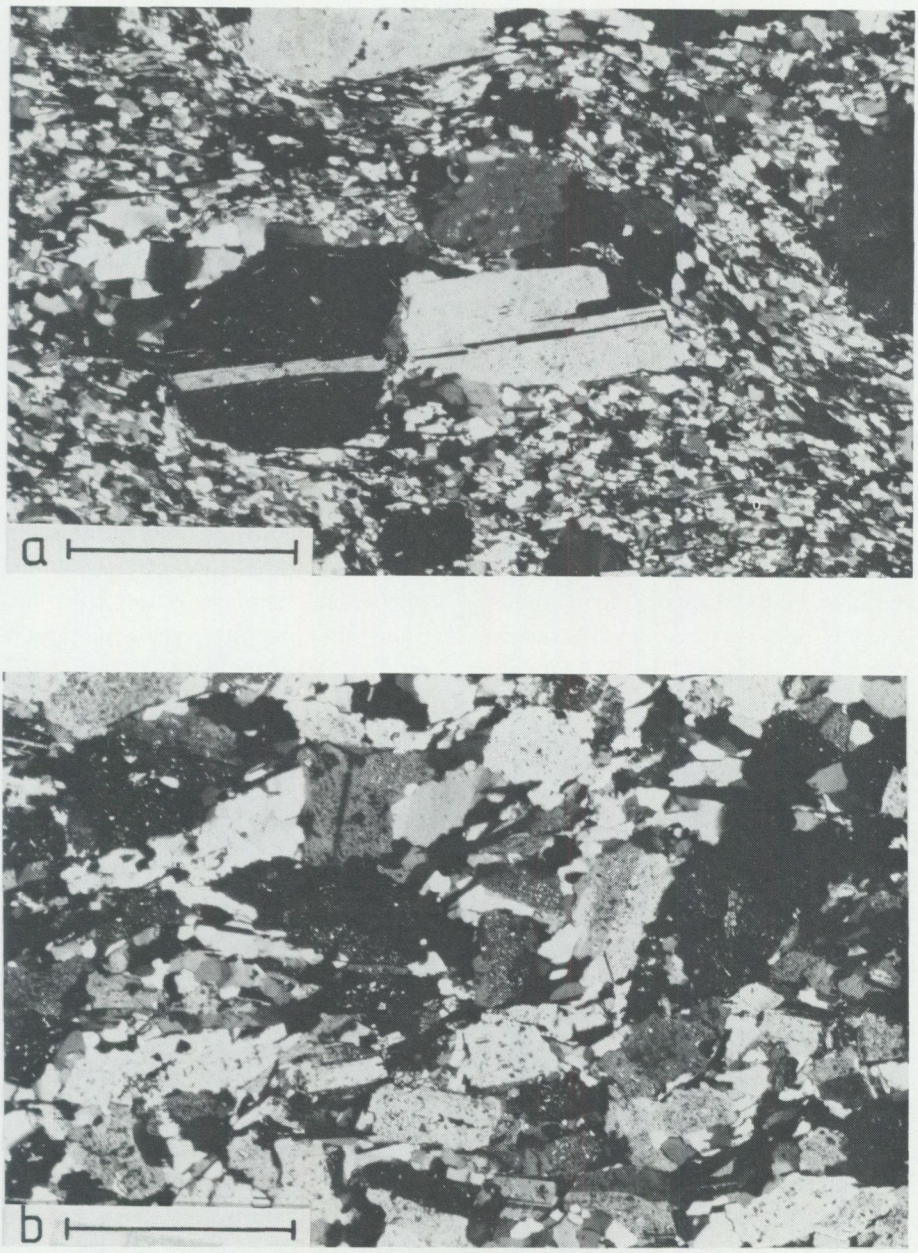

Fig. 8. a. Phyric-textured quartz keratophyre with megacrysts of albite and bluish quartz in fine-grained groundmass of albite-quartz-chlorite-epidote-biotite. This rock is thought to have originated as a vitric-crystal, ash-flow tuff. Z75:47, crossed nicols. Bar length = 1 mm.

b. Granular to faintly schistose, coarse-grained quartz keratophyre with mineralogy albite-quartz-chlorite-epidote-Fe-Ti minerals (magnetite, ilmenite, hematite); the feldspars are sericitized and c. 1 mm in grain size. A subvolcanic intrusive origin is inferred. M76:32, crossed nicols. Bar length = 1 mm.

rounding tuffites; carbonate and epidote segregations often occur along the actual contact. They are tentatively interpreted as thin, high-level, dolerite intrusions (sills or highly deformed dykes?).

The upper and major part of the volcanite sequence is composed of a cyclic alternation of more homogeneous mafic units, several tens of metres thick, and finer, phyric-textured to homogeneous, coarser quartz keratophyre (Fig. 3a).

The mafic units are composed of fine-grained, occasionally thinly layered greenschist, some layers containing scattered albite and/or amphibole phenocrysts, and occasional more massive, rubbly layers of greenstone with intergranular texture (Figs. 4 and 5). Mineral assemblages consist of chlorite-albite±amphibole±epidote± calcite. In one of the mafic units, lapilli tuff, with spherical aggregates rich in epidote (few millimetres across), occurs in association with volcanic breccia containing variably epidotized felsic fragments in a mafic rock matrix (Figs. 3a and 6). Coarser greenstones containing plagioclase laths up to 2 mm and an intergranular texture are variable in mineralogy. One group is similar in mineralogy to the finer greenschists and greenstones and consists of chlorite-albite-calcite-amphibole-epidote with small amounts of Ti-rich minerals (Fig. 7a); a second group containing chlorite-albite-calcite-Ti-rich minerals (sphene, ilmenite, leucoxene)±epidote± biotite±apatite ±white mica is often darker and similar to the greenstones found 'above' the Björkvattnet mineralization (Fig. 7b). A conspicuous feature of the mafic units is the occurrence of pre-deformation nodules of epidotite (±calcite), (see Fig. 5).

The origin of these mafic units is difficult to interpret due to the high strains. However, pyroclastic products are represented at least by the coarser lapilli tuff and volcanic breccia, while the texture of the coarser greenstones suggests that they represent high-level intrusions. The finer aphyric to phyric greenschists and more massive, rubbly greenstones are interpreted with less confidence, grain-size and texture suggesting, however, a volcanic origin (vitric to vitric-crystal tuffs and flows respectively?).

The units dominated by quartz keratophyre are composed of fine-grained, schistose quartz keratophyre, often showing a clear layered structure with alternating darker and lighter layers, and subordinate intercalations of fine-grained greenschist and greenstone. The texture is porphyritic with phenocrysts of albite and bluish quartz in a fine-grained recrystallized groundmass of albite, quartz and subordinate chlorite, biotite and epidote (Fig. 8a). Individual quartz keratophyre sheets are homogeneous over at least several metres thickness. The texture, homogeneity and thickness of the quartz keratophyres suggest that they represent vitric-crystal, ash-flow tuffs (Ross and Smith 1961). A massive quartz keratophyre up to 150 m thick with a granular to faintly schistose framework of subhedral albite (up to 2—3 mm), quartz and subordinate epidote, chlorite and Fe-Ti oxides (Fig. 8b) occurs 1.5 km west of Björkvattnet near the top of the sequence. The texture of this body suggests a possible subvolcanic intrusive origin.

STOR-BLÅSJÖN

As at Björkvattnet, the rocks immediately overlying the gabbro-intruded calcareous phyllites (Blåsjö Phyllite) are rather tuffitic, dark, quartz-rich and graphitic phyllites. A critical zone of between 1—2 m thickness, in which phyllites appear to increase in carbonate content and decrease in carbonaceous material, marks the lower contact of the volcanite-bearing formation with the calcareous phyllites. Along Storbäcken (Jormlien), the volcanites are overlain sharply by a graphitic phyllite which passes upwards into more quartz-rich phyllite with scattered quartzite pebbles; layered quartz and grey phyllites and then increasingly more pebble-rich units follow (Portfjället Conglomerate).

Within the Stor-Blåsjön area, the Stekenjokk volcanites dip regularly towards the north-west. The main foliation in the volcanites and adjacent units is often a composite, rather penetrative, variably differentiated crenulation cleavage (S_{1-2}) and the deformation appears to be strong. Mesoscopic folds include:

1. F_2, steeply plunging, reclined structures;
2. F_3, normal SW- to SSW-plunging folds with weak axial surface crenulation cleavage development; and
3. F_4, kink-like and chevron-style folds with down-dip sense of overturn and rather flat-lying axial surfaces.

Nilsson (1964) has published diagrammatic profiles through the Stekenjokk volcanites in the Stor-Blåsjön area. He estimated that the lower tuffitic phyllite unit is 50—60 m thick, while the volcanites proper lie in the range 100—200 m. The thin volcanite sequence of the Stor-Blåsjön area is dominated by finely layered greenschist and schistose quartz keratophyre; several layers contain coarser plagioclase crysts. Thin dark grey phyllite layers are intercalated in this probably tuffaceous succession. Nilsson (1964) also recorded agglomeratic greenstone and intercalations of limestone near the top of the unit.

GAUSTE (LEIPIKVATTNET)

The Gauste (Leipikvattnet) stream section provides a critical, well exposed and accessible profile through the Stekenjokk volcanites in the Gelvenåkko Nappe. The section is exposed near to the hinge zone of a macroscopic, F_3 synform which plunges south-westwards and is the northerly continuation of the Leipikvattnet Synform (Western Synform). This synform folds an earlier (F_{1-2}?), macroscopic, overturned structure, the most convincing expression of which is the repetition of the rocks of the Remdalen Group west of Leipikvattnet. As a result of this

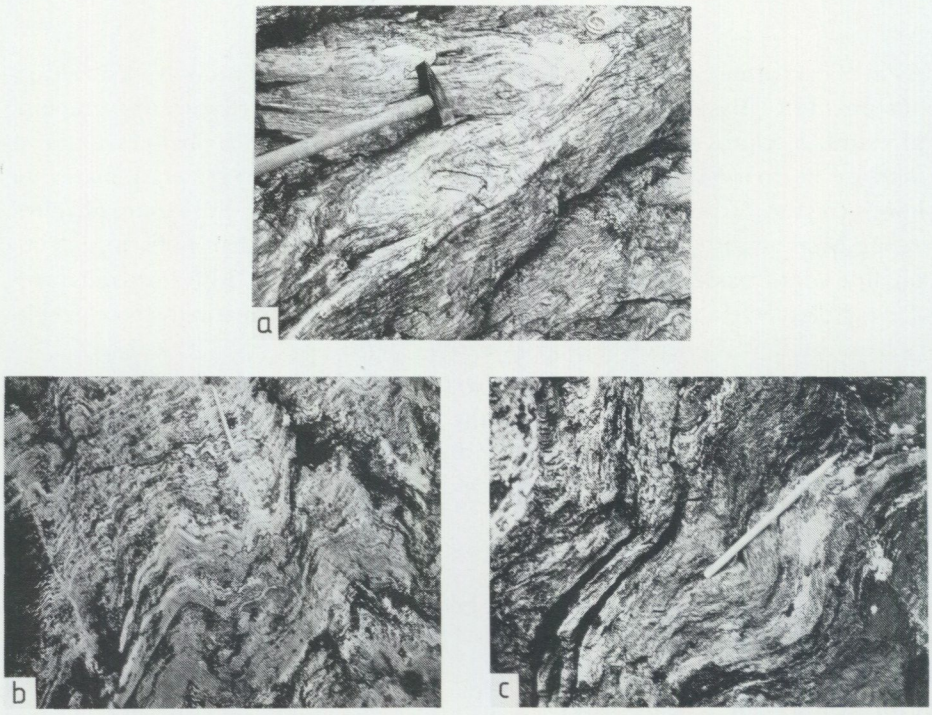

Fig. 9. Mesoscopic structures in the Stekenjokk volcanites from the Gauste stream section.
a. F_2 plunging inclined fold deforming S_{0-1} with intense differentiated crenulation cleavage (S_2) parallel to the axial surface.
b. Normal F_3 folds deforming the complex S_{1-2} main foliation.
c. Open F_4 folds with flat-lying axial surface orientation deforming steeply inclined S_3 crenulation cleavage. The S_3 cleavage contains microlithons of the penetrative S_{1-2} main foliation.

important early structure, the Stekenjokk volcanites in the Gauste section north of Leipikvattnet overlie mostly graphitic to dark, quartz phyllite with occasional lenses of quartzite conglomerate (Portfjället Conglomerate equivalent) in the contact zone, and underlie a homogeneous mafic volcanite unit (equivalent to the Lasterfjäll Greenschist of Zachrisson 1964) and the gabbro-intruded calcareous phyllites (Blåsjö Phyllite).

The main foliation (S_{1-2}) and associated lineation are deformed by abundant, F_3 mesoscopic folds (Fig. 9b), while in the structurally lower part of the profile, where the enveloping surface of the main foliation is steeper, F_4 down-dip folds with flat-lying axial surfaces are common (Fig. 9c). At a few localities, early, penetrative structures are deformed in tight, overturned folds (Fig. 9a) which are themselves deformed by the normal, F_3 folds. Morphologically these folds, with their locally intense differentiated crenulation cleavage parallel to the axial surface, resemble F_2; they plunge south-westwards and are plunging inclined rather than reclined structures.

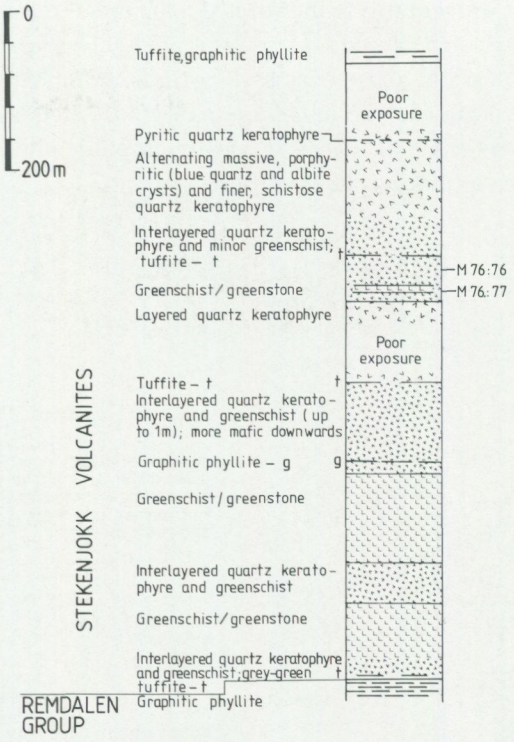

Fig. 10. Schematic section through the Stekenjokk volcanites in the Gauste (Leipikvattnet) area. The Stekenjokk volcanites here lie in the Gelvenåkko Nappe and occur on the overturned limb of a macroscopic F_{1-2} (?) fold structure. Locations of analyzed samples in this section are indicated.

The layered quartz-rich and graphitic phyllites and tuffites at the structural top of the volcanite-bearing formation are approximately 80—90 m thick while the volcanites proper on the northern limb of the early F_{1-2}(?) fold are probably up to 800 m thick.

There is a distinct polarity in the composition of the volcanites throughout the unit (Fig. 10). It appears that homogeneous, fine-grained greenschist layers (up to 100 m thick?) dominate in the structurally lower part of the sequence. These pass upwards via a well layered sequence of phyric quartz keratophyre and subordinate greenschist (up to 1 m thick) into completely felsic-dominated units composed of alternating, more massive, coarser (up to several m thick) and schistose, finer varieties of quartz keratophyre. Greenschist mineral assemblages are chlorite-albite-calcite±amphibole±epidote; textures are schistose, both aphyric and amphibole- and/or plagioclase-phyric. The quartz keratophyres contain albite, quartz and chlorite with minor epidote and white mica; albite- (and quartz-) phyric texture dominates particularly in the more massive varieties. These mafic

and felsic units are tentatively interpreted to be tuffaceous in character, representing original vitric and phyric vitric-crystal tuffs; the more massive, thicker quartz keratophyres possibly represent ash-flow tuffs. A small Zn-Cu mineralization (Malmforsen) occurs in the felsic-dominated part of this sequence (Zachrisson 1977, 1980; Stephens *et al.* 1979). A layer of graphitic phyllite (<0.5 m) has been recorded in the volcanite sequence proper.

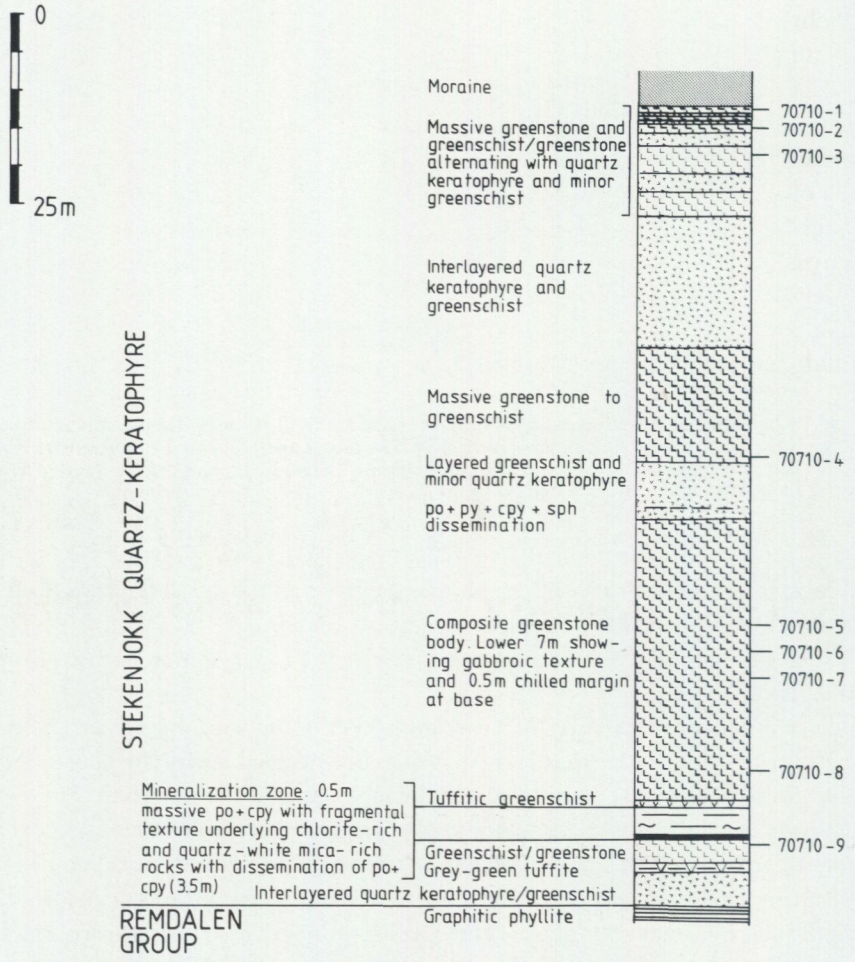

Fig. 11. Borehole section (70710) through part of the Stekenjokk volcanites (Stekenjokk Quartz-Keratophyre) in the Duoranåjje (Stekenjokk) area showing the position of the Duoranåjje Cu-rich massive sulphide deposit. Note that the strata here lie on the steeply NW-dipping, overturned limb of a major F_3 antiform. Locations of analyzed samples in this section are indicated.

DUORANÅJJE (STEKENJOKK)

On Duoranåjje, which lies 5.5 km north of the outcrop of the Stekenjokk ore body, the felsic-dominated volcanic and subvolcanic rocks of the Stekenjokk level generally underlie a packet of limey and graphitic phyllites, near the boundary to which is situated the stratabound, Cu-rich Duoranåjje mineralization (Fig. 11 and Zachrisson 1977, 1980; Stephens *et al.* 1979). A homogeneous mafic volcanite unit (Kosaåive Greenshist of Zachrisson 1964) lies above the mixed phyllites and then follows the gabbro-intruded calcareous phyllites (Fasovardo Phyllite of Zachrisson 1964).

Zachrisson (1969, Fig. 1) correlated the mixed phyllite and mafic volcanite units with the Remdalen Group, the gabbro-intruded calcareous phyllites with the Lasterfjäll Calcareous Phyllite and accordingly placed a slide at the base of the calcareous phyllites (Remdalen "repetition"). The Stekenjokk volcanites and Remdalen Group thin out north and east of Duoranåjje beneath this slide on both limbs of the F_3 Remdalen Synform (Plate 1). Considering that the F_3 folds pass through a major culmination between Stekenjokk and Duoranåjje, it is likely that this discontinuity is equivalent either to the thrust near Stekenjokk lying beneath the Gelvenåkko Nappe or the basal Gelvenåkko Nappe thrust itself.

The dominant mesoscopic structures in the Duoranåjje (Stekenjokk) area are normal, NE-plunging, F_3 folds which deform the earlier, penetrative schistosity.

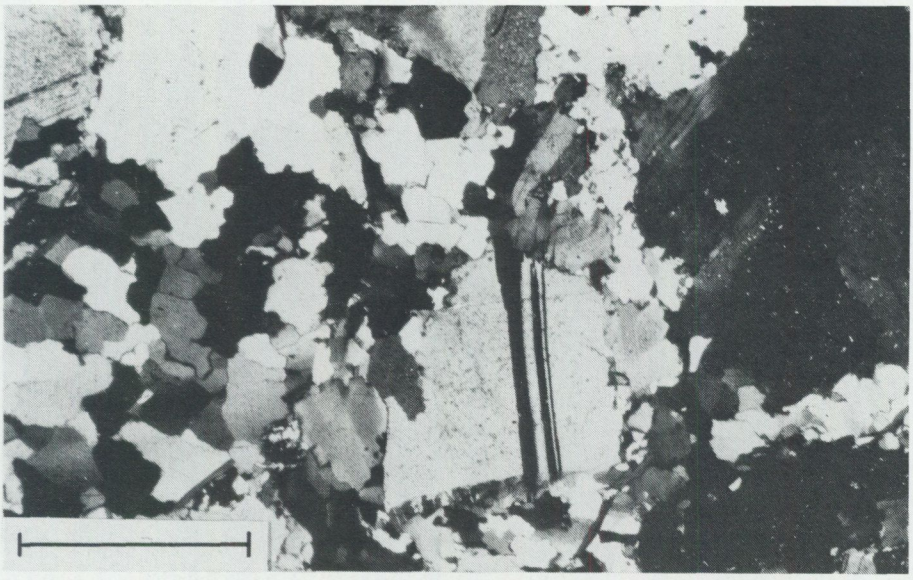

Fig. 12. Granular to pseudoporphyritic, coarse-grained quartz keratophyre with mineralogy albite-quartz-chlorite-epidote-white mica; the feldspars are often sericitized and up to c. 1—1.5 mm in grain size. A subvolcanic intrusive origin is inferred. M76:130, crossed nicols. Bar length = 1 mm.

These folds are congruent to the macroscopic, F_3 Remdalen Synform which forms part of the Western Synform.

The Stekenjokk volcanites on Duoranåjje are felsic-dominated. The quartz keratophyres are mainly composed of a massive, homogeneous type containing anhedral plagioclase and quartz crysts up to 3 mm across together with minor chlorite, white mica and epidote. The texture is granular to pseudoporphyritic (Fig. 12), the latter being due to subgrain and new grain development particularly within quartz. It is suggested that this type represents one or more high-level subvolcanic intrusions. More clearly layered, volcanic units with alternating schistose, fine-grained, albite- and quartz-phyric quartz keratophyre (dominant) and greenschist are locally conspicuous particularly near the top of the sequence (see Fig. 11). The greenschists are chlorite-albite-amphibole-epidote±calcite rocks and aphyric as well as plagioclase- and/or amphibole-phyric textures may be seen. Lenses and streaky layers of epidote with varying amounts of calcite, quartz, chlorite, amphibole, and opaque minerals are conspicuous features; these are similar to the pre-deformation nodules of epidotite observed, for example, in the Björkvattnet area.

Minor intrusions of basaltic material occur within the subvolcanic to volcanic felsic-dominated sequence described above. Several bodies, up to 2 m thick, show apophyses injecting along fissures into the adjacent quartz keratophyre (Fig. 13). Such narrow intrusive bodies (dykes?) have suffered the metamorphism and deformation shown by the adjacent quartz keratophyre (Fig. 14). Thicker, dark

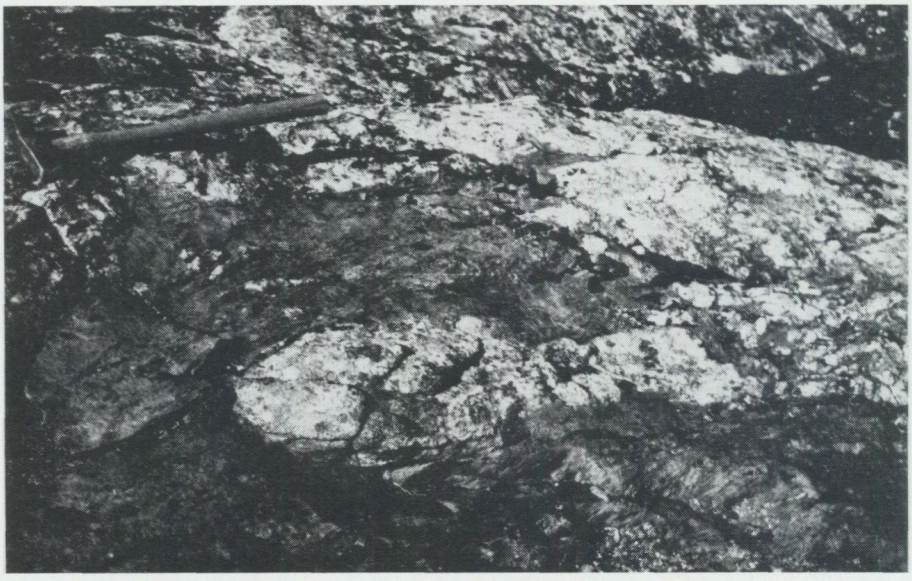

Fig. 13. Apophysis to mafic dyke intruding coarse-grained, granular-textured quartz keratophyre. Stuore Duoranåjje.

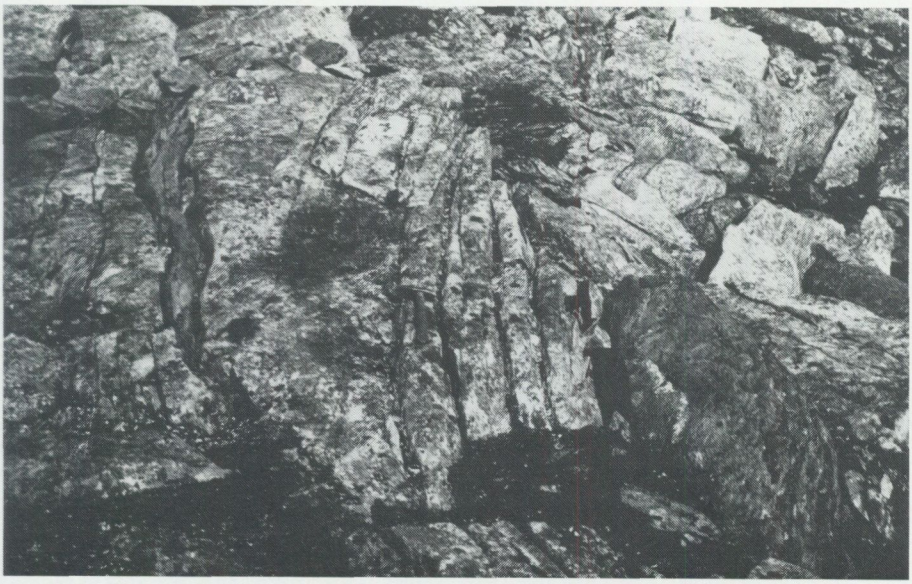

Fig. 14. Schistose greenstone lenses in coarse-grained, granular-textured quartz keratophyre. This picture is taken from the same locality as shown in Fig. 13. It is possible to map together a string of these lenses into the better preserved types showing intrusive relationship into the quartz keratophyre. Stuore Duoranåjje.

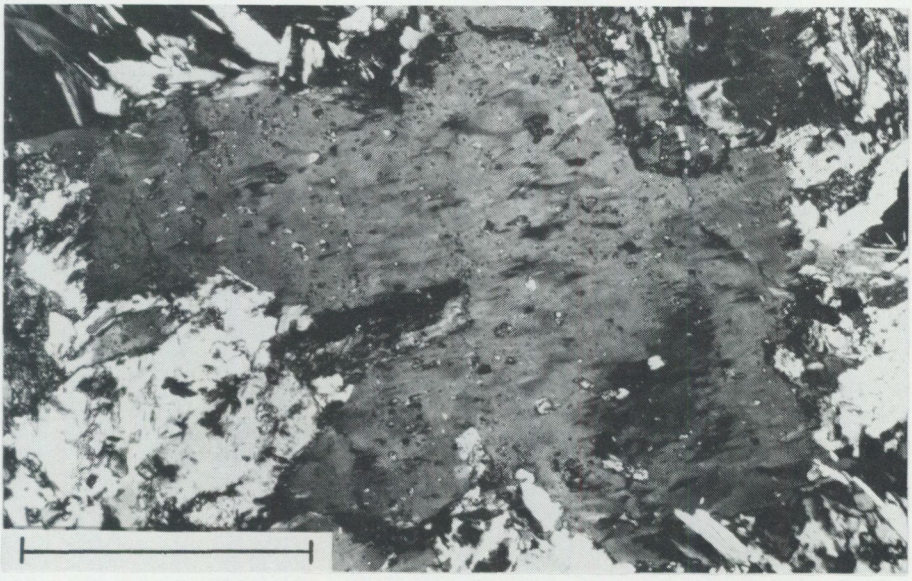

Fig. 15. Schistose, subophitic texture (amphibole-albite) in coarse-grained, dark greenstone interpreted as being high-level intrusive in origin. Mineral assemblage is amphibole-albite-chlorite-Ti-rich minerals-epidote-calcite. The coarse amphibole grains, up to 1.5 mm across, often show intragranular strain features such as undulose extinction and kinking. Bh 70710-S, 79.78—79.87m, crossed nicols. Bar length = 1 mm.

greenstone sheets are also apparent near the top of the layered volcanite sequence (Fig. 11) and also within the overlying mixed phyllites and tuffites. The most characteristic sheet is approximately 40 m thick and occurs at the same level on both limbs of the F_3 antiform on Duoranåjje. Mineralogically, this sheet consists of amphibole-albite-chlorite-epidote-sphene (leucoxene)±calcite. On the steeply NW-dipping, overturned, south-east limb of the antiform, this greenstone appears composite with alternation of finer and coarser (plagioclase laths between 0.8 and 2 mm) facies, the boundaries between which are both diffuse and sharp. All rocks are to a greater or less extent schistose but, in better preserved types, the finer facies shows intergranular to sparsely amphibole-phyric texture and the coarser types subophitic to ophitic texture (Fig. 15). This body as well as other apparently concordant sheets (for example the gabbro in the vicinity of the Stekenjokk ore body) are interpreted as pre-deformation sills. Diffuse contacts between finer and coarser facies in the composite Duoranåjje intrusion are, thus, interpreted as chilled margin contacts, while sharp contacts represent a later intrusive phase with chilled margin contacting an older intrusive phase.

REMDALEN

On the eastern limb and around the hinge of the Remdalen Synform, the Stekenjokk volcanite-bearing formation overlies a thick mafic volcanite unit (Lasterfjäll Greenschist) and gabbro-intruded calcareous phyllites (Lasterfjäll Calcareous Phyllite); towards the north-west, on the western limb of the synform, the mafic volcanite unit appears to be absent and mixed phyllites, forming the lowest part of the volcanite-bearing formation, rest directly on top of calcareous phyllites. The volcanites are overlain by lenses or more continuous layers of quartzite conglomerate or limestone interlayered with graphitic phyllite (Remdalen Quartzite—Conglomerate-bearing Formation). Normal, N-plunging F_3 folds form the dominant mesoscopic fold element in the southern Remdalen area. They deform the penetrative main foliation (S_{1-2}) and associated linear structures and are congruent to the macroscopic Remdalen Synform.

On the eastern limb of the Remdalen Synform, Zachrisson (1964) described mixed felsic and mafic volcanites at two stratigraphic levels, separated from each other and the surrounding units by often graphitic phyllite. Drilling through the lower level, associated with investigation of the Beitsetjenjunje Zn-Cu mineralization (Zachrisson 1977,1980; Stephens *et al.* 1979), revealed, in the lower part, approximately 100 m of layered tuffite (dark and graphitic to grey-green and often calcareous) with subordinate limestone (up to approx. 2 m) and graphitic phyllite interbeds (Fig. 16), remarkably similar to the layered tuffites in the lower part of the volcanite sequence in the Björkvattnet area. Overlying these tuffites,there is at least 120—130 m of well layered aphyric, variably tuffitic greenschist (chlorite-

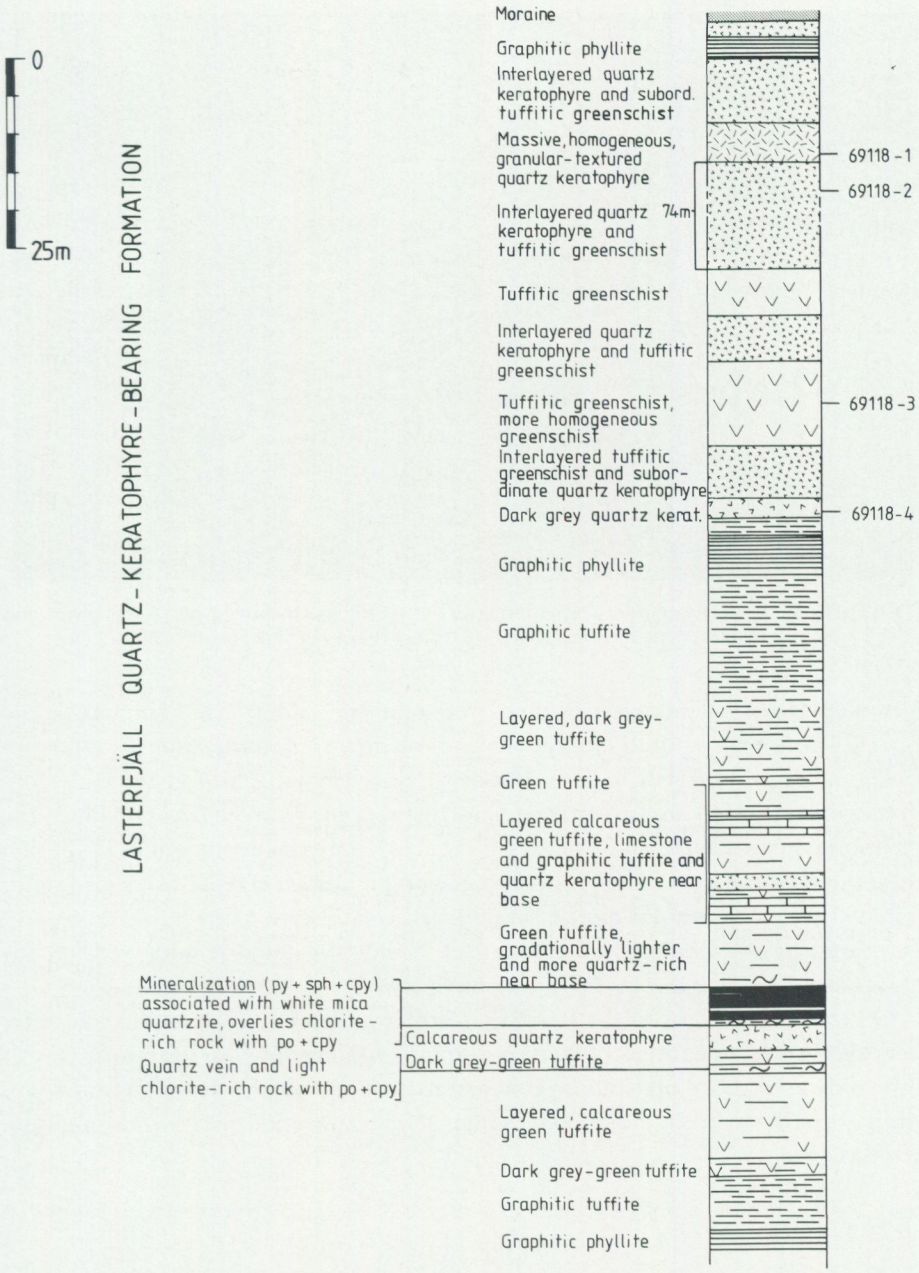

Fig. 16. Borehole section (69118) through part of the Stekenjokk volcanites (Lasterfjäll Quartz-Keratophyre-bearing Formation) in the Remdalen area showing the position of the Beitsetjenjunje Zn-Cu massive sulphide deposit. The section shown lies structurally above mafic volcanites belonging to the Lasterfjäll Greenschist. Locations of analyzed samples in this section are indicated.

Fig. 17. Distal tuff facies. Finely alternating layers of tuffitic greenschist, quartz keratophyre and biotite phyllite. Along Luoktjemjukke, approximately 2 km east of Luoktjemjaure.

albite-epidote±calcite±biotite) and fine-grained, albite- and quartz-phyric quartz keratophyre (albite-quartz-chlorite-calcite±white mica) interpreted tentatively as mainly ash-fall, vitric and phyric vitric-crystal tuffs and tuffites. More homogeneous (up to approx. 5 m) greenschist was encountered occasionally in the drillholes investigated and appears to contain conspicuous amounts of Ti-rich minerals (sphene, leucoxene, ilmenite); the origin of such greenschist is uncertain. 5 m of a coarser, granular quartz keratophyre, reminiscent of the Björkvattnet and Duoranåjje examples, was noted in one of the investigated drillholes (see Fig. 16) and is interpreted as a subvolcanic intrusive rock.

On the western limb of the Remdalen Synform, the lower part of the volcanite-bearing formation consists of layered graphitic to limey phyllites (approx. 60 m); the volcanites above are well layered greenschist and phyric quartz keratophyre, similar to the eastern limb, with some interstratification of grey to graphitic phyllite (Fig. 17).

DISCUSSION

TECTONIC POSITION OF THE LASTERFJÄLL AND REMDALEN GROUPS

On the western limb of the F_3 Fjällfjäll Antiform (Zachrisson 1969 and Plate I), the fine-grained calcareous phyllites containing gabbros overlie either quartz

wackes and calcareous phyllites without gabbro intrusions (*e.g.* west of Gränssjö) or more usually a graphitic phyllite-greenstone association. The units underlying the gabbro-intruded calcareous phyllites can be compared with the Silurian Lövfjäll (including Viris Quartzite) and Broken Formations (Kulling 1933), respectively, whose type-areas lie to the east just north of the lake Virisen (Plate I), on the eastern limb of the Fjällfjäll Antiform. Kulling's (1933) stratigraphy lies within the lowest Köli tectonic unit, referred to here as the Björkvattnet Nappe (equivalent to the low-grade, upper part of the Björkvattnet Unit of Stephens 1977 and the Joesjö Nappe of Häggbom 1980), the base of which is defined in southern and central Västerbotten (see Plate I) at the boundary to the Svartsjöbäcken Schists (Trouw 1973) and Brakko schists (Stephens 1977), respectively. The term 'Björkvattnet Nappe' is taken from the lake Björkvattnet lying 20 km north of Virisen in the county of Västerbotten. Zachrisson (1964) inferred that the stratigraphy within the Köli Nappes on the western limb of the Fjällfjäll Antiform was continuous and introduced the term Lasterfjäll Calcareous Phyllite for that part of the stratigraphy composed of calcareous phyllites, whether or not containing gabbros. Subsequently, Zachrisson (1969) correlated the Lasterfjäll Calcareous Phyllite with the Lövfjäll Formation, and noted that the upper part of the calcareous phyllite sequence and the overlying units (see Fig. 1) were simply not preserved to the east of the Fjällfjäll Antiform. The corollary followed that all the upper part of Zachrisson's (1964, 1969) stratigraphy (*i.e.* most of the Lasterfjäll Group and all of the Remdalen Group), including in particular the Stekenjokk volcanites, belonged to the same tectonic unit as Kulling's (1933) stratigraphy, the Björkvattnet Nappe of this paper, and was post-mid to late Llandovery in age. Since late-orogenic sediments from western Norway contain Lower Downton or possibly even uppermost Ludlow faunas (Roberts 1978), then all the upper part of Zachrisson's stratigraphy would appear to be Silurian and to have been deposited, metamorphosed, deformed and transported eastwards in less than 20—30 Ma (Churkin *et al.* 1979; McKerrow *et al.* 1980), a rather short time interval.

The continuity of the sequence on the western limb of the Fjällfjäll Antiform is questioned here since:

1. Gabbro intrusions are absent in the Lövfjäll Formation to the east and in the quartz wacke-bearing facies of the Lasterfjäll Calcareous Phyllite to the west of the Fjällfjäll Antiform; whether the apparently concordant gabbro sheets in the upper part of the Lasterfjäll Calcareous Phyllite are interpreted as original sills or highly deformed dykes, it would seem likely that some intrusions would occur in the immediately underlying quartz wacke and calcareous phyllite units, if there was a continuous stratigraphic succession.

2. Around Tärnaby (central Västerbotten), a thrust contact has been recognized between overlying gabbro-intruded calcareous phyllites and the underlying Lövfjäll Formation (Stephens 1977; Häggbom 1980; Sandwall 1981).

3. Locally on the western limb of the Fjällfjäll Antiform, a thrust contact and/or phyllonitic rocks have been recorded, either between calcareous phyllites with gabbros and graphitic phyllites or within calcareous phyllites, gabbros being absent in the underlying units. These localities are briefly documented below (see Plate I):

   I. North of Gränssjö, on the eastern side of Svälvetjakke (just outside the map-area shown on Plate I), a marked topographic break marks the contact between gabbro-intruded calcareous phyllites and graphitic and quartz-rich phyllites. Abundant quartz segregations in the calcareous phyllites and phyllonitic structure in the graphitic and quartz phyllites characterize this contact. Kulling (1933) also remarked on the intense deformation in this zone and its continuation northwards, although he did not favour significant movement at this level.

   II. Between Gaisarjaure and Avasjön, south of Gränssjö, over a strike length of approximately 5 km, Du Rietz (1941) marked a thrust contact between gabbro-intruded calcareous phyllites and underlying graphitic phyllites. According to Zachrisson (1964, 1969), this zone connects up with a marked topographic feature on the eastern side of Avafjället, while further south, on the north-eastern part of Lasterfjället, a zone of strong mylonitization and phyllonitization is located in the lower part of the calcareous phyllite sequence. Zachrisson (1969) suggested that this movement zone was the northerly continuation of the thrust at the base of the Remdalen "repetition".

   III. On the western side of Jalketsåive—Biellovare, Zachrisson (1964) indicated an antiform in the core of which is exposed rocks belonging to the Tjopasi Group. The western side of this antiformal structure is a thrust fault immediately above which lies gabbro-intruded calcareous phyllites. This thrust is clearly at a lower tectonic level than the Remdalen "repetition" of Zachrisson (1969).

   IV. Between Ankarvattnet and the northern shore of Stor-Blåsjön, recent mapping (K.Sundblad and M.B.Stephens) has revealed several zones of phyllonitization in the lower part of the calcareous phyllite (Blåsjö Phyllite) sequence. The uppermost zone, up to 20 m thick, and occurring some hundred metres above the Tjopasi Group rocks, dips steeply north-west and is markedly oblique to the penetrative schistosity and lithological layering in the overlying calcareous phyllites. Gabbros are absent beneath the uppermost phyllonite zone but occur higher up the succession, some 3 km north-west of this zone. It is clear that, although the movement zones mentioned here and in the preceding paragraph lie just above or at the

contact to the Tjopasi Group, the level at which calcareous phyllites are heavily intruded by gabbro intrusions appears to lie much higher in the structural succession around Ankarvattnet — Stor-Blåsjön compared with Jalketsåive — Biellovare. It is suggested that either the gabbros are cutting up through the calcareous phyllite succession from Biellovare towards Ankarvattnet or lithological units belonging to the calcareous phyllite sequence and lying beneath the gabbro-intruded level are cutting out between Ankarvattnet and Biellovare, along a tectonic contact situated at or just above the contact to the Tjopasi Group rocks. The mapping relations between Ankarvattnet and Stor-Blåsjön suggest that the latter hypothesis is more likely. It is uncertain whether the main tectonic break should be placed along the lower contact of the calcareous phyllite or along the uppermost phyllonite zone; the latter solution is shown on Plate I.

The correlation (Zachrisson 1969), both as regards tectonic level and age, of the quartz wacke—calcareous phyllite and graphitic phyllite—greenstone associations with the Silurian Lövfjäll and Broken Formations (Björkvattnet Nappe), respectively, is accepted (Fig. 1). However, it is suggested that the upper part of the stratigraphy described by Zachrisson (1964, 1969), *i.e.* the bulk of the Lasterfjäll Calcareous Phyllite, including the gabbro-intruded part, and higher units, occurs within two thrust nappe units lying structurally above and separate from the fossiliferous Björkvattnet—Virisen stratigraphy of Kulling (1933). The lower of these units is referred to here as the Stikke Nappe and the upper one is the already defined Gelvenåkko Nappe (Zachrisson 1969). Based on the local evidence discussed above, the contact between the Stikke and Björkvattnet Nappes is indicated in Plate I.

The tectonic solution presented above needs to be compared with earlier solutions proposed by Sjöstrand (1978) and Kollung (1979) for the tectonostratigraphy in the Köli Nappes. The mapping by K. Sundblad around Ankarvattnet has provided no support for the fold nappe hypothesis of Sjöstrand (1978) with an "inversion line" located in the central part of the Blåsjö Phyllite. Such a hypothesis demands correlation of two quite distinct lithostratigraphic sequences, *i.e.* the Tjopasi Group and Bellovare Formation on the right way up eastern limb of the postulated fold nappe and the upper part of the Lasterfjäll and Remdalen Groups on the inverted western limb (see Fig. 1). Furthermore, no evidence is apparent for a tectonic break at the top of the Blåsjö Phyllite, as proposed by Kollung (1979), *i.e.* at the contact between his Renselvann and Huddingsdalen Groups. Work in progress (Stephens 1981a) indicates that both mafic and subordinate felsic intrusions in the Blåsjö Phyllite are comagmatic with some of the mafic rocks and the felsic rocks, respectively, within the Stekenjokk volcanites. This data

provides strong support for field relationships suggesting stratigraphic continuity in the upper part of the Blåsjö Phyllite and into the Stekenjokk volcanites.

WAY UP OF THE LASTERFJÄLL AND REMDALEN GROUPS

Inversion of the Lasterfjäll and Remdalen Groups and the inferred fold nappe solution presented by Sjöstrand (1978) were based on his stratigraphic correlation of the rocks within the Lasterfjäll and Remdalen Groups with lithologies in the Eastern Trøndelag area, Norway (southern side of the Grong-Olden Culmination). Studies of metal zonation and position of alteration assemblages in the Stekenjokk (Juve 1977) and Ankarvattnet (Sundblad 1980) massive sulphide deposits, which occur within the Stekenjokk volcanites and Blåsjö Phyllite of the Stikke Nappe respectively, support the inversion hypothesis. Furthermore, Juve (1977) implied that the position of the Stekenjokk ore body near the structural base of the volcanites would favour local inversion at Stekenjokk. Evidence for such local inversion of these sulphide deposits does not necessarily imply regional inversion of the whole upper part of the Lasterfjäll—Remdalen stratigraphy, since the presence of attenuated F_{1-2} overturned folds and minor thrusts within major lithological or tectonic units is highly probable. As stated earlier, such folds are present in the Gelvenåkko Nappe. Nevertheless, it would appear that the majority of the Zn-Cu deposits associated with the Stekenjokk volcanite-bearing formation, not only the Stekenjokk ore body itself, occur towards the calcareous phyllite side of the formation. Since this is usually the structural base of the formation, then such a distribution may well argue for regional-scale inversion of the Lasterfjäll-Remdalen stratigraphy.

AGE OF THE LASTERFJÄLL AND REMDALEN GROUPS

Applying the tectonic re-interpretation presented above, involving division of Zachrisson's (1969) Lower Köli unit into the Björkvattnet and Stikke Nappes, the age of the gabbro-intruded calcareous phyllites, Stekenjokk volcanites and overlying Remdalen Group is no longer necessarily Silurian but may be older. Arguments for a possible Ordovician age for the Stekenjokk volcanites are now presented. A similar conclusion based, in part, on different arguments was also put forward by Sjöstrand (1978).

As pointed out by Sjöstrand (1978), gabbro-intruded calcareous phyllites and metagreywackes similar to the Lasterfjäll and Blåsjö Phyllites occur in the Eastern Trøndelag area. In particular, near and south of Kjølhaugan (Eastern Trøndelag), heavily gabbro-intruded calcareous phyllites lie west of and structurally above graptolite-bearing (Getz 1980), Llandovery black phyllites which in turn lie west of and above calcareous sandstones, phyllites and conglomerates (see Wolff 1976).

Earlier interpretations (Chaloupsky and Fediuk 1967; Siedlecka 1967; Wolff 1967) indicated that the Llandovery black phyllites (Slågån Group) formed the youngest stratigraphic unit and were situated in a tight overturned syncline, while the calcareous sediments on either side were the same stratigraphic unit (Kjølhaugan Group) and older. More recent, detailed, structural mapping of the eastern calcareous sandstones and phyllites in the Kjølhaugan area (Hardenby 1980) has demonstrated that this unit lies itself in a syncline overturned to the east, the right way up eastern limb lying with tectonic contact (Trondheim Nappe Complex) on underlying Seve mica schists and amphibolites, and the stratigraphically *older* Slågån Group and heavily gabbro-intruded calcareous phyllites lying in an inverted position on the overturned western limb. These results suggest that the western, heavily gabbro-intruded calcareous phyllites are not the same stratigraphic level as the eastern calcareous sandstones and phyllites. Assuming a continuous succession from the Slågån Group upwards and westwards into the western, heavily gabbro-intruded phyllites, it follows that the latter are pre-Llandovery in age. On the basis of the correlation of the Lasterfjäll and Blåsjö Phyllites with the heavily gabbro-intruded calcareous phyllites of the Kjølhaugan Group (Trondheim Nappe Complex), a pre-Llandovery age for the Lasterfjäll and Blåsjö Phyllites may also be inferred. Since crinoids have been noted in the structurally lower part of the Remdalen Group in the Remdalen (Högbom 1925) and Kvarnbergsvattnet (Sjöstrand 1978) areas, an early Ordovician minimum age can be determined for the rocks immediately above the Stekenjokk volcanites. Thus, it follows that if the Remdalen Group is stratigraphically older than the Lasterfjäll Group, as argued earlier, the Stekenjokk volcanites should be Ordovician in age.

REVISED TECTONOSTRATIGRAPHIC SCHEME

Based on the discussion above, a revised tectonostratigraphic scheme for the Köli east and west of the Fjällfjäll Antiform in Sweden is presented in Fig. 18. The Björkvattnet Nappe containing diagnostic Ordovician and Silurian fossils essentially contains a right way up sequence. This stratigraphy is separated by a tectonic break from lithologies (including the Stekenjokk volcanites) in the Stikke Nappe thought to lie in an inverted position and to be Ordovician (and older?) in age. The term Lasterfjäll Group has not been used here, since it groups together lithologies occurring in separate tectonic units. The term Blåsjö Phyllite (Lasterfjäll Calcareous Phyllite), as used here, is restricted to the gabbro-intruded calcareous phyllites in the Stikke Nappe. It excludes the calcareous phyllites and quartz wackes thought to be equivalent to the Lövfjäll Formation and belonging to the Björkvattnet Nappe. The base of the Blåsjö Phyllite was not defined when the term was introduced (Nilsson 1964). Sjöstrand (1978), however, included all the calcareous phyllites down to the equivalent of the Broken, Slätdal and Vojtja Formations in the Blåsjö Phyllite.

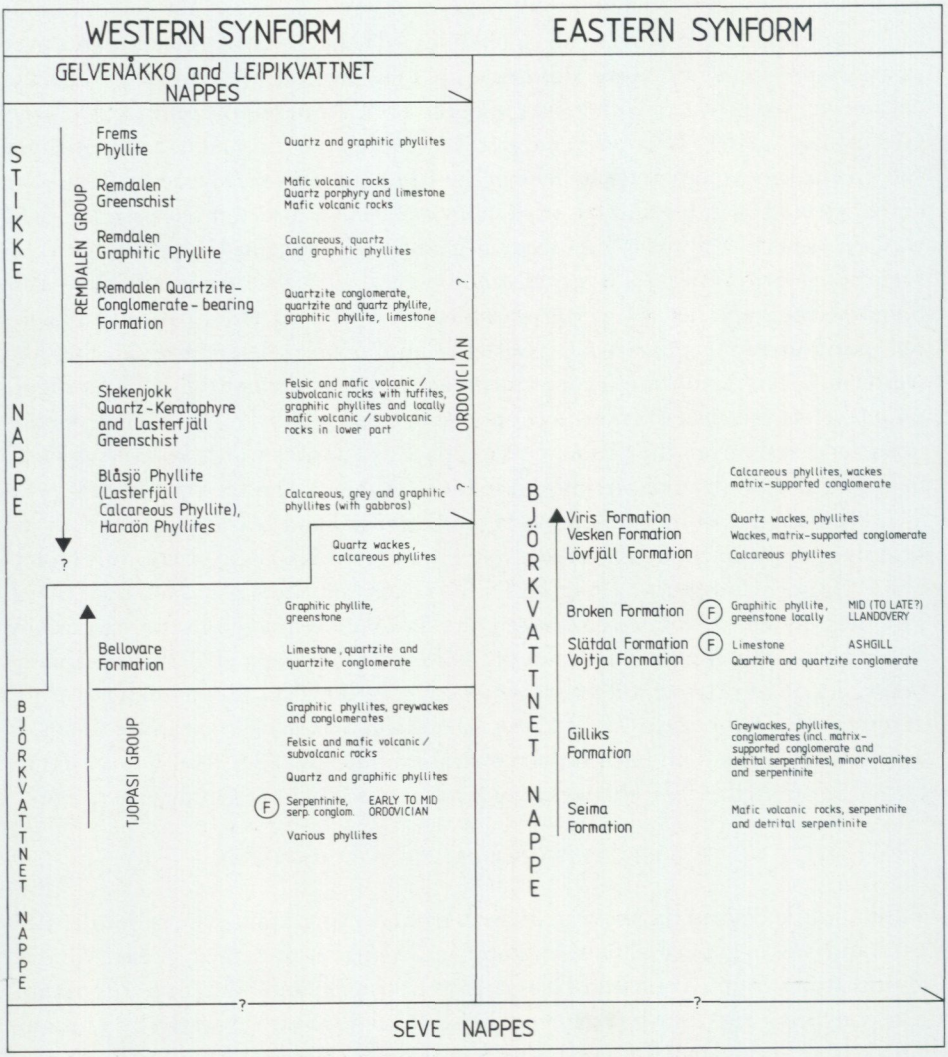

Fig. 18. Revised interpretation of the tectonostratigraphy of the Köli Nappes in northern Jämtland and southern Västerbotten (cf. Fig. 1), vertical arrows indicating way up of the different successions. The lithological sequences shown for the Björkvattnet Nappe are right way up. The lithological sequence shown for the Stikke Nappe is of less certain stratigraphic polarity; inversion of the whole sequence is tentatively indicated here. The Gelvenåkko Nappe includes lithologies belonging to the Lasterfjäll and Remdalen Groups, and the Leipikvattnet Nappe lithologies correlatable possibly with the Lasterfjäll and Remdalen Groups. F indicates diagnostic fossil occurrence.

SUMMARY OF RESULTS AND CONCLUDING REMARKS

1. The Stekenjokk volcanites have been studied from Björkvattnet in northern Jämtland to Remdalen in southern Västerbotten, a strike length of some 90 km. The Stekenjokk volcanite-bearing formation is usually underlain by gabbro-intruded calcareous phyllites (Blåsjö Phyllite) with, in some areas (Leipikvattnet, Stekenjokk, east Remdalen), the development of a mafic volcanite unit (Lasterfjäll Greenschist) between the Stekenjokk volcanite-bearing formation and the calcareous phyllites. The Stekenjokk volcanites are usually overlain by a unit of graphitic phyllite containing lenses or thicker, more continuous layers of quartzite conglomerate and limestone (Portfjället Conglomerate or Remdalen Quartzite—Conglomerate-bearing Formation). The structurally lower (*i.e.* towards the mafic volcanite-calcareous phyllite side) 50—100 m within the Stekenjokk volcanite-bearing formation is composed of various proportions of layered tuffite, graphitic and limey phyllite, and minor limestone. Zn-Cu-dominated stratabound sulphide mineralizations occur within this tuffite unit, at the border between graphitic phyllite and volcanite, and within the volcanites mostly on the tuffite-mafic volcanite-calcareous phyllite side, *i.e.* towards the usual structural base of the formation. This stratigraphy is coherent and consistent over the total strike length which has been studied and is interpreted here to be stratigraphically continuous.

2. Zachrisson (1969) recognized that the Stekenjokk volcanites occurred within two distinct tectonic units, a lower one he loosely referred to as the Lower Köli unit, including minor nappes and repetitions (*e.g.* Remdalen "repetition"), and an upper one referred to as the Gellvernokko Nappe (Gelvenåkko Nappe in this study). The essential premise that the structural sequence within the Lower Köli unit west of the Fjällfjäll Antiform, which includes in its lower part elements correlatable with the fossiliferous Ordovician and Silurian stratigraphy of Kulling (1933) further east, is a continuous stratigraphic succession, is questioned here. It is suggested, instead, that the gabbro-intruded calcareous phyllites, Stekenjokk volcanites and Remdalen Group within Zachrisson's Lower Köli unit belong to a higher tectonic unit — here referred to as the Stikke Nappe — lying above the fossiliferous stratigraphy of Kulling (1933); Kulling's stratigraphy lies in the lowest Köli unit, here referred to as the Björkvattnet Nappe.

3. Within most of the Stikke Nappe and near Leipikvattnet in the Gelvenåkko Nappe, the lithostratigraphic sequence is as described with volcanites etc. on top of gabbro-intruded calcareous phyllites. However, in most of the Gelvenåkko Nappe, the tuffite-phyllite complex overlies the volcanites proper in a continuous succession. Such complexities are related to early $F_{1-2}(?)$ folds.

Local stratigraphic inversion within major lithological units has been described at Stekenjokk (Juve 1977) and Ankarvattnet (Sundblad 1980), both in the Stikke Nappe. Such evidence, when considered with the occurrence of most of the massive sulphide deposits near the usual structural base of the volcanites (calcareous phyllite side), support Sjöstrand's (1978) suggestion that the gabbro-intruded calcareous phyllites are stratigraphically younger than the Stekenjokk volcanites. Correlation of the gabbro-intruded calcareous phyllites with the western part of the Kjølhaugan Group in the Eastern Trøndelag stratigraphy (Trondheim Nappe Complex), and use of available fossil evidence and the inversion hypothesis indicate an Ordovician age for the Stekenjokk volcanites.

4. Although the Stekenjokk volcanites have suffered polyphase deformation and chlorite to biotite grade metamorphism under pressures of c. 5 kbar, it is still possible to recognize some primary textures and, thus, speculate, at least in part, on their original nature:

   I. Mafic rocks constitute possibly up to one third of the volcanites and high-level intrusions in the Stekenjokk volcanite-bearing formation. The bulk of the mafic material is composed of fine-grained greenschists and greenstones with mineral assemblages chlorite -albite±amphibole±epidote ±calcite±Ti-rich minerals, here referred to as Group 1 mafic rocks. Group 1 greenschists and greenstones showing finer aphyric to plagioclase- and/or amphibole-phyric textures are interpreted as being volcanic (vitric to vitric-crystal tuffs and flows?); coarser pyroclastic products, lapilli tuff and volcanic breccia, have been recognized locally in the Björkvattnet area. Group 1 greenstones with coarser intergranular texture are thought to represent high-level intrusions. A subordinate mafic component, referred to here as Group 2 mafic rocks, is composed of often darker greenstone and dolerite to gabbro sheets with mineral assemblages, amphibole-albite-chlorite-epidote-Ti-rich minerals (sphene, ilmenite, leucoxene) ±calcite and chlorite-albite-calcite-Ti-rich minerals ±biotite±epidote±apatite±white mica. Intergranular and occasionally subophitic to ophitic textures and chilled margins are conspicuous in this group and attest to the intrusive origin of these rocks. They occur either as concordant sheets, at one locality composite and up to 40 m thick, or narrow, dyke-like (?) bodies and, based on their occurrence in other rock-types, define the latest phase of magmatic activity in the Stekenjokk volcanites. A conspicuous feature of the mafic units is the occurrence of pre-deformation nodules and veinlets of epidotite (±calcite).

   II. Felsic rocks (quartz keratophyres) dominate (approximately two thirds?) the Stekenjokk volcanites and consist of the mineral assemblages albite-quartz-chlorite±epidote±mica±calcite±Fe-Ti oxides. Both albite- and

quartz-phyric as well as coarser granular textures occur; such rocks are interpreted as phyric vitric-crystal tuffs and subvolcanic intrusions, respectively. The more homogeneous, thicker, phyric tuffs are thought to represent ash-flows (note especially Björkvattnet and Gauste areas), while the finely layered phyric quartz keratophyre and greenschist sequences intimately intermixed with more tuffitic or even phyllitic material (note especially Stor-Blåsjön and Remdalen areas) are more tentatively interpreted as ash-fall and reworked ash-fall deposits. Felsic subvolcanic intrusions are particularly well represented in the Björkvattnet and Duoranåjje (Stekenjokk) areas.

5. The volcanite packet appears to be thicker (500—1000 m) where more varied — including particularly coarser pyroclastics and subvolcanic felsic intrusions — sequences occur. Such sequences are, thus, thought to represent accumulations somewhat closer to major eruptive centres. Finely layered, thin (<200 m) units with occasional sedimentary intercalations are tentatively interpreted as a more distal pyroclastic facies. On this basis, it is suggested, for example, that, in the Stikke Nappe, the Björkvattnet and Stekenjokk successions represent a more proximal position to major centres, while the Stor-Blåsjön sequence may represent a more distal facies of the volcanite pile.

6. Sedimentary intercalations, which are frequent in the more distal pyroclastic facies but rare in the thicker more proximal sequences, consist of grey to graphitic phyllite and limestone; they are interpreted as marine and attest to the submarine nature of the ongoing volcanism. Such intercalations are thought to represent less violent phases or real pauses in the largely explosive volcanic activity.

Part II: PETROCHEMISTRY AND PETROGENESIS

ANALYTICAL METHODS AND RESULTS

69 whole rock samples were analyzed for major and minor elements at SGU (Geological Survey of Sweden). Sampling (localities indicated on Plate I) was carried out on a regional basis over the total strike length of the volcanites and away from the influence of alteration around known massive sulphide deposits. Epidotites and carbonate-rich zones were also not included in the sampling. Mafic rocks analyzed were chosen so as to avoid as much as possible porphyritic specimens (plagioclase and/or amphibole-phyric) and finely layered specimens. Textures in felsic rocks analyzed include both porphyritic (albite- and quartz-phyric) and granular, aphyric.

SiO_2, TiO_2, Al_2O_3, FeO* (total Fe as FeO), MnO, MgO, and CaO were determined by optical emission spectroscopy (tape machine method) using prefabricated, fused, synthetic standards, while Na_2O and K_2O were determined by atomic absorption. Prior to determination, the samples were powdered, mixed with a lithium borate-strontium carbonate buffer, fused, quenched in distilled water and the resulting granules ground to a powder. The details of the techniques

TABLE 1. Determinations of USGS standard rocks at the Geochemical Laboratories of the Geological Survey of Sweden (SGU — major elements) and the Geological Survey of Norway (NGU — trace elements). SGU major element determinations were made during a routine run of Stekenjokk volcanite samples. NGU[1] trace element determinations are reported in Faye and Ødegård (1975), while NGU[2] trace element determinations were made during a routine run of Stekenjokk volcanite samples. Recommended values are as reported in Flanagan (1973).

	Basalt USGS BCR-1		Andesite USGS AGV-1		Granodiorite USGS GSP-1		Granite USGS G-2	
	SGU	Recomm. value	SGU	Recomm. value	SGU	Recomm. value	SGU	Recomm. value
SiO_2 (%)	53.7	54.50	58.0	59.00	66.7	67.38	68.4	69.11
TiO_2	2.22	2.20	1.04	1.04	0.66	0.66	0.48	0.50
Al_2O_3	12.9	13.61	16.3	17.25	14.6	15.25	14.7	15.40
Fe_2O_3	5.6	3.68	5.4	4.51	1.8	1.77	1.5	1.08
FeO	8.8	8.80	2.2	2.05	2.8	2.31	1.5	1.45
MnO	0.18	0.18	0.09	0.097	0.03	0.042	0.03	0.034
MgO	3.4	3.46	1.47	1.53	0.98	0.96	0.79	0.76
CaO	7.0	6.92	4.9	4.90	2.0	2.02	1.9	1.94
Na_2O	3.3	3.27	4.3	4.26	2.8	2.80	4.1	4.07
K_2O	1.6	1.70	2.9	2.89	5.4	5.53	4.3	4.51
P_2O_5	0.29	0.36	0.44	0.49	0.28	0.28	0.15	0.14
H_2O^+	0.5	0.77	0.6	0.81	0.6	0.57	0.5	0.55
H_2O^-	1.0	0.80	1.3	0.16	0.2	0.12	0.2	0.11
CO_2	0.04	0.03	0.06	0.06	0.12	0.15	0.13	0.08
Total	100.5	100.28	99.0	99.05	99.0	99.84	98.7	99.73

	NGU[1]	NGU[2]	Recomm. value	NGU[1]	NGU[2]	Recomm. value	NGU[1]	NGU[2]	Recomm. value	NGU[1]	NGU[2]	Recomm. value
Zr (ppm)	195	185	190	228	228	225	624	469	500	335	296	300
Y	34	43	37.1	13	22	21.3	23	23	30.4	4	8	12
Cu	14	24	18.4	62	70	59.7	32	34	33.3	31	12	11.7
Zn	128	91	120	86	82	84	97	113	98	81	103	85
Ni	9	15	15.8	15	19	18.5	6	9	12.5	4	6	5.1
Cr	24	5	17.6	7	< 5	12.2	0	< 5	12.5	0	< 5	7

used are described by Danielsson (1967), where also remarks on precision, accuracy and sensitivity are included. FeO and P_2O_5 were determined by wet chemical methods as described in Asklund *et al.* (1966), while $H_2O>105°$, $H_2O<105°$ and CO_2 were determined by various gravimetric methods.

A suite of six trace elements, Zr, Y, Cu, Zn, Ni, and Cr, was determined on 58 samples at NGU (Geological Survey of Norway) by X-ray fluorescence using a Philips PW1540 machine and synthetic standards. Determinations were made on fused rock powders. Details of the methods used, correction procedures, precision and accuracy estimates are provided by Faye and Ødegård (1975).

A 'blind' run of four USGS standard rocks, BCR-1, AGV-1, GSP-1, and G-2, was carried out at both the SGU and NGU laboratories during routine determination of major and trace elements of unknown samples, respectively. The results are shown in Table 1. By comparing these values with recommended values (Flanagan 1973), some measure of the accuracy of the analyses presented in this paper is obtained.

Individual analyses with locality coordinates are presented in the Appendix, while means, standard deviations and ranges of different types of mafic and felsic rocks are summarized in Table 2. Fe_2O_3/FeO values (0.2—1.3) as well as $H_2O>105°$(0.2—4.8 %) and CO_2(<0.01—4.1 % with two extreme values at 5.5 and 8.0 %) contents are variable in the mafic and felsic Stekenjokk volcanites (see Appendix), indicating varying degrees of oxidation, hydration and carbonation. It is probable that such processes took place during both pre-deformation alteration as well as syn-deformation regional metamorphism events. In order to gain some insight into original compositions and to be able to compare the analyses both with each other and with published analyses from other areas, all analyses have been recalculated and plotted on the various diagrams on a volatile-free basis.

The Group 1 and Group 2 mafic rocks in Table 2 correspond to the field/microscope-distinguishable mafic rock groups defined in Part I (see page 34). The chemical characteristics of Groups 1 and 2 are discussed in the following section. Careful inspection of the chemical data, emphasizing, in particular, distribution of the critical elements Ti, Mg, K, P, Zr, Y, Ni, and Cr as well as the ratios FeO*/MgO and Zr/Y, suggests refinement of each of the mafic groups into two subgroups (1A and 1B, 2A and 2B), the chemical differences between which are also discussed below. The breakdown of Group 1 into two subgroups is based entirely on chemical data. However, the breakdown of the darker Group 2 mafic rocks into two subgroups appears to correspond to certain mineralogical differences, Group 2A containing the amphibole-albite-chlorite-epidote-Ti-rich minerals ±calcite and Group 2B the chlorite-albite-calcite-Ti-rich minerals±biotite±epidote±apatite mineral assemblages. The felsic rocks, both volcanic and high-level intrusions, are shown in a separate column in Table 2.

TABLE 2. Means, standard deviations and ranges of chemical analyses of mafic and felsic volcanites and high-level intrusive rocks within the Stekenjokk volcanites. N = number of analyses unless otherwise stated in brackets, x = mean, s = standard deviation, analyses recalculated on a volatile-free basis. Group 1A (Basalt) includes one sample with 56.0 % SiO_2 but trace element characteristics compatible with basalt; Group 1B (Basalt) includes one sample with 53.5 % SiO_2 (remaining 14 samples have <53 % SiO_2).

	MAFIC ROCKS															FELSIC ROCKS (N=20)		
	Group 1A - Basalt (N=6)			Group 1A - Basaltic andesite (N=3)			Group 1B - Basalt (N=15)			Group 2A - Tholeiitic basalt (N=17)			Group 2B - Alkalic basalt (N=8)					
	$\bar{x}$	s	Range	$\bar{x}$	s	Range	$\bar{x}$	s	Range	$\bar{x}$	s	Range	$\bar{x}$	s	Range	$\bar{x}$	s	Range
SiO_2 (%)	52.4	1.9	50.6-56.0	54.0	1.4	53.0-55.6	50.2	1.6	47.3-53.5	49.2	1.6	44.7-51.2	49.7	1.7	47.1-51.5	75.2	5.2	63.0-83.0
TiO_2	0.54	0.16	0.31-0.77	0.67	0.07	0.63-0.75	0.75	0.26	0.42-1.28	2.73	0.56	1.79-3.92	3.45	0.45	2.88-4.11	0.34	0.23	0.10-0.83
Al_2O_3	16.3	0.8	14.7-16.9	16.8	0.5	16.4-17.3	15.8	1.3	13.3-18.3	14.2	0.7	13.2-15.7	14.5	1.0	12.8-15.9	11.8	1.5	9.0-14.3
Fe_2O_3	3.2	1.1	1.9-5.0	4.2	1.3	3.0-5.5	3.0	0.9	1.4-4.7	4.7	1.1	2.6-7.4	4.9	1.8	2.5-7.8	1.6	1.3	0.4-5.3
FeO	7.9	1.4	5.9-9.9	7.5	1.2	6.3-8.7	7.3	0.7	6.0-8.6	8.5	1.7	5.6-12.9	9.4	1.6	6.9-11.8	2.1	1.1	0.8-4.6
MnO	0.21(5)	0.03	0.18-0.25	0.18(2)	0.02	0.17-0.20	0.19(14)	0.04	0.13-0.31	0.25	0.06	0.15-0.41	0.24	0.02	0.22-0.27	0.07(16)	0.04	0.01-0.17
MgO	7.3	1.2	5.9-8.5	6.5	0.2	6.3-6.7	8.0	1.4	5.7-10.9	6.2	0.6	5.0-7.0	4.3	0.7	3.4-5.4	1.3	0.9	0.3-3.2
CaO	6.7	1.5	5.7-9.7	6.0	1.3	4.5-6.8	10.9	1.9	7.5-13.1	10.5	1.6	7.3-12.4	7.9	1.0	6.5-9.1	1.7	1.6	0.1-5.8
Na_2O	4.8	1.1	2.7-6.0	4.5	0.5	4.0-4.9	3.7	1.1	2.0-6.2	2.8	0.7	2.1-4.4	3.9	0.7	3.1-5.0	5.2	0.8	3.3-6.6
K_2O	0.2	0.2	0.1-0.7	0.2	0.1	0.1-0.2	0.2	0.2	0.1-0.7	0.2	0.1	0.1-0.5	0.8	0.6	0.1-1.9	0.4	0.4	0.1-1.4
P_2O_5	0.06(5)	0.01	0.05-0.08	0.06(2)	0.01	0.05-0.06	0.08(14)	0.03	0.04-0.16	0.29(16)	0.09	0.17-0.48	0.91	0.4	0.45-1.54	0.06(16)	0.05	0.01-0.15
Total	99.6			100.6			99.8			99.6			100.0			99.8		
Zr(ppm)	24	10	13-39	35	3	33-38	50(14)	21	25-93	210(14)	81	140-368	220(7)	35	153-252	97(14)	36	24-151
Y	13	3	9-16	21	2	20-24	19(14)	6	12-31	57(14)	18	29-93	43(7)	10	33-56	39(14)	12	17-55
Cu	31	14	16-55	66	46	24-115	39(14)	29	1-74	46(15)	14	21-79	30(7)	25	1-60	10(14)	11	1-42
Zn	79(5)	10	65-91	60(1)	-	-	62(14)	15	33-86	148(15)	76	70-381	97(7)	26	60-122	50(14)	33	5-123
Ni	25(5)	7	19-35	28(1)	-	-	106(13)	49	47-190	57(15)	25	12-93	11(7)	8	0-21	<5	-	0-6
Cr	48	30	11-86	31	17	18-50	365(14)	164	101-644	148(14)	87	0-257	17(7)	33	0-89	<5	-	0-<5
FeO^*/MgO	1.51	0.32	1.08-1.90	1.87	0.38	1.48-1.94	1.27	0.22	0.89-1.70	2.08	0.44	1.37-2.94	3.30	0.60	2.33-4.09	3.22	1.62	0.80-6.50
Zr/Y	1.74	0.24	1.44-2.44	1.68	0.27	1.38-1.90	2.57(14)	0.53	1.82-3.47	3.69(14)	0.49	3.04-4.83	5.31(7)	1.04	4.21-7.18	2.42	0.62	1.26-3.56

GENERAL PETROCHEMICAL CHARACTER OF THE STEKENJOKK VOLCANITES

Using the ratio FeO*/MgO as an index of differentiation (Kuno 1959; Thompson *et al.* 1962), it is apparent that, while there is some overlap in FeO*/MgO values between Groups 1 and 2, TiO_2, P_2O_5 and Zr contents are distinctly higher in the Group 2 mafic rocks, although the compositional gaps are small (Table 2 and Fig. 19). Y contents and Zr/Y values are also higher in Group 2, although a small overlap is apparent for these parameters (Table 2 and Fig.19).

The presumed mainly volcanic greenschists and greenstones of mafic Group 1 consist of basalts ($44\% \leqslant SiO_2 < 53\ \%$) and basaltic andesites ($53\ \% \leqslant SiO_2 < 56\ \%$). Consideration of the minor and trace elements Ti, P, Zr, Y, Ni, and Cr as well as Zr/Y ratios, *i.e.* the relatively more incompatible and more compatible elements, suggests that this group is not homogeneous. It may be subdivided on a chemical basis into two subgroups (1A and 1B) which as a consequence, however, remain meso- and microscopically indistinguishable. Over a similar range of FeO*/MgO values, the Group 1A rocks have distinctly lower Ni and Cr contents than the Group 1B rocks (Table 2 and Fig. 19). Although TiO_2, P_2O_5, Zr, and Y contents as well as Zr/Y ratios overlap, there is a bias towards *higher* values (Fig. 19 and mean values in Table 2) for the Group 1B rocks, *i.e.* those rocks with distinctly *higher* Ni and Cr contents. The Group 1A rocks (9 analyses) consist of basalts and basaltic andesites, while the Group 1B rocks (15 analyses), with the exception of one analysis with 53.5 % SiO_2, are entirely basaltic. It is important to note also that average Zr and Y contents in the Group 1B basalts are higher and comparable respectively to Zr and Y contents in the Group 1A basaltic andesites. Application of Q-mode cluster analysis (Davis 1973, p. 456—473) to the Group 1 mafic rocks, using the contents of TiO_2, MgO, K_2O, P_2O_5, Zr, Y, Ni, and Cr as well as the ratios FeO*/MgO and Zr/Y as parameter variables, suggests breakdown into two major subgroups (Fig. 20a). All Group 1A samples recognized by inspection of the chemical data fall in the upper cluster (Analyses 1 down to 5), while the lower cluster (Analyses 20 down to 13) is made up entirely of Group 1B samples. The classification predicted by the cluster analysis does not exactly correspond to that suggested by data inspection, since three 1B samples (Analyses 11, 14 and 15) with lower Ni and Cr contents and higher FeO*/MgO ratios (most differentiated 1B samples?) lie in the upper cluster together with the 1A samples (Analyses 1, 2, 3, 5, 6, and 8); their immediate neighbours in a less significant cluster are two 1A samples (Analyses 1 and 8) showing higher Ni and Cr contents and lower FeO*/MgO ratios (most primitive 1A samples?). Apart from these probably more differentiated 1B samples, the cluster analysis supports the chemical classification of the Group 1 mafic rocks into two subgroups.

A majority of Group 1 samples show enrichment of Na_2O with or without CaO depletion when compared with unaltered, Recent basalts from different tectonic

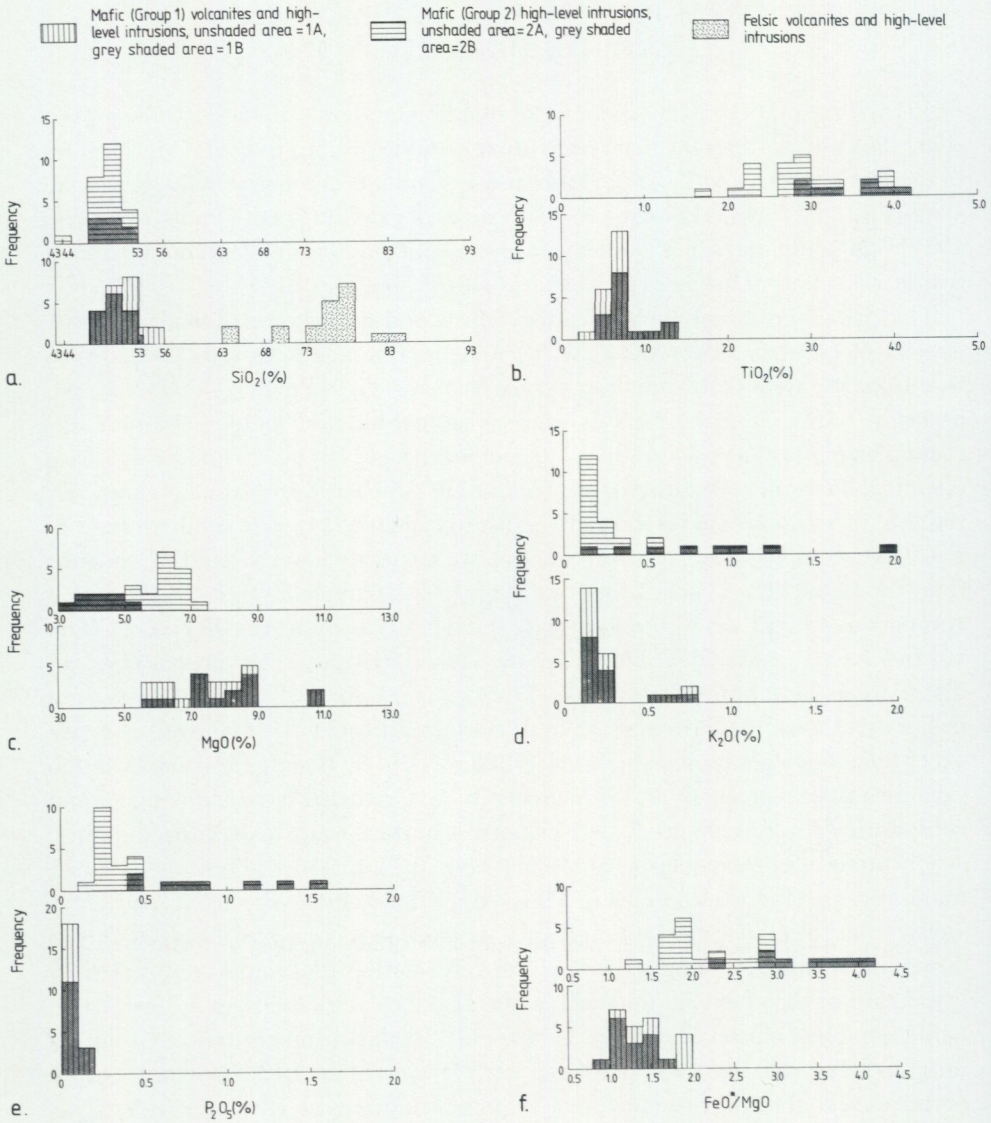

environments (Fig. 21a, b); chemically such rocks are spilites (Graham 1976). It is, however, worth emphasizing that approximately one third of the samples analyzed show more or less 'normal' Na_2O and CaO contents (LeMaitre 1976). The process or processes leading to the formation of the typical Na_2O-enriched/CaO-depleted chemistry of spilites was areally extensive but not completely pervasive.

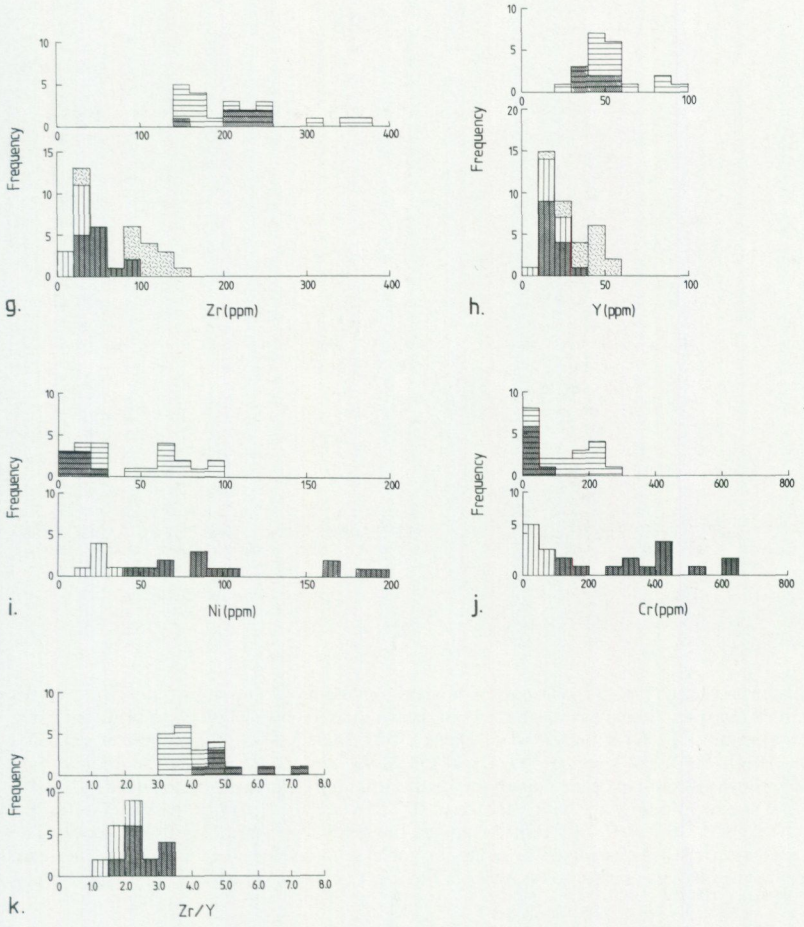

Fig. 19. (p. 40—41). Histograms indicating the distributions of SiO_2 (a), TiO_2 (b), MgO (c), K_2O (d), P_2O_5 (e), FeO*/MgO (f), Zr (g), Y (h), Ni (i), Cr (j), and Zr/Y (k) in analyzed Stekenjokk mafic volcanites and high-level intrusions. Felsic rocks are also shown on the SiO_2, Zr and Y histograms.

The late intrusive greenstones and dolerite to gabbro sheets of mafic Group 2 consist solely of basalts. Consideration of the elements Mg, P and Ni as well as the FeO*/MgO and Zr/Y ratios suggest subdivision into two subgroups (2A and 2B) which, as stated earlier, appear also to be mineralogically different. Group 2A greenstones etc. (17 analyses) with amphibole and without visible biotite or apatite show higher MgO and Ni contents, lower P_2O_5 content and lower FeO*/MgO and Zr/Y ratios than Group 2B greenstones (8 analyses— Table 2 and Fig. 19). Other points of significance include the following (see Fig. 19):

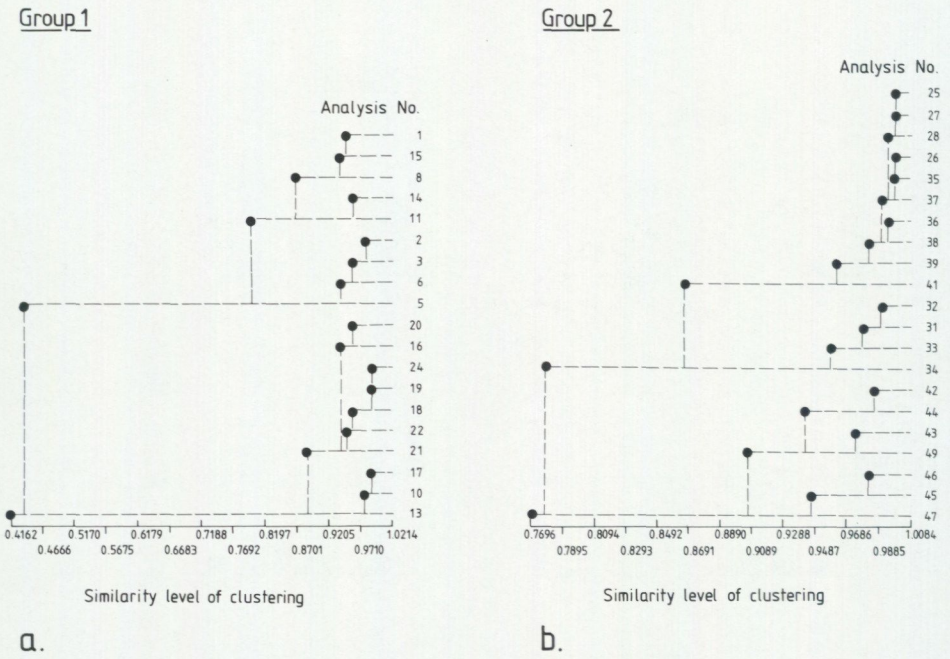

Fig. 20. Dendrograms, based on Q-mode cluster analysis, grouping Group 1 (a) and Group 2 (b) mafic rock analyses. The diagrams have been drawn directly from a computer print-out using the programme CLUSTR presented in Davis (1973, p. 467—473). 10 parameter variables (TiO_2, MgO, K_2O, P_2O_5, Zr, Y, Ni, Cr, FeO*/MgO, and Zr/Y) were employed and only samples showing complete sets of analyses for these oxides/elements were included. The data were first standardized by applying the factors 10^0, 10^{-1} (Group 1) and 10^0 (Group 2), 10^0, 10^0, 10^{-2}, 10^{-2}, 10^{-2}, 10^{-2}, 10^0, 10^0 respectively to the parameter variables listed above. The similarity matrix was constructed by using the correlation coefficient as a similarity measure between all possible pairs of samples. Analysis No. refers to the list of analyses in the Appendix.

1. K_2O values are less variable in Group 2A and lie entirely in the lower part of the range of Group 2B K_2O values, *i.e.* consistent with the occurrence of biotite in Group 2B samples;

2. TiO_2 values are less variable in Group 2B and lie in the upper part of the range of Group 2A TiO_2 values;

3. Cr *as well as Zr and Y* are less variable in Group 2B basaltic rocks and lie in the lower part of the range of Group 2A.

Application of cluster analysis to the Group 2 mafic rocks, using the same parameter variables as for the Group 1 mafic rocks, indicates breakdown into three clusters (Fig. 20b). The most distinct cluster (Analyses 42 down to 47)

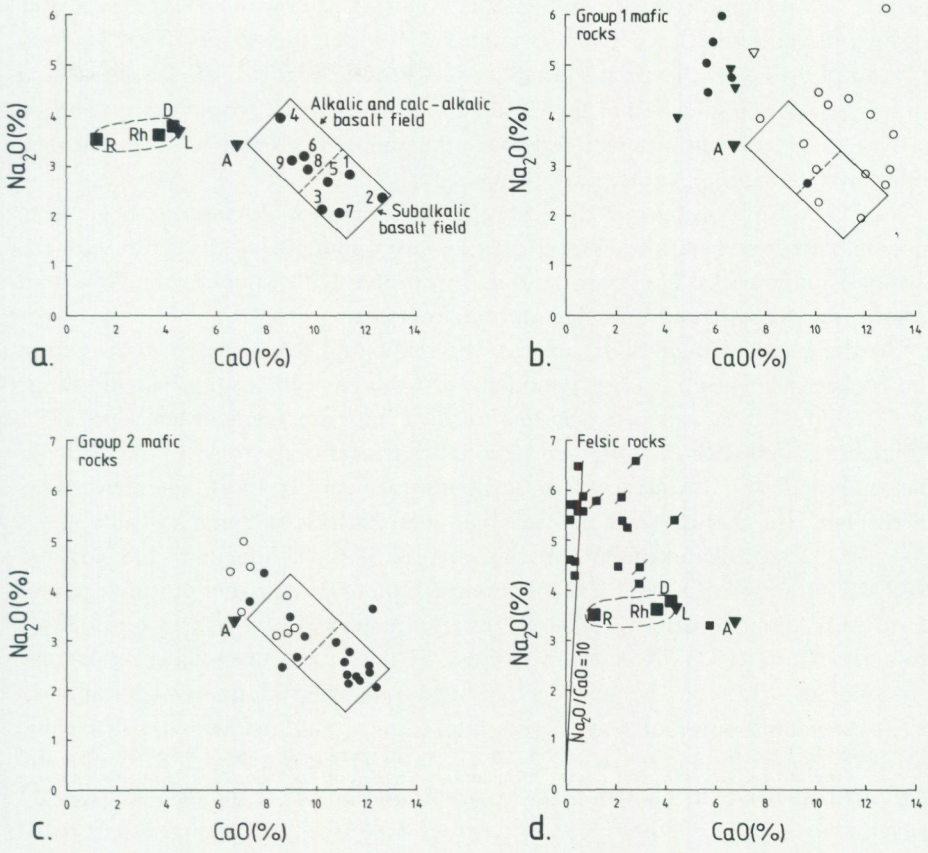

Fig. 21 Na_2O-CaO diagrams

a. Some average, 'normal' (unaltered) igneous rocks. *Basalts* (filled circles, rectangular field) - 1. Mid-ocean ridge basalt (66 analyses; Cann 1969, Engel and Engel 1970, Shido *et al.* 1971). 2. Back-arc basin basalt (11 analyses; Hawkins 1976). 3. Ocean-island tholeiite (193 analyses; MacDonald and Katsura 1964, Brooks and Jakobsson 1974). 4. Ocean-island alkalic basalt (88 analyses; MacDonald and Katsura 1964, Engel *et al.* 1965, Brooks and Jakobsson 1974). 5. Continental tholeiite (25 analyses; Waters 1961, Frey *et al.* 1978, Nielsen 1978). 6. Continental alkalic basalt (6 analyses; Frey *et al.* 1978, Nielsen 1978). 7. Island arc tholeiite (56 analyses; Stark 1963, Baker 1968, Gill 1970, Bryan *et al* 1972, Ewart *et al.* 1973, 1977). 8. Calc-alkalic basalt (75 analyses; Pearce 1976). 9. Shoshonitic basalt (21 analyses; Pearce 1976). *Intermediate rocks* (filled inverted triangles; A = Andesite, L = Latite) - Le Maitre 1976. *Felsic rocks* (filled squares, elliptical field; D = Dacite, Rh = Rhyodacite, R = Rhyolite) - Le Maitre 1976.

b. Group 1 mafic rocks (1A - filled circles = basalt, smaller filled inverted triangles = basaltic andesite; 1B - open circles = basalt, open inverted triangle = basaltic andesite). Average 'normal' basalt field and average 'normal' andesite (A) shown for comparison in Figs. 21b and c.

c. Group 2 mafic rocks (2A - filled circles = basalt; 2B - open circles = basalt).

d. Felsic rocks (filled squares = extrusive; filled squares with diagonal line = subvolcanic intrusive). Average 'normal' intermediate and felsic rocks shown for comparison.

corresponds to Group 2B recognized by inspection of the data, while the upper two clusters (Analyses 25 down to 41 and Analyses 32 down to 34) correspond to Group 2A; the middle cluster on Fig. 20b (Analyses 32 down to 34) comprises the highly differentiated (low Ni and Cr, high FeO*/MgO, high Zr and Y etc.) Group 2A samples. Thus, the cluster analysis programme confirms the chemical and mineralogical classification of the Group 2 mafic rocks into two subgroups and, at a lower level of significance, separates the more differentiated from the less differentiated samples within Group 2A.

Na_2O and CaO contents in the Group 2 greenstones etc. lie closer to the range of 'normal' unaltered basalts (Fig. 21c); they are apparently less spilitic than the Group 1 mafic rocks. However, the highly variable K_2O values in the Group 2B basaltic rocks may be a result of alteration processes.

On the basis of their SiO_2 content, the mafic and felsic compositions within the Stekenjokk volcanites are bimodally distributed, compositions in the range $56\ \% \leq SiO_2 < 63\ \%$, *i.e.* corresponding to silicic andesite, being absent (Fig. 19a). This agrees well with the observed bimodal character of the rocks in the field and the analytical data are believed to be significant in this respect. The felsic rocks themselves are characterized by variable, often high SiO_2 content (Table 2 and Fig. 19a), total alkali contents in the range 3.5—6.8% (mean = 5.6.%), and Na_2O/K_2O and Na_2O/CaO (except in one sample) ratios greater or much greater than unity; their mineralogy and chemistry are typical of a quartz keratophyre (Schermerhorn 1973). It is of importance to note that Na_2O/CaO ratios vary widely (0.6—54.0) but while the phyric-textured, volcanic quartz keratophyres occupy the full range of Na_2O/CaO ratios, the granular-textured subvolcanic intrusions lie in the lower part (1.2—8.4) of this range (see Fig. 21d). As for the mafic rocks, it would appear that the process or processes giving rise to Na_2O enrichment with or without CaO depletion was areally extensive but reached variable stages of advancement; in particular, the quartz keratophyres more confidently interpreted as magmatic (intrusive) rocks never reached the same degree of Na_2O enrichment and/or CaO depletion as the volcanites (phyric tuffs).

The mineralogical and chemical inhomogeneity within the Stekenjokk volcanites is apparently not related systematically to either tectonic units or particular centres. Indeed, the area Björkvattnet, which has been more intensively studied as it appears to represent closer proximity to one volcanic centre, contains the whole range of compositional and textural types, mafic (1A, 1B, 2A and 2B) and felsic as well as volcanic and high-level intrusive.

MAFIC ROCKS

ALTERATION PROCESSES, ELEMENT MOBILITY AND PRINCIPLES OF GEOCHEMICAL STUDY

Since the mafic Stekenjokk volcanites are thought to be, at least in part, pyroclastic and to have been deposited under submarine conditions, it is apparent that their original chemistry would have been highly susceptible to various types of alteration processes, even prior to the effects of the Silurian deformation and low-grade regional metamorphism. From the studies of mainly Recent basalts on or beneath the sea-floor, the following processes are relevant:

1. Low-temperature (<25°C) sea-floor weathering (Hart 1969, 1971; Hart 1970; Cann 1971; Hekinian 1971; Matthews 1971; Thompson 1973; Hart *et al.* 1974; Aumento *et al.* 1976).
2. Higher temperature, sub-greenschist to greenschist (spilitization) or even amphibolite facies sub-sea-floor metamorphism involving replacement reactions without significant textural modification and thought to occur after deposition, extrusion or emplacement (Vallance 1965, 1969, 1974; Melson and van Andel 1966; Smith 1968; Cann 1969; Miyashiro *et al.* 1971; Spooner and Fyfe 1973; Loeschke 1976; Vallier and Batiza 1978).

Smith (1968), after a detailed study of spilites in an Ordovician marine sequence from New South Wales, Australia, invoked conditions of deep burial (P_{load}>2 kb) as a means of providing the temperatures necessary for the replacement reactions to proceed at an appreciable rate. More recently, several authors (Spooner *et al.* 1974; Bonatti *et al.* 1975; Stern *et al.* 1976; Spooner *et al.* 1977) have proposed models explaining sub-sea-floor metamorphism in terms of water-rock interaction during hydrothermal convection of heated sea-water, the convective cells being driven by heat from igneous intrusions at depth; in such models, alteration occurred in high heat-flow regimes under relatively shallow burial conditions (P_{load}<1.5 kb). A recent Sr-isotope study of the Troodos ophiolitic rocks (Spooner *et al.* 1977) confirms the hypothesis that sea-water was involved in the replacement reactions, requires interaction of rock with large volumes of water and shows that mass transfer through the rock pile occurred in a flow system. A fully referenced summary of ideas pertaining to the genesis of spilite and emphasizing alternative "deuteric" and, in particular, "primary" viewpoints is given by Amstutz (1968).

The extent of metasomatism in the whole rock pile during sub-sea-floor metamorphism (spilitization) has provoked considerable discussion. Vallance (1969) indicated that sampling bias against monomineralic Ca-rich veins and pods often

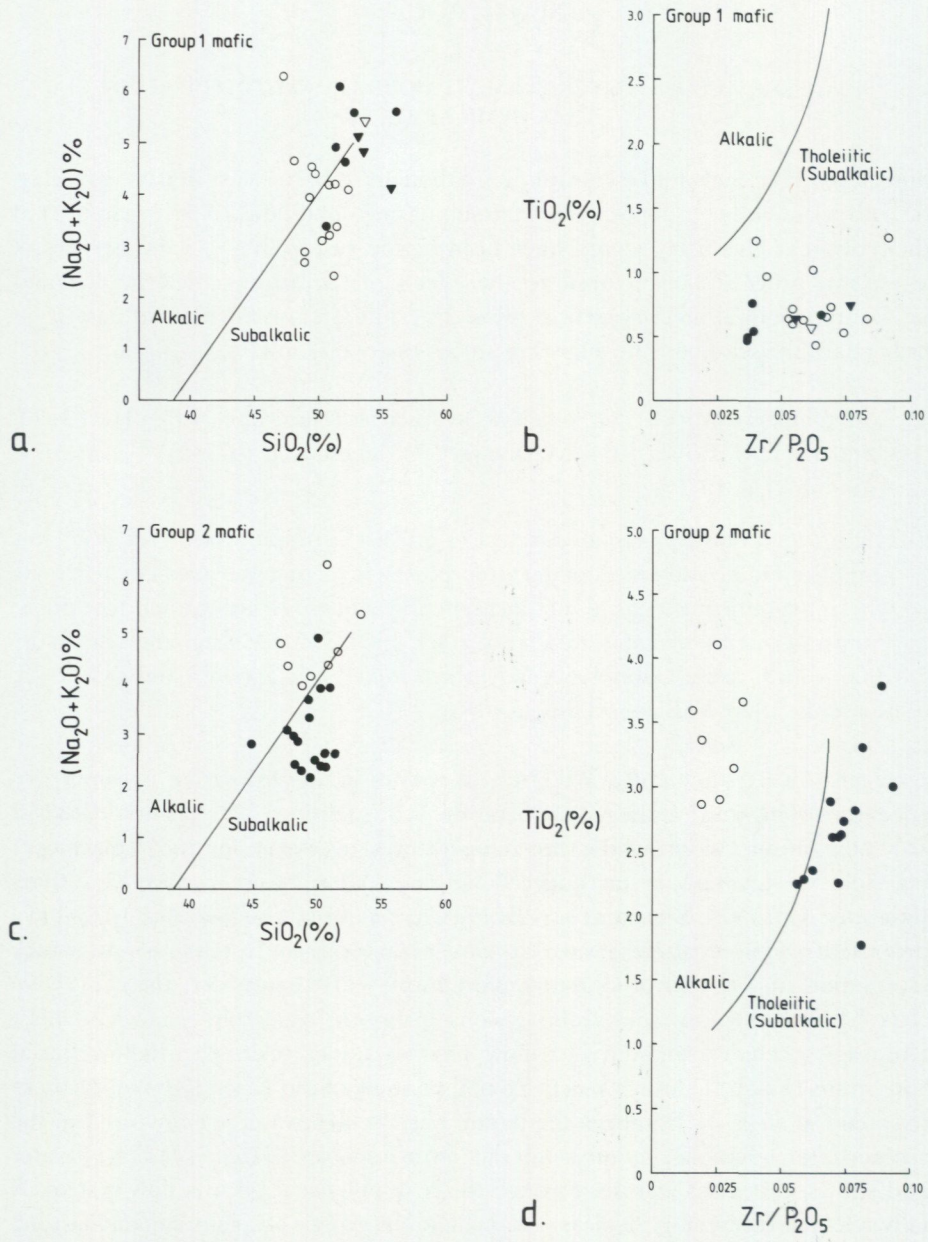

Fig. 22. Assessment of alkalinity in the Stekenjokk mafic volcanites and high-level intrusive rocks. Total alkalis *versus* silica diagram after MacDonald and Katsura (1964); TiO_2 *versus* Zr/P_2O_5 diagram after Floyd and Winchester (1975) and Winchester and Floyd (1976). a, b = Group 1 mafic rocks. 1A - filled circles = basalt, filled inverted triangles = basaltic andesite; 1B - open circles = basalt, open inverted triangle = basaltic andesite. c, d = Group 2 mafic rocks. 2A - filled circles = basalt; 2B - open circles = basalt.

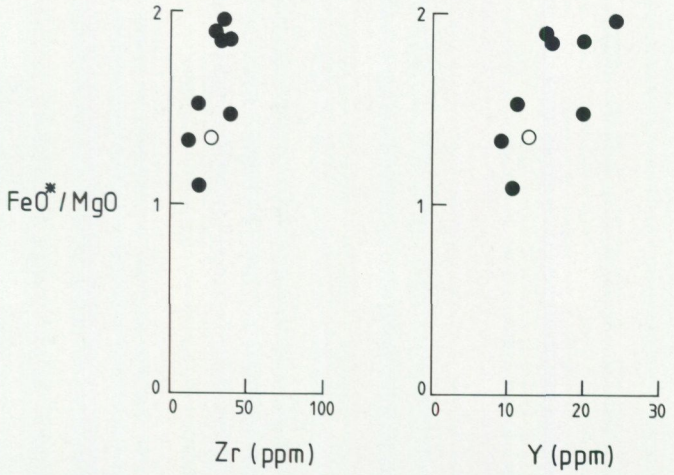

Fig. 23. Variation of FeO*/MgO ratio with the supposedly less mobile elements Zr and Y (Group 1A mafic rocks). Filled circles = more spilitic basalt and basaltic andesite; open circle = less spilitic basalt (see Fig. 21b).

associated with spilitic basalts may lead to erroneous conclusions concerning addition or subtraction of elements to the whole rock pile, when spilitic basalt is compared with unaltered basalt. However, various authors (Cann 1969; Spooner *et al.* 1977; Vallier and Batiza 1978; Stephens 1980b) have demonstrated addition and/or loss of material to the rock pile during spilitization.

Element mobility during deformation and low-grade regional metamorphism may well be restricted to oxidation, hydration and carbonation processes and small-scale transport of material (recrystallization and nucleation and growth of new grains). However, the occurrence of syntectonic veins (mainly syn-S_1) and variably differentiated crenulation cleavages (particularly S_2, S_3) in the Stekenjokk volcanites are indicative of extensive — at least on the largest mesoscopic fold scale — element mobility during deformation. In this regard, Elliott (1973) and Field and Elliott (1974) have suggested that quite significant changes in chemistry occur during the deformation and retrogressive metamorphism of gabbro to amphibolite. Furthermore, work on the syn-deformation, low-grade metamorphism of mafic rocks (Kerrich *et al.* 1977) as well as greywackes (Williams 1972; Beach 1974; Gray 1977; Stephens *et al.* 1979) suggests that many elements are particularly mobile along discrete zones (*e.g.* shear zones, limb areas of small-scale folds developing into differentiated crenulation cleavage), much of the material lost from the system being deposited in syntectonic veins and/or fold hinges.

Careful avoidance of areas showing abundant folding, metamorphic differentiation or veining should restrict the effects of alteration in the Stekenjokk volcanites

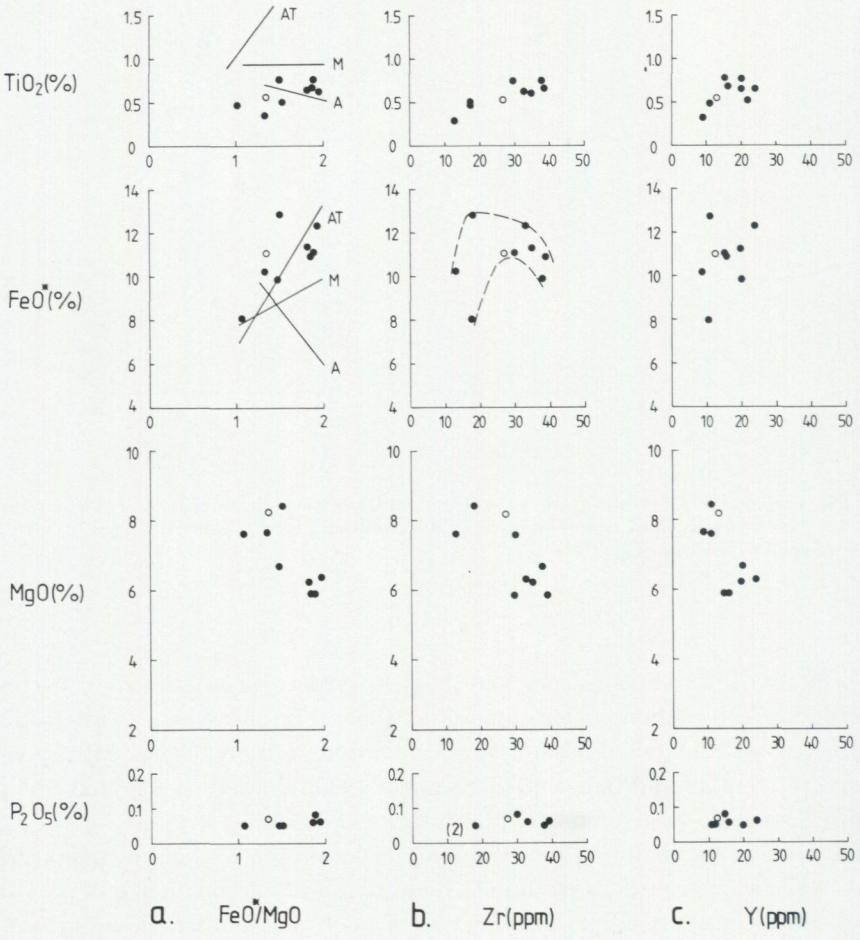

to either sea-floor weathering and/or sub-sea-floor metamorphism. As indicated earlier, many samples show significant enrichment in Na_2O, often accompanied by depletion in CaO. Furthermore, the epidotite (±calcite) nodules present in these rocks attest to considerable, pre-deformation redistribution of elements, including in particular Ca, under sub-greenschist or greenschist facies conditions. These points suggest that sub-sea-floor metamorphism (spilitization) was the more important alteration process in the Stekenjokk volcanites.

From the studies on spilitization processes cited above, it is apparent that the major elements Si, Al, Ca, Na, and K and the trace elements Rb, Ba and Sr are particularly susceptible to migration during sub-sea-floor metamorphism (spilitization). Furthermore, assuming little or no volume change, petrological conclu-

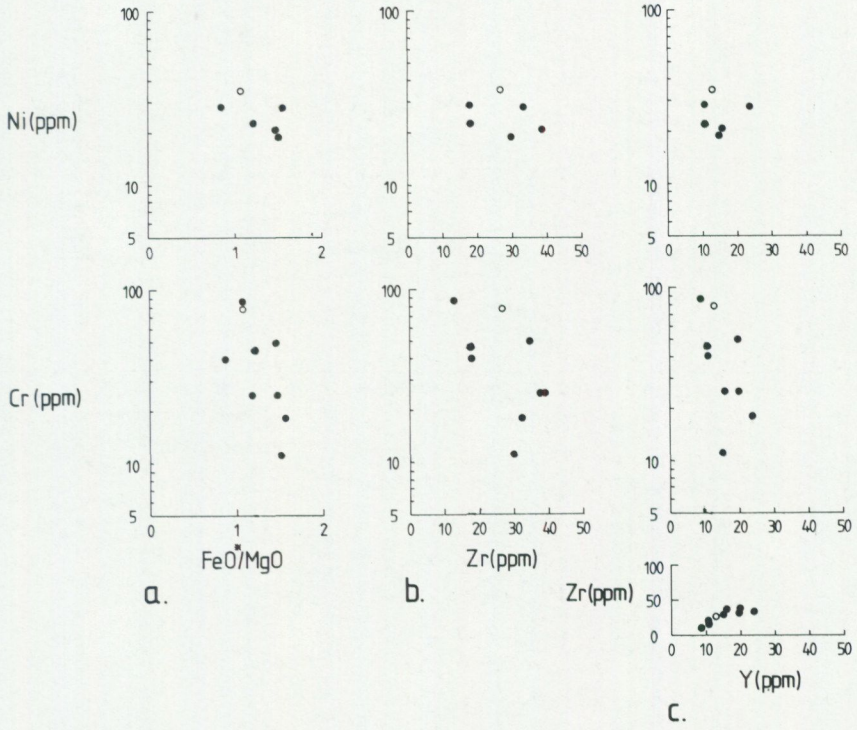

Fig. 24. (p. 48—49). Variation of the elements Ti (as TiO_2), total Fe (as FeO*), Mg (as MgO), P (as P_2O_5), Ni, and Cr with increasing FeO*/MgO (a), Zr (b) and Y (c) for the Group 1A mafic rocks. Zr variation with increasing Y is also shown under (c).
Calc-alkalic, mildly tholeiitic and tholeiitic reference trends from Amagi Volcano (Japan) (A), Macauley Island (Kermadec Island Group) (M) and abyssal tholeiites (AT) respectively are indicated on the TiO_2 and FeO* *versus* FeO*/MgO diagrams (from Miyashiro 1975). Filled circles = more spilitic basalt and basaltic andesite; open circle = less spilitic basalt (see Fig. 21b).

sions based on the major and minor elements Ti, total Fe, Mg, P as well as the trace elements Zr, Y, Nb, Cr, Ni should be more valid than those based on the more obviously mobile components cited above. Recent studies (for example, Pearce and Cann 1971, 1973; Pearce 1975; Floyd and Winchester 1975; Winchester and Floyd 1976) have made use of the supposed relative immobility of the elements Ti, P, Zr, Y, Nb, and Cr for classifying altered and metamorphosed mafic igneous rocks and discriminating the tectonic environments to which they are related. A study of the chemical changes occurring during spilitization of the Group 1B Stekenjokk mafic rocks (Stephens 1980b) suggests conservation of Si, Ti, Al, total Fe, P, and Y, small loss of Mg, Ca, Zr, and Ni and more significant loss of K and Cr.

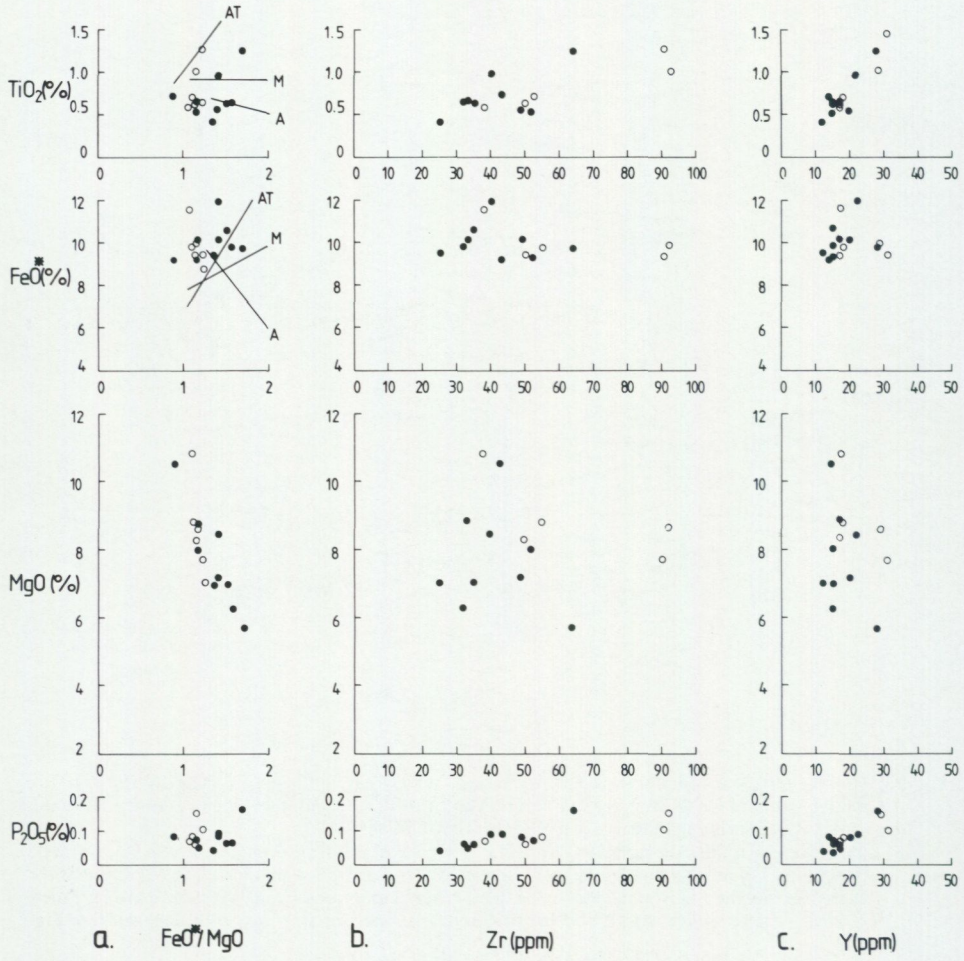

In the geochemical study of the Stekenjokk volcanites presented here, emphasis is, thus, placed on the supposedly less mobile elements Ti, total Fe, Mg, P, Zr, Y, Cr, and Ni, special care being taken with Mg, Zr, Ni, and especially Cr in the Group 1B rocks. Conclusions based on the conventional total alkalis *versus* silica (MacDonald and Katsura 1964) and AFM diagrams are viewed critically, while normative classifications (see, for example, Irvine and Baragar 1971) are avoided.

RECOGNITION OF VOLCANIC (IGNEOUS) ROCK SERIES

Although the Group 1 volcanites and high-level intrusive rocks spread over the dividing line between the fields of alkalic and nonalkalic (subalkalic) rock series

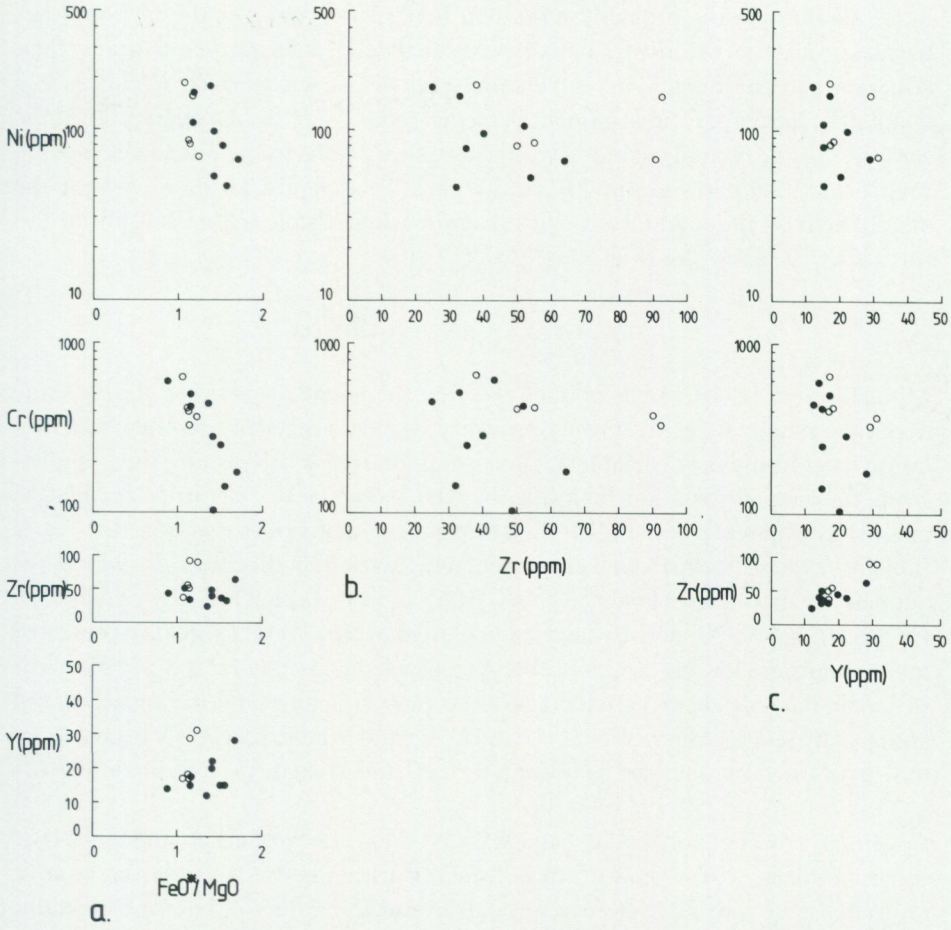

Fig. 25. (p. 50—51). Variation of the elements Ti (as TiO_2), total Fe (as FeO*), Mg (as MgO), P (as P_2O_5), Ni, Cr, Zr, and Y with increasing FeO*/MgO (a), Zr (b) and Y (c) for the Group 1B mafic rocks. Trends on TiO_2 and FeO* *versus* FeO*/MgO diagrams as for Fig. 24. Filled circles = more spilitic basalt; open circles = less spilitic basalt (see Fig. 21b and Stephens 1980b).

(Miyashiro 1975) on the total alkalis-silica diagram (Fig. 22a), this is dictated by their variably spilitic nature. Using the supposedly less mobile elements Ti, P and Zr, it is clear that all samples analyzed for these elements, even the spilitic samples showing apparent alkalic tendencies in Figure 22a, lie in the nonalkalic (subalkalic) field of Figure 22b.

The Group 2 basaltic intrusions likewise spread over the dividing line on the total alkalis-silica diagram (Fig. 22c). However, since these rocks are apparently less spilitic, the pattern of dominating nonalkalic (subalkalic) and subordinate

more alkalic types is probably more real here. All except 2 of the 17 Group 2A basaltic rocks lie within the nonalkalic (subalkalic) field on this diagram; their adherence to the nonalkalic (subalkalic) rock series is confirmed in Figure 22d using the supposedly less mobile elements (only 1 of the 2 apparently alkalic samples has been analyzed for Zr; this sample also falls in the nonalkalic field on Figure 22d). All of the Group 2B basaltic rocks lie along the dividing line or in the alkalic field on the total alkalis-silica diagram; their alkalic nature is confirmed in the TiO_2-Zr/P_2O_5 plot (Fig. 22d).

CHEMICAL VARIATION TRENDS

Miyashiro (1974, 1975) has pointed out that the boundary between the tholeiitic and calc-alkalic series is entirely arbitrary as they represent end-members in a family of continuously variable magma evolution trends. Miyashiro, thus, emphasized the use of variation diagrams in which certain key elements are plotted against a differentiation index (FeO*/MgO) to distinguish varying degrees of tholeiitic versus calc-alkalic characteristics. Variation diagrams in which the supposedly more inert elements Ti (as TiO_2), total Fe (as FeO*), Mg (as MgO), P (as P_2O_5), Zr, Y, Ni, and Cr have been plotted against FeO*/MgO are presented for each group (1A, 1B, 2A, and 2B). As a check on possible Fe and Mg mobility, in particular, all elements have also been plotted against the incompatible and supposedly less mobile elements, Zr and Y. Zr and Y have previously been used as indices of fractionation (see, for example, Sceal and Weaver 1971; Graham 1976).

Group 1A — The nonalkalic (subalkalic) Group 1A volcanites and high-level intrusive rocks, which show a range in SiO_2 contents between basalt and basaltic andesite, have low TiO_2 contents (<0.8%) and low values of both incompatible (Zr<40 ppm, Y<25 ppm) as well as compatible elements (Ni<40 ppm, Cr<90 ppm); MgO values vary between 5.9 and 8.5%. The probably inert behaviour of the fractionation index FeO*/MgO is supported from Figure 23 which indicates that the ratio FeO*/MgO increases regularly with increasing Zr and Y contents.

TiO_2 and P_2O_5 show positive to flat trends on all types of variation diagram (Figs. 24a—c). FeO* appears to increase with increasing FeO*/MgO but possibly rises, reaches a peak and then falls off with respect to Zr (Figs. 24a, b). In contrast to these elements negative trends are apparent on MgO and Cr diagrams (Figs. 24 a—c). Finally, a flattening-off of Zr values with increasing Y is apparent (Fig. 24 c). As far as the elements cited above are concerned, the one apparently non-spilitic sample (see Fig. 21b) behaves in the same way as the spilitic samples.

The trends indicated are continuous and consistent with one another and are interpreted as a result of fractional crystallization. In particular, a mildly tholeiitic differentiation trend is inferred from the TiO_2 and FeO* variation diagrams (compare Miyashiro 1975). An important point is that even the least fractionated

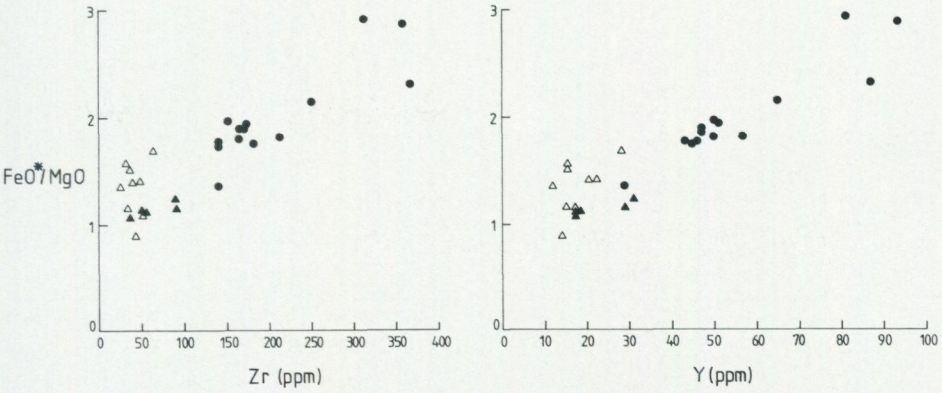

Fig. 26. Variation of FeO*/MgO ratio with the supposedly less mobile elements Zr and Y for mafic rock Groups 1B and 2A. Open triangles = more spilitic 1B basalt, filled triangles = less spilitic 1B basalt, filled circles = 2A basalt.

of the samples here, all of which represent magmas which reached or nearly reached the earth's surface, have undergone extensive fractionation at depth. This is indicated by the consistently low Ni, Cr and to a less extent MgO contents. Thompson *et al.* (1972) have suggested that Ni and Cr decrease rapidly in basaltic rocks where fractionation of olivine has been important; Cr-spinel and possibly pyroxene need also to be considered. After initial concentration in the liquid, TiO_2, P_2O_5 and probably FeO* were depleted due to fractionation of the appropriate phases, possibly amphibole, ilmenite and/or magnetite (see also Miyashiro and Shido 1975) and apatite. Mild fractionation of a Zr-bearing phase is suggested as Zr values appear to flatten off, while Y remained truly incompatible.

Group 1B — The nonalkalic (subalkalic) Group 1B volcanites and high-level intrusive rocks, all except one sample (SiO_2 = 53.5%) lying in the basalt range of SiO_2 values, have low to moderate TiO_2 contents (0.54—1.28%), low to moderate values of incompatible elements (Zr = 25—93 ppm, Y = 12—31 ppm) and often high contents of MgO (5.7—10.9%), Ni (47—190 ppm), and Cr (101—644 ppm).

Comparison of the chemistries of the average more and less spilitic Group 1B samples (Stephens 1980b) indicates that the supposedly more inert elements Mg, Zr, Ni, and, in particular, Cr were not conserved during the spilitization process; apparent loss of these elements is indicated. Thus, the distributions on the various FeO*/MgO variation diagrams can be expected to be significantly influenced by element mobility.

Scattered distribution patterns, thought to be dictated by Mg mobility, occur in those diagrams involving a conserved element (*e.g.* Ti, total Fe, P, Y) and the differentiation index FeO*/MgO (Fig. 25a). More ordered distributions for the conserved elements Ti and P are apparent on the Y (and Zr) variation diagram

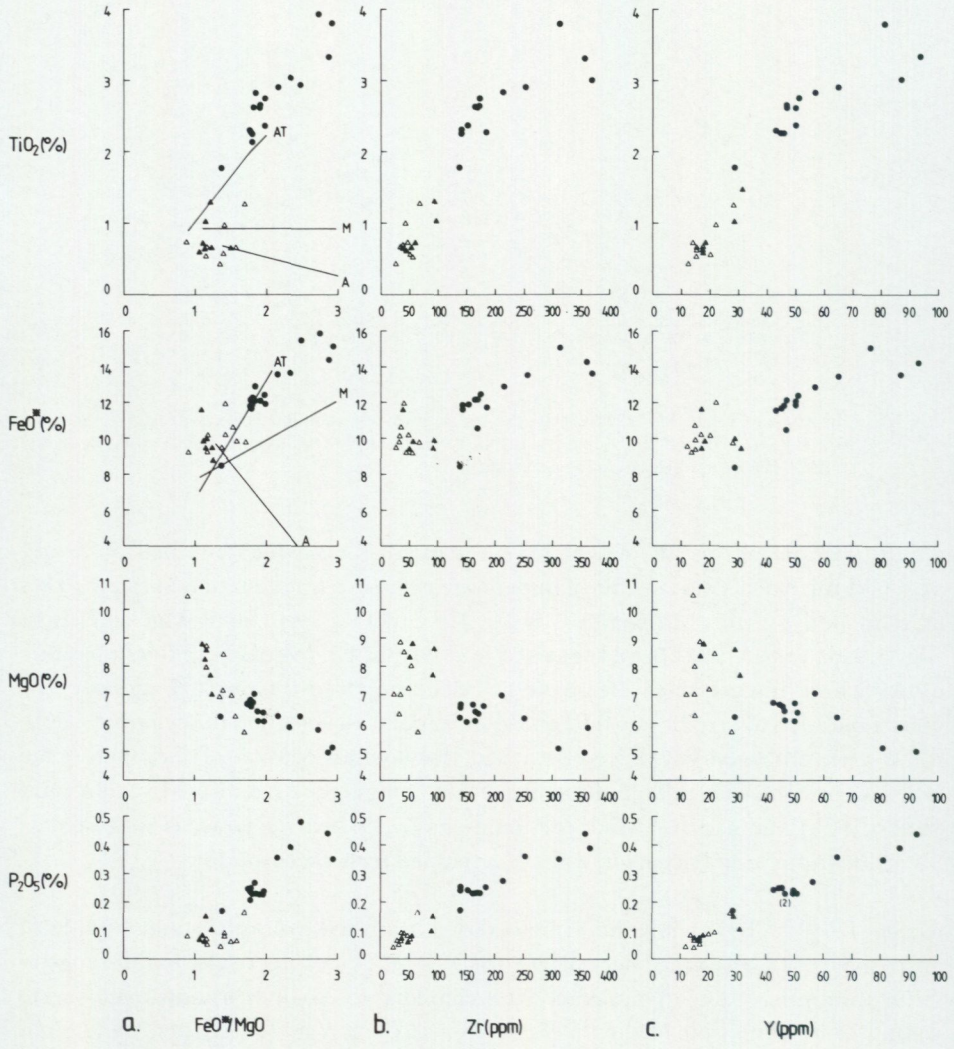

(Figs. 25c and b), where both TiO_2 and P_2O_5 appear to increase with increasing Y (and Zr). FeO* appears to remain fairly steady over the whole range of Zr values (Fig. 25b), while no clear trend emerges from the Y diagram (Fig. 25c). MgO, Ni and Cr show apparently well-defined negative trends on FeO*/MgO variation diagrams (Fig. 25a), while more scattered distributions dominate when these elements are plotted against the conserved element Y (and Zr), (Figs. 25c and b). Such contrasting behaviour is interpreted as being due to significant Mg, Ni and Cr mobility. Less spilitic samples on MgO, Ni and Cr *versus* Y (and Zr) variation diagrams tentatively suggest negative trends for these three elements. It is note-

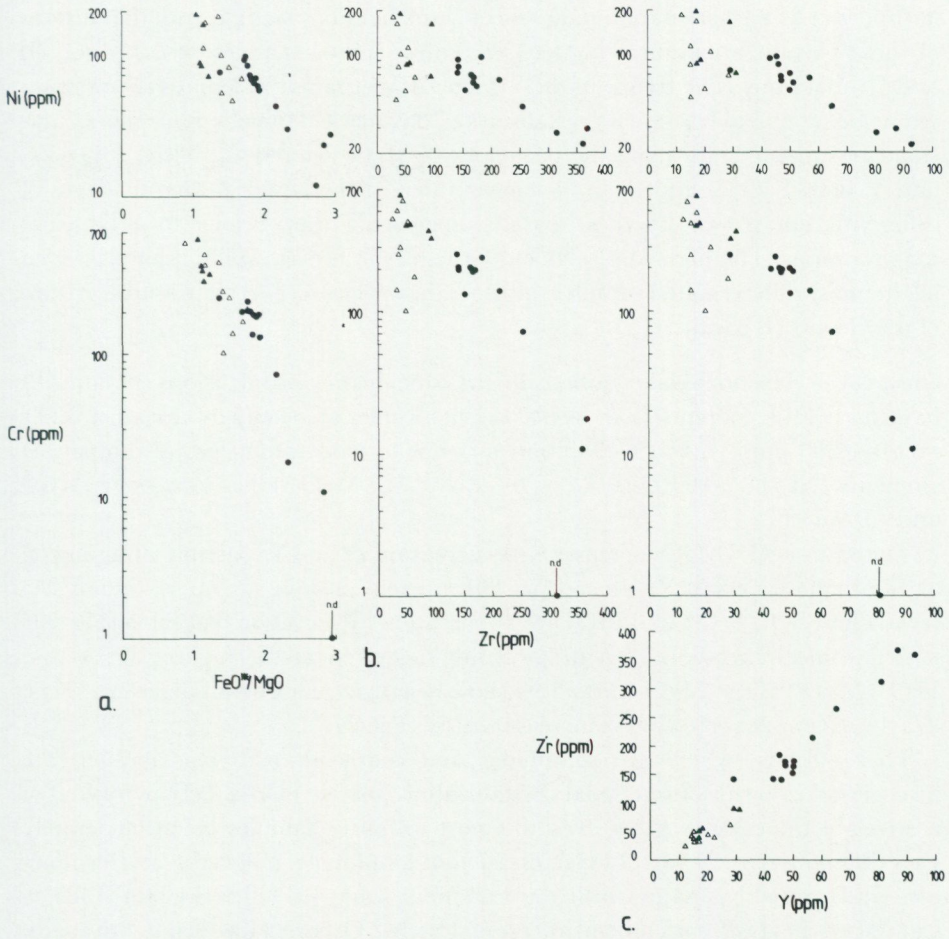

Fig. 27. (p. 54—55). Variation of the elements Ti (as TiO_2), total Fe (as FeO*), Mg (as MgO), P (as P_2O_5), Ni, and Cr with increasing FeO*/MgO (a), Zr (b) and Y (c) for mafic rock Groups 1B and 2A. Zr variation with increasing Y is also shown under (c). Trends on TiO_2 and FeO* *versus* FeO*/MgO diagrams as for Fig. 24. n.d. = not detected during analysis. Open triangles = more spilitic 1B basalt, filled triangles = less spilitic 1B basalt, filled circles = 2A basalt.

worthy that Zr and Y rise steadily with one another in a tight, 'well-behaved' manner, less spilitic and more spilitic samples deviating little from one another (Fig. 25c).

FeO*/MgO variation diagrams are difficult to interpret for the Group 1B basalts due to mobility of Mg (loss), leading to too high FeO*/MgO values, as well as mobility (loss) of Cr and to a less extent Ni; scattered distribution patterns and apparent fractionation trends result. However, use of the more inert element

Y (and Zr) as a fractionation index sheds some light on the differentiation history of these basalts, attention being focused on less spilitic samples on the MgO, Ni and Cr diagrams. The trends in the Y (and Zr) diagrams are tentatively interpreted as being due to fractional crystallization, olivine+Cr-spinel±pyroxene separation presumably controlling the behaviour of MgO, Ni and Cr. TiO_2, P_2O_5, Zr, and Y (and FeO*?) appear to be concentrated in the liquid during all stages of differentiation shown by these basalts, suggesting they belong to a tholeiitic magma series. The high MgO, Ni and Cr values in the less spilitic samples, even in the most differentiated samples, indicate, however, the overall primitive nature of the Group 1B basalts.

Group 2A — The nonalkalic (subalkalic) basaltic, high-level intrusions (Group 2A) have high TiO_2 contents (1.79—3.92%), high values of incompatible elements (Zr = 140—368 ppm, Y = 29—93 ppm) and low to moderate values of compatible elements (Ni = 12—93 ppm, Cr = 0—257 ppm); MgO values vary between 5.0 and 7.0 %.

The ratio FeO*/MgO increases with increasing Zr and Y, possibly dropping off at the highest Zr and Y values (Fig. 26). Steeply positive (compare Group 1A) trends for TiO_2, FeO* and P_2O_5 are apparent on all variation diagrams (Figs. 27 a—c); some indications of a drop-off are suggested at the highest Zr, Y and FeO*/MgO values. MgO, Cr and Ni show negative trends on all diagrams (Figs. 27a—c). Zr appears to always increase with Y (Fig. 27c).

These trends, which are continuous and consistent with one another, are interpreted in terms of fractional crystallization (olivine+Cr-spinel±pyroxene) of a strongly tholeiitic magma, even the most primitive samples being moderately well differentiated. Delay of crystallization of amphibole, magnetite and/or ilmenite and probably apatite until the very final stages of differentiation leads to significant Fe-Ti-P enrichment in residual melts. Osborn (1962) and Miyashiro (1974) have indicated cooling and crystallization under conditions of relatively low f_{O_2} for such melts. Zr and Y remained truly incompatible. A final point is the rather low Al_2O_3 content (13.2—15.7%), possibly suggesting significant plagioclase separation.

Group 2B — The Group 2B, mildly alkali basaltic, high-level intrusions show high TiO_2 values (2.88—4.11%), high values of incompatible elements (Zr = 153—252 ppm, Y = 33—56 ppm) and low MgO (3.4—5.4%), Ni (<25 ppm) and Cr (<90 ppm) values; as indicated earlier, they also show high P_2O_5 content (0.45—1.54%) and occasionally high K_2O content (0.1—1.9%).

FeO*/MgO appears to increase rapidly with increasing Zr and probably also Y (Fig. 28), all three parameters being of potential use as fractionation indices. TiO_2 appears to firstly increase with increasing FeO*/MgO but a negative trend rapidly takes over (Fig. 29a); distribution patterns are more scattered on TiO_2 *versus* Zr

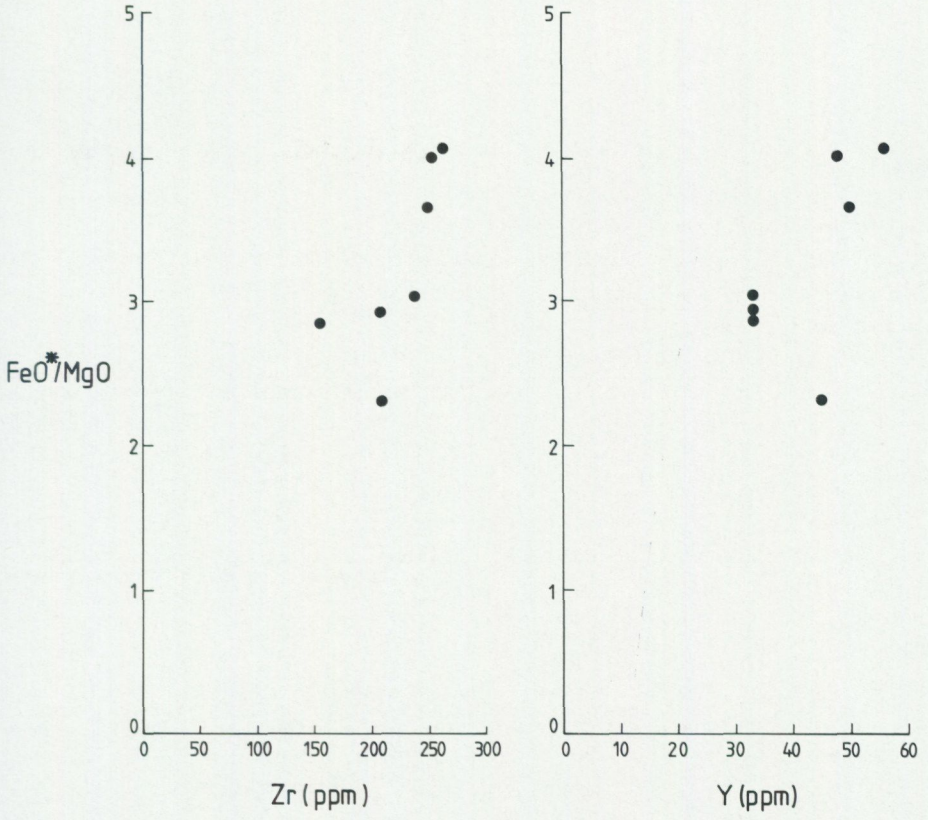

Fig. 28. Variation of FeO*/MgO with the supposedly less mobile elements Zr and Y (Group 2B mafic rocks).

and Y variation diagrams but a negative trend is suggested in Figure 29c. FeO* shows a positive to flat trend on FeO*/MgO and Y diagrams (Figs. 29a and c), while positive trends for P_2O_5 are clear from Figures 29b and c. Negative trends are indicated on all MgO diagrams (Figs. 29a—c). A somewhat scattered positive trend is apparent on the Zr—Y diagram (Fig. 29c).

Absolute MgO, Ni and Cr values indicate that the Group 2B mildly alkali basaltic rocks are highly differentiated. It is suggested that they are derived from a melt that had already undergone extensive olivine+Cr-spinel±pyroxene crystallization at depth. The trends indicated above suggest that fractionation of a Ti-rich phase and concentration of P_2O_5, Zr, Y, and to a less extent FeO* in residual melts are also important characteristics of these basalts. As for Group 2A, the rather low Al_2O_3 values (12.8—15.9%) may well be indicating significant plagioclase removal.

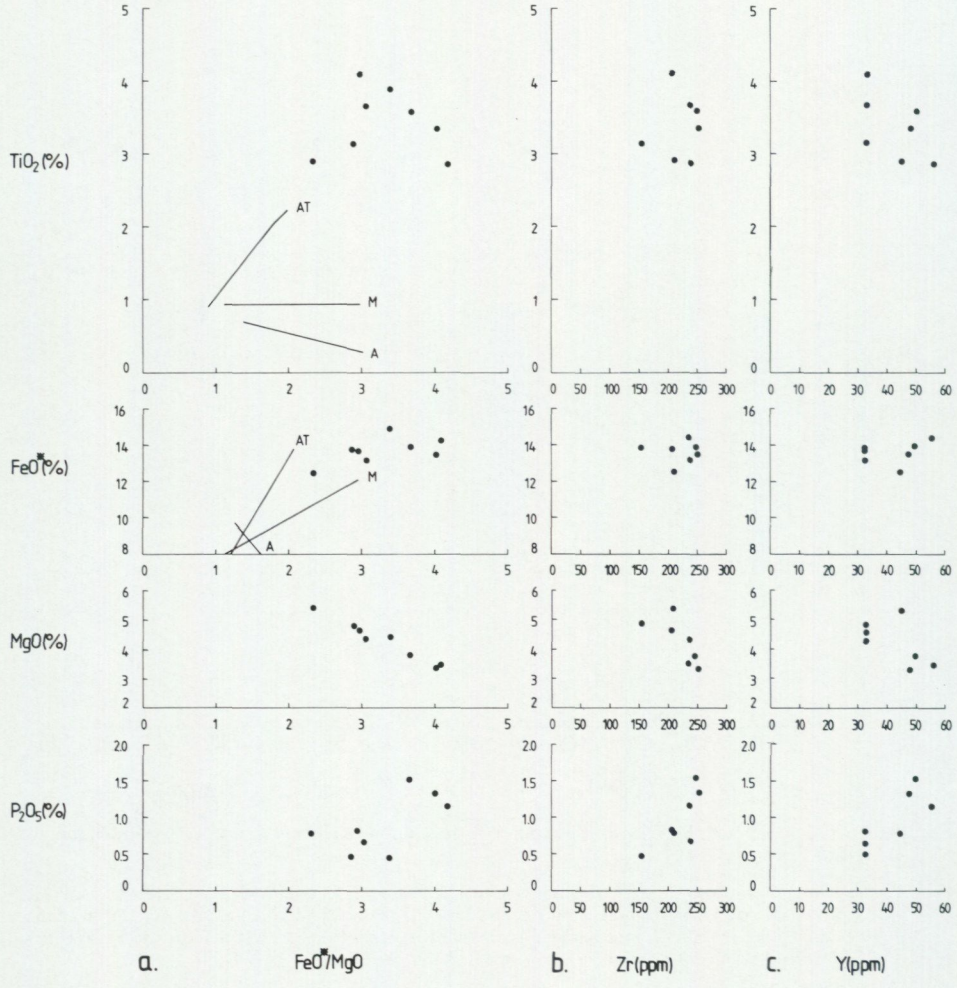

Two points deserve emphasis when comparing Group 2A and 2B chemistries:

1. At comparable FeO*/MgO ratios, Zr and Y values are lower in Group 2B, *even though MgO and Ni values are also lower*; however, the steeper trends on the FeO*/MgO *versus* Zr and Y diagrams (Fig. 28, compare with Fig. 26) suggest that the Zr and Y contents of more parental magmas may well have been higher in the Group 2B alkali basaltic rocks.

2. The Group 2B rocks are enriched in P_2O_5 and K_2O compared with Group 2A.

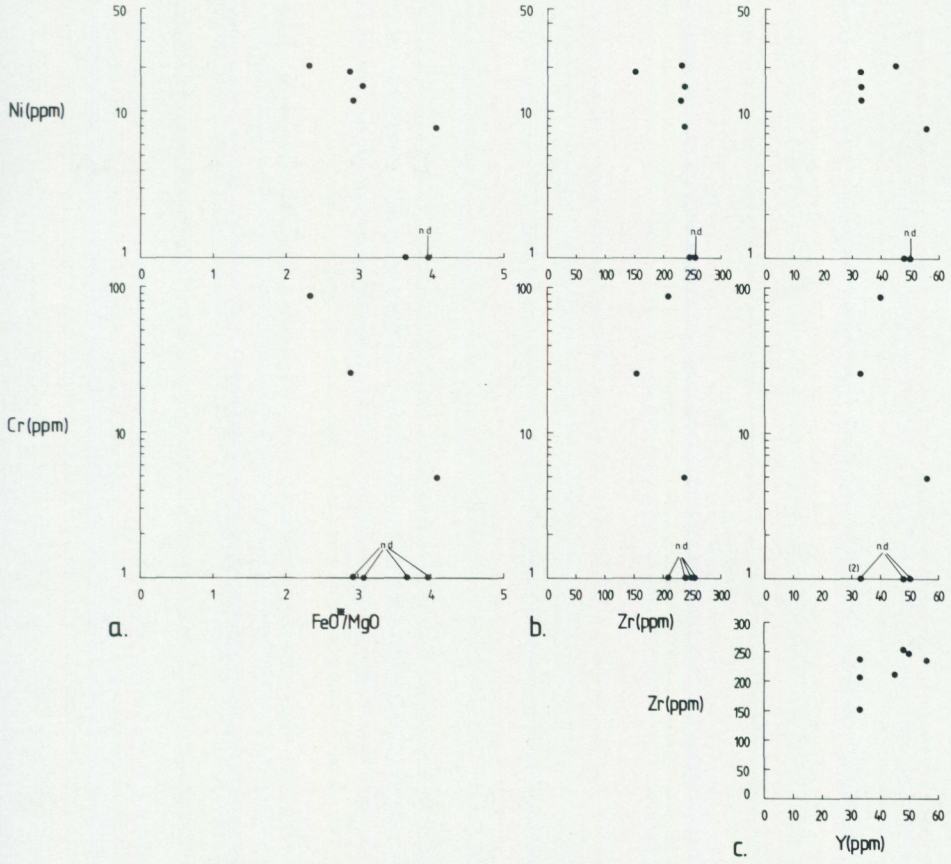

Fig. 29. (p. 58—59). Variation of the elements Ti (as TiO_2), total Fe (as FeO*), Mg (as MgO), P (as P_2O_5), Ni, and Cr with increasing FeO*/MgO (a), Zr (b) and Y (c) for the Group 2B mafic rocks. Zr variation with increasing Y is also shown under (c). Trends on TiO_2 and FeO* *versus* FeO*/MgO diagrams as for Fig. 24. n.d. = not detected during analysis.

APPLICATION OF AFM-DIAGRAM TO VARIABLY ALTERED MAFIC ROCKS

The bulk of the Group 1A rocks are enriched in Na_2O relative to normal unaltered basalts, while many of the Group 1B basalts appear to have undergone both Na_2O addition and MgO depletion during early sub-sea-floor metamorphism (spilitization). These changes would, in the first case, displace points towards the total alkali apex on the AFM-diagram such that the F/M ratio remains the same and, in the second case, move points so that the F-value remains constant, assuming that the change in MgO balances that in Na_2O. In both cases a shift into the calc-alkali field (Irvine and Baragar 1971) would result (see also MacGeehan 1978).

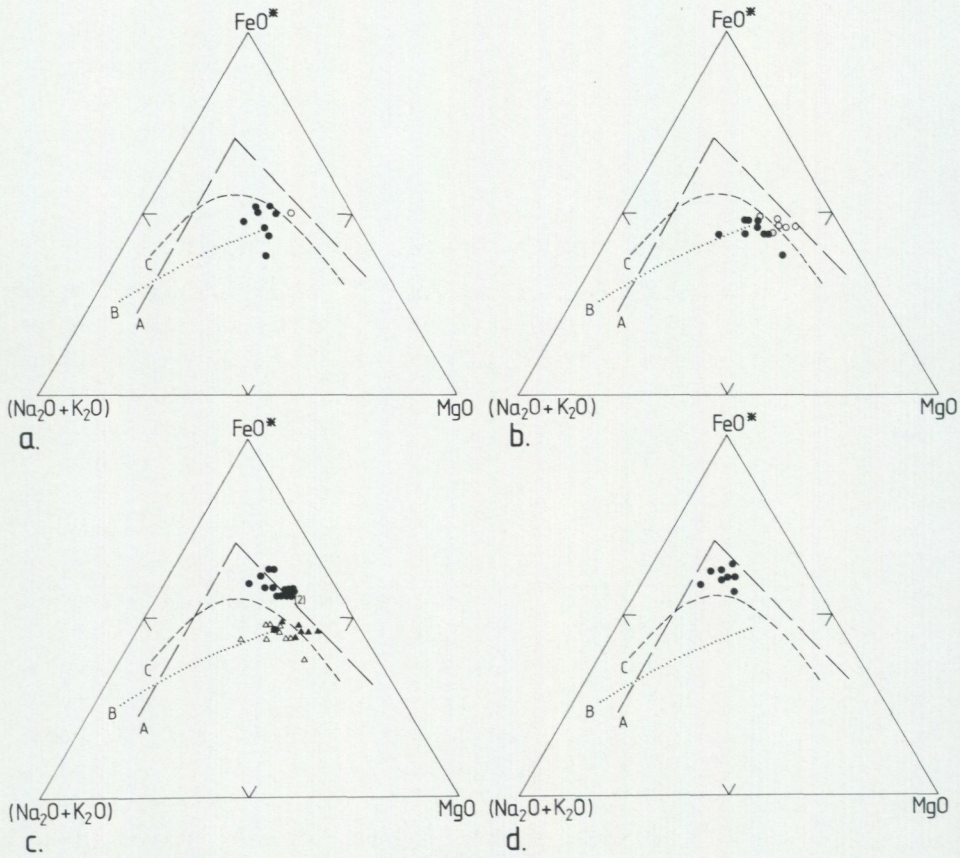

Fig. 30. A (Na_2O+K_2O) — F (FeO*) — M (MgO) diagrams. a. Group 1A mafic rocks. Filled circles = more spilitic basalt and basaltic andesite; open circle = less spilitic basalt. b. Group 1B mafic rocks. Filled circles = more spilitic basalt; open circles = less spilitic basalt. c. Mafic Groups 1B and 2A. Open triangles = more spilitic 1B basalt, filled triangles = less spilitic 1B basalt, filled circles = 2A basalt. d. Group 2B mafic rocks.
The trends shown represent Hawaiian tholeiitic suite, A, (from MacDonald and Katsura 1964), Cascades calc-alkalic suite, B, (from Graham 1976) and Irvine and Baragar's (1971) dividing line, C, between tholeiitic (above line) and calc-alkalic (beneath line) fields.

The Group 1 data, when plotted on an AFM-diagram (Figs. 30a, b), follow this predicted pattern. All Group 1A rocks, except the one non-spilitic sample, lie along Irvine and Baragar's dividing line or within their calc-alkali field. The Group 1B basalts lie along an elongate trend parallel to the AM base line; more spilitic samples lie in the calc-alkali field, while the less spilitic samples lie closer to the dividing line or within the tholeiite field. Thus, spilitization gives rise to *apparent* calc-alkalic characteristics on the AFM-diagram and obscures the tholeiitic nature of the Group 1 basalts suggested on the basis of the data discussed in the preceding section.

An AFM plot for the Group 2 basaltic high-level intrusive rocks (Figs. 30c, d), which are apparently less altered than the Group 1 mafic rocks, illustrates the strong Fe-enrichment within the suite and a firm commitment of the nonalkalic (subalkalic) Group 2A rocks to the tholeiite field of Irvine and Baragar (1971). This supports the conclusions made in the previous section.

FRACTIONATION SERIES IN THE STEKENJOKK MAFIC ROCKS

The contents of relatively more incompatible (Ti, P, Zr, and Y) and more compatible (Ni and Cr) elements in the Groups 1A and 1B mafic rocks, as well as the varying behaviour of the elements Ti, total Fe, P, and Zr with increasing differentiation suggest that these rocks do not belong to the same fractionation series. Similar arguments apply when a comparison is made between the Groups 1A och 2A mafic rocks. Furthermore, the mildly alkalic nature of the Group 2B basaltic rocks, their enrichment in P and K and probably Zr and Y in more parental magmas compared with all other groups, and the distinctive behaviour of Ti during fractionation clearly distinguish the Group 2B rocks as a separate fractionation series. By contrast, the distribution of the Group 1B data on the Group 2A variation diagrams (Figs. 26 and 27a—c) and AFM-diagram (Fig. 30c) suggest that the more primitive 1B basalts may well complement the more differentiated 2A basaltic rocks in a continuous differentiation series. Well-defined positive (strongly tholeiitic) trends are particularly apparent for the less mobile elements Ti, total Fe, P, and Zr on the Y (and Zr) diagrams (Figs. 27c and b). Allowance is necessary for Mg, Ni and Cr mobility in the Group 1B basalts when dispersion from a 'tight', well-defined trend is noted in the combined 1B—2A plots.

Thus, three quite separate mafic fractionation series are proposed for the Stekenjokk volcanites:

1. Group 1A — mildly tholeiitic basalts and basaltic andesites showing chlorite—albite±amphibole±epidote±calcite±Ti-rich mineral assemblages and probably with both volcanites and high-level intrusions represented.

2. Groups 1B+2A — strongly tholeiitic basaltic rocks showing a wide fractionation series. The more primitive basalts (1B) are probably both volcanic and high-level intrusive, and field/microscope-indistinguishable from the 1A mafic rocks; the more differentiated basaltic rocks (2A) are entirely high-level intrusive and, on the basis of their darker colour and higher content of Ti-rich minerals, are field/microscope-distinguishable from the Group 1 mafic rocks.

3. Group 2B — mildly alkalic basalts with chlorite-albite-calcite-Ti-rich minerals ±biotite±epidote±apatite mineral assemblages and only high-level intrusions represented.

AFFINITY OF DIFFERENT FRACTIONATION SERIES TO MAFIC ROCKS IN MODERN TECTONIC ENVIRONMENTS

Following earlier work by Chayes (1964), discrimination of the tectonic setting of basalts and basaltic andesites using their major, minor and trace element geochemistry has been demonstrated to a greater or less extent by the works of Miyashiro (1974, 1975), Pearce (1976) and Pearce *et al.* (1975, 1977) using major and minor elements, and Pearce and Cann (1971, 1973), Bloxam and Lewis (1972), Herrmann *et al.* (1974), Floyd and Winchester (1975), Miyashiro and Shido (1975), Pearce (1975), and Pearce and Norry (1979) using trace elements.

Several major elements potentially useful for distinguishing basalts and basaltic

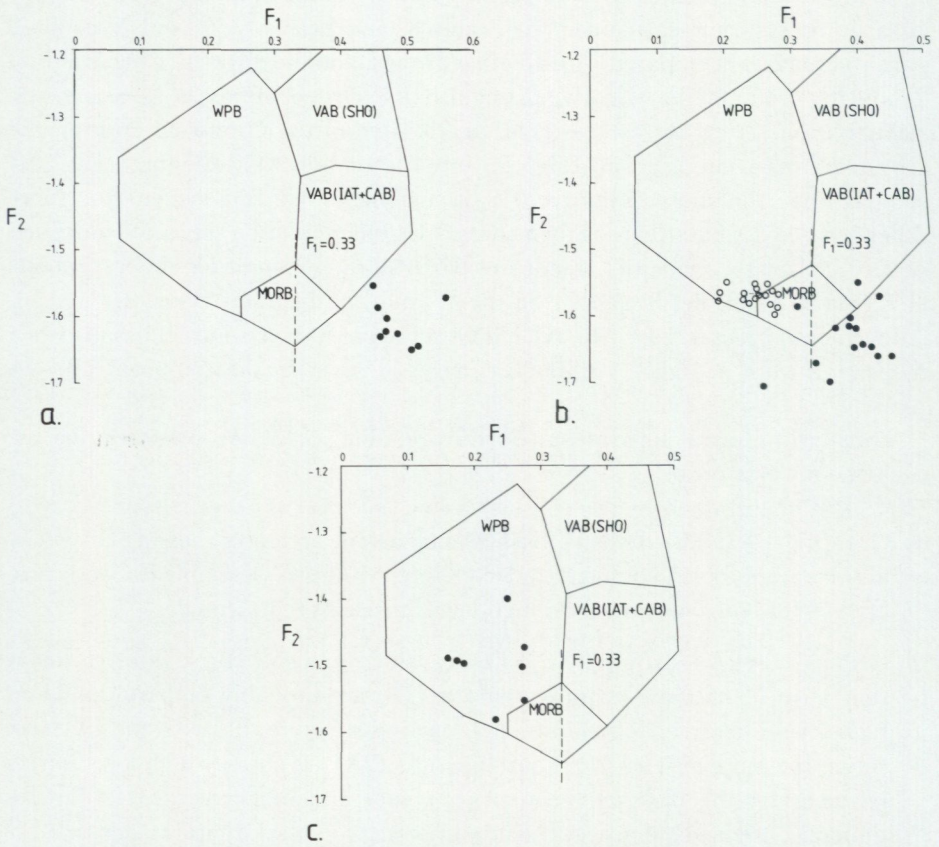

Fig. 31. Plot of discriminant functions F_1-F_2 (Pearce 1976) for different mafic rock fractionation series. a. Group 1A series. b. Groups 1B+2A series; filled circles = 1B basalt, open circles = 2A basalt. c. Group 2B series. MORB = Mid-ocean ridge basalt; VAB = Volcanic arc basalt; IAT = Island arc tholeiite; CAB = Calc-alkalic basalt; SHO = Shoshonitic basalt; WPB = Within-plate basalt.

TABLE 3. Mean values of mafic rocks in the three mafic fractionation series (1A, 1B+2A and 2B) and comparison with mean values of basaltic rocks from different tectonic environments; IAT includes both basalts and basaltic andesites (up to 56 % SiO_2). N = number of analyses unless otherwise stated in brackets; all analyses recalculated on a volatile-free basis.

	1A	1B+2A	2B	MORB	IAT	CAB	OIT	OIAB
N	9	32	8	66	97	75	193	88
SiO_2 (%)	52.9	49.7	49.7	50.20	54.00	52.12	49.43	48.31
TiO_2	0.58	1.80	3.45	1.50	0.73	1.07	2.50	3.00
Al_2O_3	16.5	15.0	14.5	16.25	17.13	18.07	13.92	16.10
FeO^x	10.9	11.5	13.8	9.63	9.53	8.89	11.40	9.47
MnO	0.20 (7)	0.22 (31)	0.24	0.18	0.18	-	0.16	0.17
MgO	7.0	7.0	4.3	7.74	5.13	5.00	8.26	5.70
CaO	6.5	10.7	7.9	11.30	9.95	9.67	10.23	8.58
Na_2O	4.7	3.2	3.9	2.84	2.34	2.95	2.15	3.97
K_2O	0.2	0.2	0.8	0.20	0.51	0.94	0.39	1.47
P_2O_5	0.06 (7)	0.19 (30)	0.91	0.13	0.12	-	0.26	0.64
Total	99.5	99.5	99.5	99.97	99.62	98.71	98.70	97.41
Zr (ppm)	28	130 (28)	220 (7)	95 (10)	42 (67)	106 (60)	165 (21)	333 (10)
Y	16	38 (28)	43 (7)	43 (10)	19 (61)	23 (60)	25 (20)	54 (10)
Cu	43	43 (29)	30 (7)	77 (10)	117 (67)	-	91 (36)	36 (10)
Zn	76 (6)	106 (29)	97 (7)	-	87 (50)	-	-	-
Ni	26 (6)	80 (28)	11 (7)	97 (10)	23 (67)	25 (?)	-	47 (14)
Cr	42	257 (28)	17 (7)	297 (10)	49 (67)	40 (?)	-	73 (14)

MORB = Mid-ocean ridge basalt (Engel *et al.* 1965; Cann 1969; Miyashiro *et al.* 1969; Engel and Engel 1970)

IAT = Island arc tholeiite (Stark 1963; Baker 1968; Gill 1970; Bryan *et al.* 1972; Ewart *et al.* 1973; Ewart *et al.* 1977)

CAB = Calc-alkali basalt (Jakeš and White 1972; Pearce and Cann 1973; Pearce 1976)

OIT (WPB) = Ocean-island tholeiite (Within-plate basalt) (MacDonald and Katsura 1964; Pearce and Cann 1971; Brooks and Jakobsson 1974)

OIAB (WPB) = Ocean-island alkali basalt (Within-plate basalt) (MacDonald and Katsura 1964; Engel *et al.* 1965; Brooks and Jakobsson 1974)

= Data not presented

andesites from different tectonic settings (*e.g.* Si, K) are of doubtful significance owing to the spilitic type of alteration that many of these rocks have suffered (see earlier discussion). On the other hand, use of trace elements generally considered to be immobile, for example REE, Ti, Y, Zr, Ni, Cr, should reduce the problems of element redistribution. An important consideration here is volume change during alteration. Comparison of absolute values between altered and unaltered samples as well as the use of defined fields on binary plots are of dubious significance, if alteration proceeds non-isovolumetrically; ternary plots of conserved elements will, however, overcome this problem. A more important problem arises from studies which indicate that certain of these so-called immobile elements, for

example REE (Hellman and Henderson 1977), Ti (Loeschke 1976; Vallier and Batiza 1978) and Cr (Stephens 1980b; Grenne *et al.* 1980) may not, in fact, be always conserved during spilitization. Another problem arises when it is considered that the supposed immobile elements constitute such a small proportion of the total rock chemistry and may, indeed, be sited in a single phase; the question of a representative sample arises.

The general approach used here is to extract as much information as possible from major and minor elements, and then to see how the trace element data compare with this picture. For purposes of comparison, mean values of basalts from various modern environments are presented in Table 3. Since the mean values of several supposedly stable elements (Ti, total Fe, P, and Y) are similar in the more and less spilitic Group 1B mafic rocks, it was considered likely that the spilitization process in these rocks proceeded isovolumetrically (Stephens 1980b). On this basis, minor loss of Mg, Zr and Ni and more significant loss of Cr were suggested. No such analysis can be applied to the Group 1A mafic rocks due to their more pervasive spilitic character. However, in the analysis of chemical variation trends presented earlier, there was an internal consistency between the different plots involving the supposedly less mobile elements, suggesting limited mobility of these elements. On the basis of the results for the Group 1B mafic rocks, spilitization of the Group 1A samples is assumed to have proceeded isovolumetrically. Conclusions drawn from data for the Group 2 high-level intrusive rocks are considered to be even more reliable due to their apparently less altered nature when compared to the Group 1 mafic rocks.

Group 1A mafic fractionation series — The chemical variation trend on the TiO_2 versus FeO*/MgO diagram (Fig. 24a) is similar to that observed in island arc tholeiites (IAT), (see Miyashiro 1975); in particular this trend is remarkably similar to that observed in the tholeiites from the Tonga group of islands in the western Pacific (Miyashiro 1975; Ewart *et al.* 1977). Use of Pearce's (1976) discriminant analysis functions, which include the more mobile elements Si, Na, Ca, and K, is problematic since the Group 1A rocks are mostly spilitic; addition of Na_2O and possible loss of K_2O during spilitization combined with their conspicuously low TiO_2 contents are the critical factors controlling the distribution of points outside all fields (Fig. 31a). On account of mainly the low TiO_2 content, these basalts and basaltic andesites plot well to the right of the critical $F_1 = 0.33$ line (Pearce 1976). When considered in the light of the highly fractionated nature of these rocks, this is consistent with the conclusion that the Group 1A rock chemistries are similar to basalts from modern day convergent plate margins.

On the Ti-Zr-Y diagram of Pearce and Cann (1973), the Group 1A rocks plot in or immediately around the field of IAT (Fig. 32a). Use of a Ti-Cr discriminant (Pearce 1975) and the Zr/Y *versus* Zr diagram of Pearce and Norry (1979) confirms their chemical affinity to IAT (Figs. 33a and 34a).

In summary, the Group 1A mildly tholeiitic, fractionated (low Ni and Cr) basalts and basaltic andesites are highly depleted in the more incompatible elements (Zr, Y, Ti, P) as well as the Zr/Y ratio relative to mid-ocean ridge basalt (MORB), (Table 3, compare columns 1 and 4). These features together with their occurrence in a mixed mafic and felsic volcanic sequence are typical for the IAT series (Table 3, column 5). TiO_2 fractionation trends and use of discriminant functions are in agreement with this conclusion.

Groups 1B+2A mafic fractionation series — The positive trends of variation on the combined 1B-2A TiO_2 and FeO* *versus* FeO*/MgO diagrams lie in a similar position to the trends for MORB and within-plate basalts (WPB), (see Miyashiro 1975). The Group 1B data plot mostly outside the delimited fields on the F_1-F_2 diagram (Fig. 31b) of Pearce (1976), the more spilitic samples generally having lower F_2 values, consistent with Na_2O enrichment and possible K_2O depletion. An important consideration here is the primitive nature of these rocks and, in particular, their low TiO_2 contents. Allowance for the variably spilitic and primitive nature of these basalts suggests closest affinity to MORB. The Group 2A data straddle the boundary between the MORB and WPB fields on the F_1-F_2 discriminant diagram (Fig. 31b), the most differentiated samples lying in the WPB field, probably due mainly to their high TiO_2 contents. Allowance for the differentiated nature of the 2A basaltic rocks suggests closest affinity to MORB.

On the Ti-Zr-Y diagram (Pearce and Cann 1973), the Group 1B and 2A basaltic rocks lie within the ambiguous field including both MORB and IAT (Fig. 32b). Use of a Ti-Cr discriminant (Pearce 1975) suggests a MORB affinity, only a few spilitic 1B samples passing over into the IAT field presumably due to Cr loss (Stephens 1980b) during alteration (Fig. 33b). Allowing for the primitive and differentiated character of the Group 1B and Group 2A basaltic rocks, respectively, and minor loss of Zr during spilitization of the 1B basalts, the distribution on the Zr/Y *versus* Zr diagram of Pearce and Norry (1979) also suggests affinity to MORB (Fig. 34b).

In summary, the proposed fractionation series involving Group 1B and 2A basaltic rocks is strongly tholeiitic and involves both more primitive (1B) and more differentiated (2A) samples. Data on the various discriminant diagrams indicate affinity to MORB, when allowance is made for the broad range in degree of fractionation in this series as well as Cr and minor Zr losses during spilitization of the 1B basalts. Thus, the low and high TiO_2, P_2O_5, Zr, and Y values in the 1B and 2A basaltic rocks, respectively, compared with MORB (Table 2, columns 7—12 and Table 3, column 4) are due to varying degrees of fractionation. The average 1B—2A basalt (Table 3, column 2) compares well with the average MORB basalt cited in Table 3 (column 4).

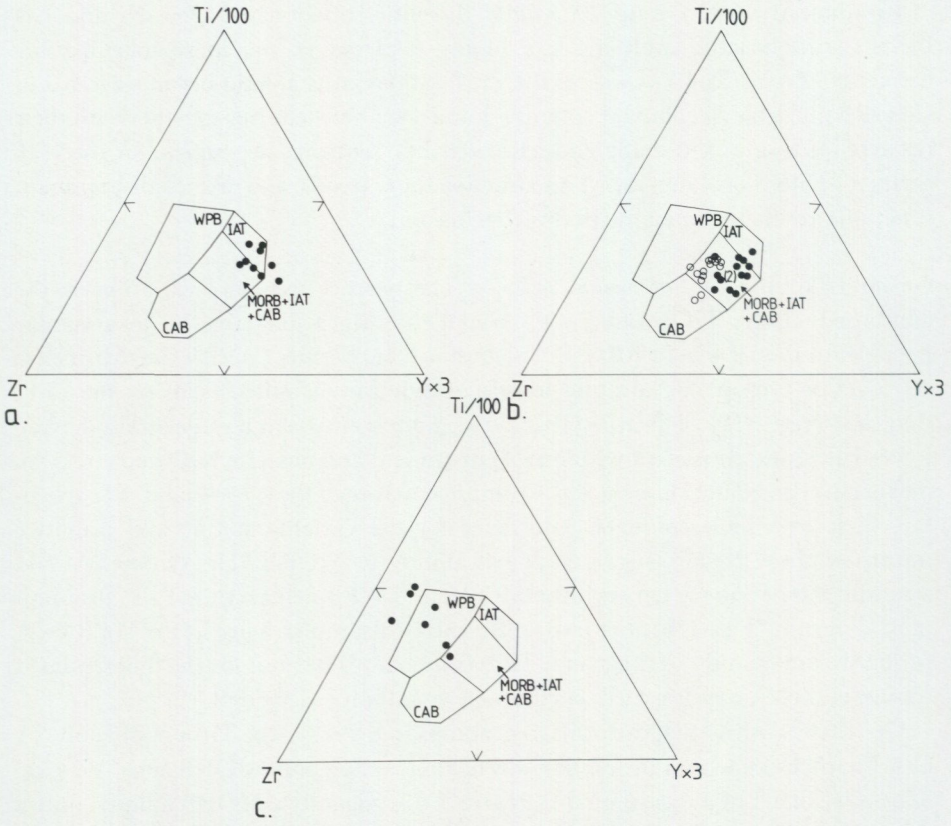

Fig. 32. Ti-Zr-Y discriminant diagram (Pearce and Cann 1973) for different mafic rock fractionation series. a. Group 1A series. b. Groups 1B+2A series; filled circles = 1B basalt, open circles = 2A basalt. c. Group 2B series. For explanation of abbreviations, see Fig. 31.

Group 2B mafic fractionation series — The mildly alkalic Group 2B basaltic rocks fall firmly within the WPB field on the F_1-F_2 major element discriminant diagram (Fig. 31c). Similarly, they lie within or just outside the WPB field on the Ti-Zr-Y diagram (Fig. 32c) and firmly within the WPB field on the Zr/Y *versus* Zr plot (Fig. 34c).

The Group 2B rocks are highly differentiated and show a firm WPB affinity (compare also Table 3, columns 3 and 8). In particular, they are enriched in P and K and probably Zr and Y in more parental magmas compared with the other groups of mafic rocks. Since even primitive within-plate alkalic basalts appear to be characterized by enrichment of, for example, Ti, K, P, Zr, and Y relative to MORB (compare, for example, analyses in Frey *et al.* 1978 with MORB in Table

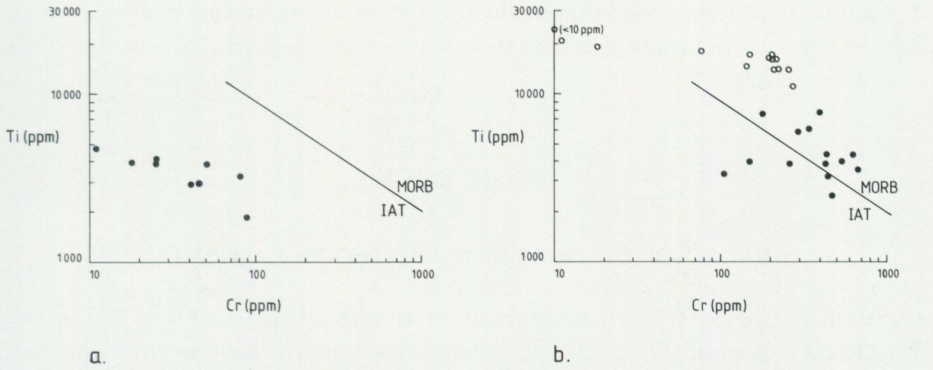

Fig. 33. Ti-Cr diagram (Pearce 1975) applied to Group 1A (a) and Groups 1B+2A (b) mafic fractionation series; on Fig. 33b filled circles = 1B basalt, open circles = 2A basalt. All mafic rocks plotted lie in and just outside the IAT and ambiguous MORB+IAT+CAB fields on Fig. 32. For explanation of abbreviations, see Fig. 31.

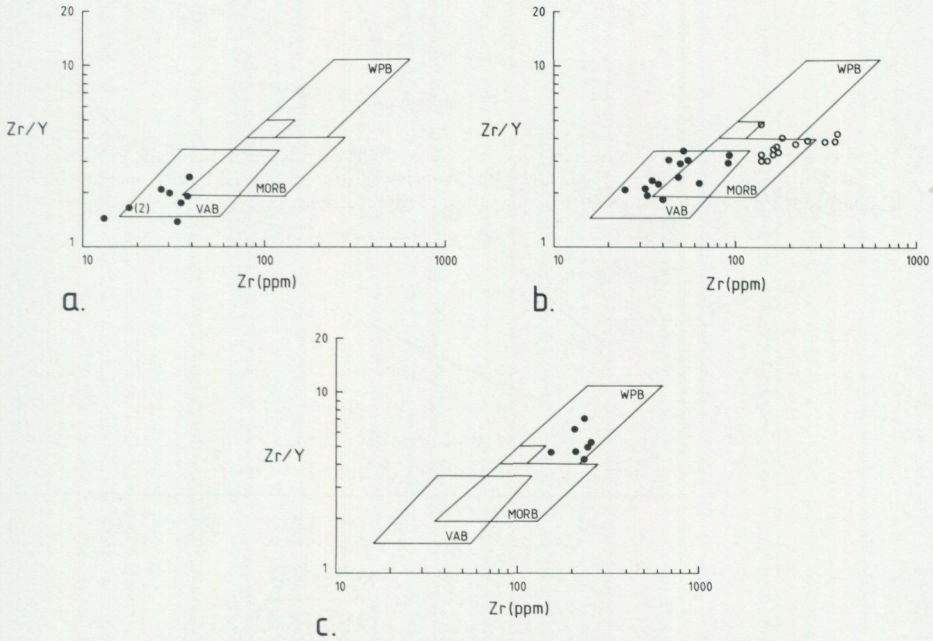

Fig. 34. Zr/Y-Zr discriminant diagram (Pearce and Norry 1979) for different mafic rock fractionation series. a, Group 1A series. b, Groups 1B+2A series; filled circles = 1B basalt, open circles = 2A basalt. c, Group 2B series. For explanation of abbreviations, see Fig. 31.

3, column 4), it is suggested that the high values of these elements in the Group 2B basaltic rocks is not due entirely to their highly differentiated character (see later discussion, p 82).

FELSIC ROCKS

NATURE OF THE PROBLEM AND METHODS OF APPROACH

On both the igneous spectrum diagram of Hughes (1973), (see Fig. 35), and a Na_2O-CaO diagram (Fig. 21d), the Stekenjokk quartz keratophyres plot well away from the andesite—dacite—rhyolite fields. Most of the quartz keratophyres cluster on the left-hand side of the igneous spectrum diagram reflecting their extremely low $K_2O/(K_2O+Na_2O)$ ratios and total alkali contents in the range 3.5—6.8%. As stated earlier, SiO_2 and Na_2O/CaO values vary widely and most significantly there is a relationship between texture and chemistry, in that granular-textured subvolcanic intrusions have SiO_2 and Na_2O/CaO values which

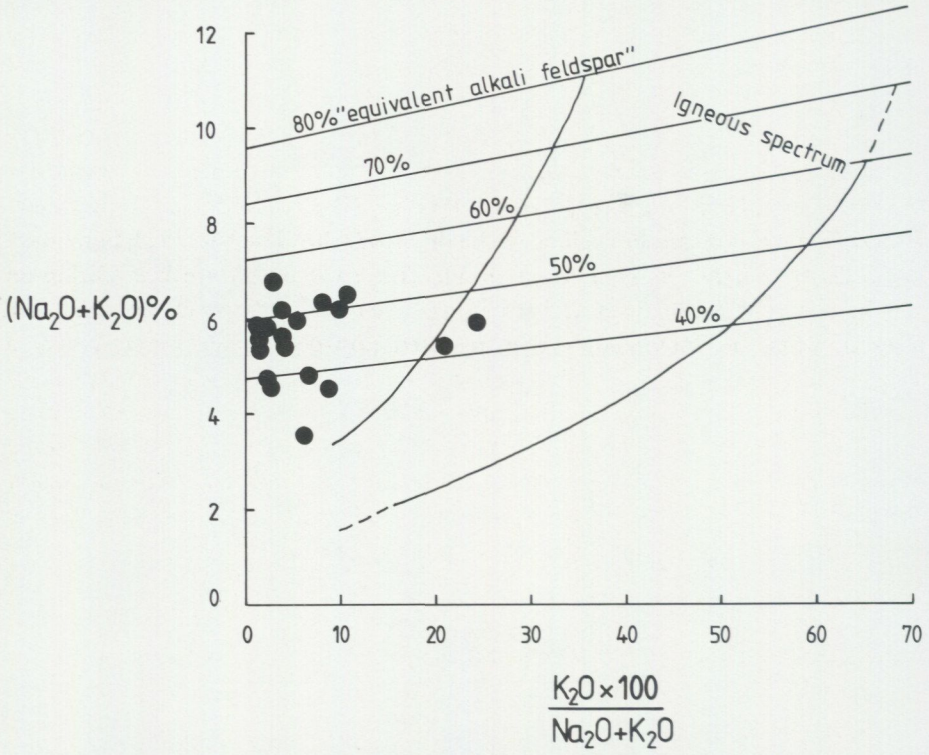

Fig. 35. (Na_2O+K_2O) — $K_2Ox100/(Na_2O+K_2O)$ diagram (Hughes 1973) for the felsic rocks. "Equivalent alkali feldspar" content is calculated assuming all Na_2O and K_2O is in the form of pure albite (11.8 % Na_2O) and pure K-feldspar (16.9 % K_2O) respectively (Hughes 1973).

lie in the lower part of the range of respective values for the phyric-textured, volcanic quartz keratophyres. Compared with the felsic end-members of the spectrum basalt—andesite—dacite—rhyolite, the Stekenjokk quartz keratophyres are chemically anomalous; the hypothesis that they are the alteration product of more 'normal' igneous rocks is strongly suggested.

Discussion of the origin of quartz keratophyre can be found in Battey (1955), Hughes (1973), Schermerhorn (1973) and in several contributions in Amstutz (1974). As with the spilites, there remains the controversy concerning the relative roles of 'primary' *versus* 'secondary' processes, the latter including alteration post-dating deposition, extrusion or emplacement. However, the amount of literature concerned with the origin of quartz keratophyre is far less than that concerned with the origin of spilite (see, for example, list of references cited earlier). This is somewhat surprising since in many orogenic belts (see, for example, Battey 1955; Donnelly 1966) quartz keratophyre occurs intimately associated with spilite, an association typically demonstrated in the Stekenjokk volcanites of the present study. It is also of interest that these rocks share their most characteristic chemical peculiarity — high Na_2O/CaO ratios — compared with the corresponding members in the spectrum basalt—andesite—dacite—rhyolite. It is, therefore, considered reasonable here to suppose that the processes giving rise to the peculiar chemistry of the quartz keratophyres are similar to those which apply to the development of the spilites. It is worth recalling the role that sub-sea-floor metamorphism is thought to have played in the conversion of basalt and basaltic andesite to spilite.

Following on from the alteration hypothesis, further debate arises as to whether quartz keratophyre represents altered rhyolite (Battey 1955) or altered more plagioclase-rich volcanites such as dacite or rhyodacite (Hughes, 1973; Schermerhorn 1973). Further light on these problems is shed by the work of Dickinson (1962). Using relict textures and stratigraphic continuity between less and more altered parts, he convincingly demonstrated post-depositional alteration of a submarine, rhyodacite vitric tuff into a quartz keratophyre felsite composed predominantly of albite and quartz; this alteration occurred under conditions of deep burial during diagenesis. Recent works in the Caribbean (see, for example, Gunn and Roobol 1976; Jackson and Smith 1978) have also indicated that the quartz keratophyres there represent metasomatized calc-alkalic dacites; they appear to have formed as a result of metamorphism post-dating extrusion of dacite.

The analysis which follows seeks answers to the following questions:

1. What is the nature of the chemical alteration in the felsic rocks and, thus, the original magmatic compositions?

2. Are the Stekenjokk quartz keratophyres related by fractionation to the mafic rocks in the Stekenjokk volcanites, bearing in mind their close spatial relationship in the field, yet the extreme bimodality of the Stekenjokk mafic and felsic

rocks on the SiO_2 histogram (Fig. 19)? Since the levels of the consistently most incompatible elements P, Zr and Y in the mafic rocks are similar or *lower* in the felsic rocks compared with the two fractionation series defined by the Groups 1B+2A and Group 2B basaltic rocks, it is inferred that the felsic rocks cannot belong to these fractionation series. However, there remains the possibility that they are related by fractionation to the Group 1A island arc tholeiite series.

When assessing possible alteration, three factors governing the chemistry of the quartz keratophyres must be considered:

1. Changes in absolute values due to real losses or gains.
2. Changes in absolute values related to volume and/or specific gravity changes during alteration, *i.e.* apparent losses or gains.
3. Chemical variation related to normal igneous processes *e.g.* fractional crystallization.

Since the chemistry of quartz keratophyres is characterized by high Na_2O and low CaO values (Schermerhorn 1973) relative to 'normal' intermediate and felsic magmatic rocks (andesite, dacite, rhyodacite, rhyolite), the parameter Na_2O/CaO is used below as a means of expressing the deviation of the Stekenjokk felsic rocks from these 'normal' rocks. Values of Na_2O/CaO for andesite, dacite, rhyodacite and rhyolite from LeMaitre's (1976) data are 0.51, 0.88, 1.01, and 3.11, respectively. However, the index Na_2O/CaO is only an index of alteration with respect to the mineral plagioclase feldspar. Five of the twenty quartz keratophyre samples (see Appendix) show both low Na_2O/CaO ratios (<3) and reasonable SiO_2 values ($63\% \leq SiO_2 < 75\%$) when compared with 'normal' felsic compositions and four of these have been interpreted as subvolcanic intrusions. These samples are suggested to represent less altered compositions with respect to the elements Na, Ca, Si, and Al, *i.e.* those elements constituting plagioclase feldspar. Other phases need not be altering at the same rate as the plagioclase feldspar and, thus, redistribution of the elements contained in these phases may be less or even more advanced than the Na-Ca exchange, for example, in the plagioclase feldspar. The criteria for estimating less altered and more altered compositions for other groups of elements besides Na, Ca, Si, and Al are discussed in detail below.

Assuming the specific gravities of altered and unaltered rocks are the same, the effects of volume changes $\pm$ 10% and $\pm$ 20% on absolute abundances of an element conserved during the alteration process are shown in Table 4.

TABLE 4. Effect of volume change during alteration on the concentration of a conserved element in unaltered rock. The effect of 10 % and 20 % volume gain/loss on unaltered compositons ranging from 1 to 10 %, 12 %, 15 %, 60 %, 65 %, and 70 % and 10—100 ppm are tabulated. Specific gravities of altered and unaltered rock compositions are assumed to be the same.

	Wt % of conserved element in unaltered rock														
	1	2	3	4	5	6	7	8	9	10	12	15	60	65	70
10 % gain	0.9	1.8	2.7	3.6	4.6	5.5	6.4	7.3	8.2	9.1	10.9	13.6	54.6	59.1	63.6
10 % loss	1.1	2.2	3.3	4.4	5.6	6.7	7.8	8.9	10.0	11.1	13.3	16.7	66.7	72.2	77.8
20 % gain	0.8	1.7	2.5	3.3	4.2	5.0	5.8	6.7	7.5	8.3	10.0	12.5	50.0	54.2	58.3
20 % loss	1.3	2.5	3.8	5.0	6.3	7.5	8.8	10.0	11.3	12.5	15.0	18.8	75.0	81.3	87.5

	ppm of conserved element in unaltered rock									
	10	20	30	40	50	60	70	80	90	100
10 % gain	9.1	18.2	27.3	36.4	45.5	54.5	63.6	72.7	81.8	90.9
10 % loss	11.1	22.2	33.3	44.4	55.6	66.7	77.8	88.9	10.0	111.1
20 % gain	8.3	16.7	25.0	33.3	41.7	50.0	58.3	66.7	75.0	83.3
20 % loss	12.5	25.0	37.5	50.0	62.5	75.0	87.5	100.0	112.5	125.0

ASSESSMENT OF ALTERATION EFFECTS

Zr, Y behaviour and establishment of alteration models — When plotted against the index Na_2O/CaO, the trace elements Zr and Y show no tendency to vary systematically with Na_2O/CaO (Fig. 36); two samples (Analyses 59 and 66 in the Appendix) show, however, distinctly lower values of Zr than the remainder as well as showing the lowest Y and Zr/Y values.

Bearing in mind the supposedly immobile behaviour of Zr and Y during alteration of mafic rocks, this data may well be reflecting the relative stability of these elements during formation of the quartz keratophyres (see also Jackson and Smith 1978). It is unlikely that the lower Zr values for Analyses 59 and 66 can be explained by volume changes, as, from Table 4, unrealistically high changes are required to eliminate the gap between these two samples and the main group. A more reasonable explanation is that these samples, highly depleted in incompatible elements Zr and Y and having lower Zr/Y ratios, represent a separate pre-alteration type and do not belong to the main group of felsic rocks. The variation that does exist within the main group is thought to be largely due to primary magmatic variation.

Four samples in the main group of felsic rocks (Analyses 50, 54, 55, and 57), all subvolcanic intrusions, are, on the basis of Na-Ca-Si criteria discussed earlier, apparently less altered. Assuming that these samples also represent less altered compositions with respect to the elements Zr and Y, then a comparison of their

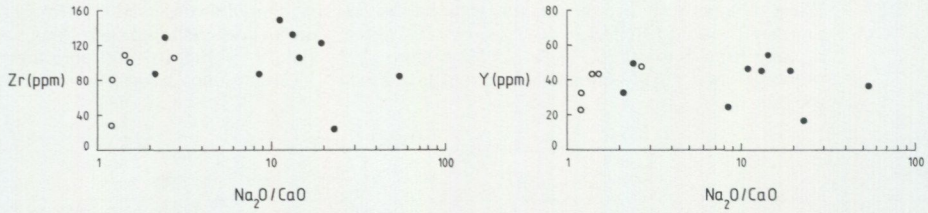

Fig. 36. Variation of Zr and Y with Na_2O/CaO ratio in the felsic rocks. Open circles = felsic rocks, all except one being subvolcanic intrusive, showing both low Na_2O/CaO ratios and reasonable SiO_2 values when compared with 'normal' felsic rock compositions (see text); filled circles = remaining felsic rocks, mostly extrusive.

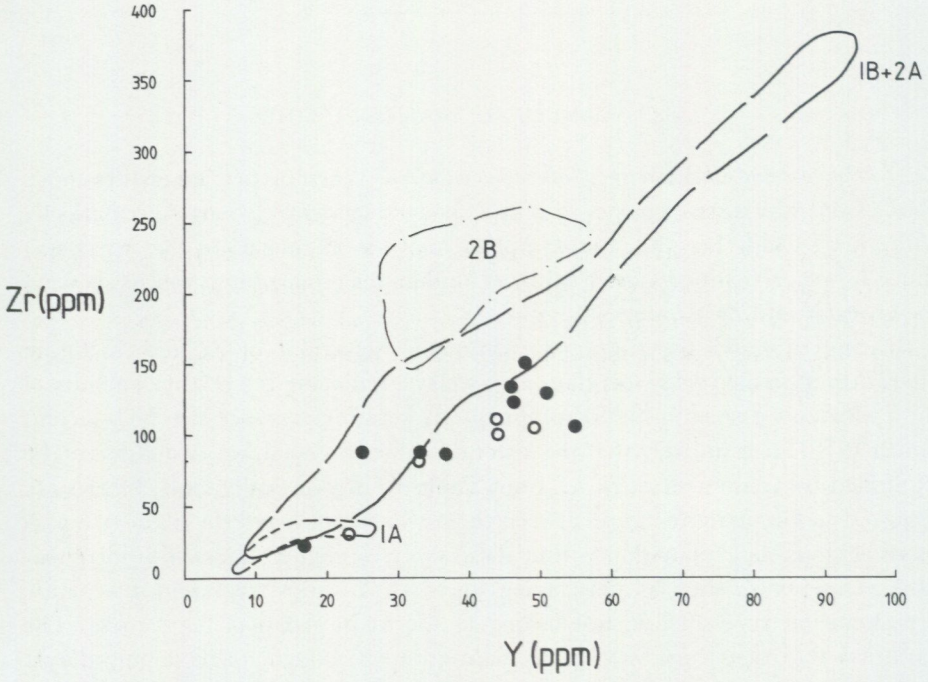

Fig. 37. Zr-Y variation diagram for the felsic rocks. Open circles = felsic rocks, all except one being subvolcanic intrusive, showing both low Na_2O/CaO ratios and reasonable SiO_2 values when compared with 'normal' felsic rock compositions (see text); filled circles = remaining felsic rocks, mostly extrusive. Trends for the 1A, 1B+2A and 2B mafic fractionation series are taken from Figs. 24, 27 and 29 respectively. The two samples lying along the 1A trend are Analyses 59 and 66 in the Appendix.

mean Zr (100 ppm) and Y (43 ppm) values with the mean Zr (114 ppm) and Y (43 ppm) values in the remaining apparently more altered samples permits discussion of two alteration models. Model A assuming Zr conservation implies a 10—15 % volume loss (see Table 4) and a small (10—15 %) real loss of Y during alteration; model B assuming Y conservation implies no volume change and a small (10—15 %) real gain of Zr during alteration. It is now possible to interpret a Zr-Y plot for the felsic rocks with greater confidence (Fig. 37). The main group of samples lies along a trend suggesting an early rapid increase and then a fall-off of Y with increasing Zr. This trend is quite distinct both in form and position from that indicated by the Group 1A mafic rocks. Furthermore, neither a 15 % volume loss with Zr conserved (model A) nor a 15 % gain in Zr under isovolumetric conditions (model B) can account for the important 'Zr gap' between the trends. It appears, therefore, unlikely that the main group of felsic rocks was generated by fractional crystallization of the same magma that produced the Group 1A mafic rock series. Analyses 59 and 66, however, plot along the Group 1A trend together with the basaltic andesites. It is feasible that these samples, with their low Zr, Y, and Zr/Y values, are variably altered fractionation products of the Group 1A island arc tholeiite series; these two samples are excluded in the following discussion which aims to assess the nature of the main group of felsic rocks.

Na — Na_2O content in the main group of felsic rocks is anomalously high over the whole range of Na_2O/CaO values when compared with 'normal' andesite (3.5 %), dacite (3.8%), rhyodacite (3.7 %) and rhyolite (3.6 %), (see LeMaitre 1976 and Fig. 38). It is considered likely that the flat trend on the Na_2O diagram is a result of pervasive Na_2O concentration in all these rocks. Thus, the mean Na_2O content of four apparently less altered (based on Na-Ca-Si criteria) samples (5.0 %) is probably a maximum estimate of the mean pre-alteration Na_2O content. The mean Na_2O content of the remaining apparently more altered (based on Na-Ca-Si criteria) samples is 5.5 %. Since the maximum volume losses (15 and 0% respectively) in the proposed alteration models are insufficient (see Table 4) to explain the concentration of Na_2O values from 'normal' levels of between 3.5 and 4.0 % up to values ranging between 4.2 and 6.6 % (mean of 18 values=5.4 %), real addition of Na_2O is required.

Si, Al, Ca — It appears that for the elements Si, Al and Ca there is a smoother correlation of change in element content — increase in the case of Si, decrease in the case of Al and Ca — with increasing Na_2O/CaO ratio (Fig. 38). Comparison of mean values of the four apparently less altered (based on Na-Ca-Si criteria) and the remaining more altered samples should provide some estimate of pre-alteration *versus* altered compositions. However, since no truly unaltered rocks are present, the pre-alteration values will probably be somewhat too high for SiO_2 and too low for Al_2O_3 and CaO.

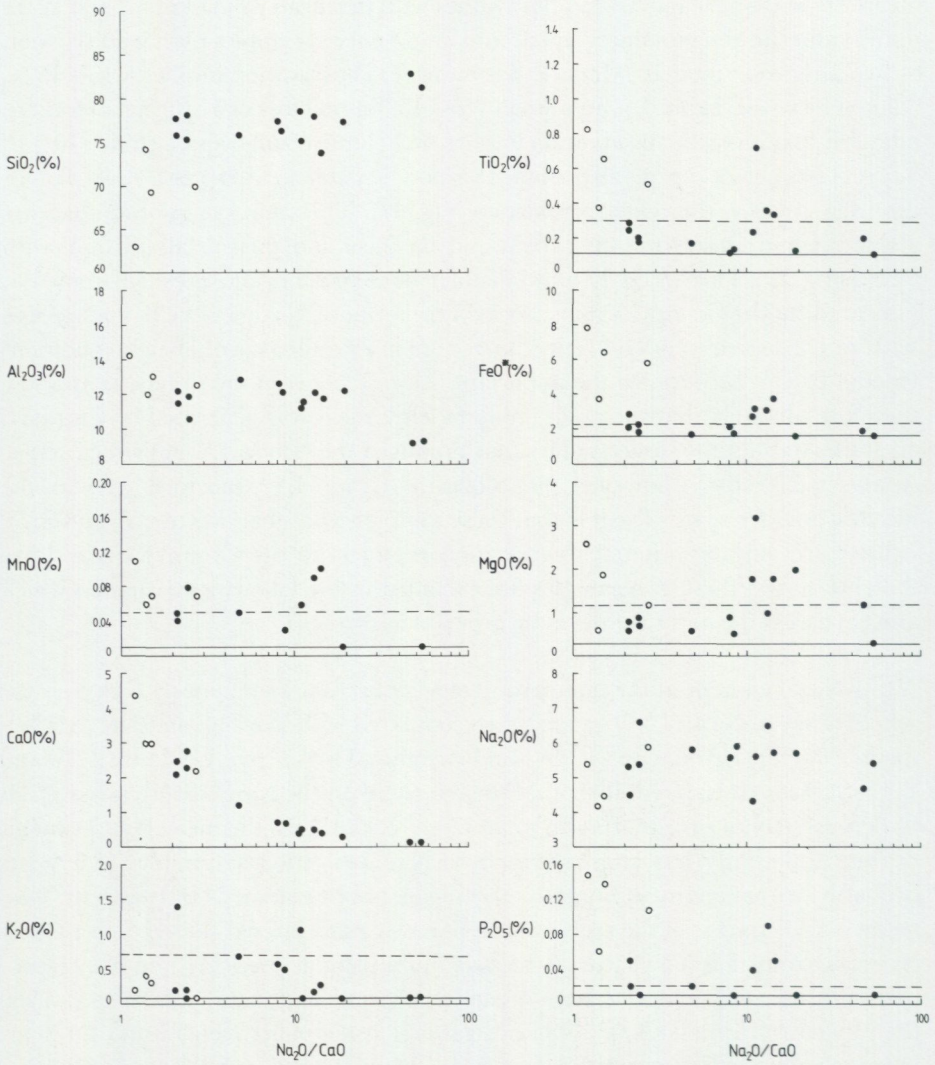

Fig. 38. Variation of major and minor elements with Na_2O/CaO ratio for the main group of felsic rocks. Open circles = subvolcanic felsic intrusions showing both low Na_2O/CaO ratios and reasonable SiO_2 values when compared with 'normal' felsic rock compositions (see text); filled circles = remaining felsic rocks, mostly extrusive. Plateau distribution patterns showing low values, defined by lower continuous (more confident) and upper non-continuous (less confident) lines, are apparent for the elements Ti, Fe, Mn, Mg, K, and P.

Ti, total Fe, Mn, Mg, K, P — The distribution patterns on the Ti, total Fe, Mn, Mg, K, and P *versus* Na_2O/CaO diagrams (Fig. 38) show plateaux development (low values), the various plateaux being established at quite low Na_2O/CaO ratios (c. 2); a variable number of samples showing higher values plot above the plateaux

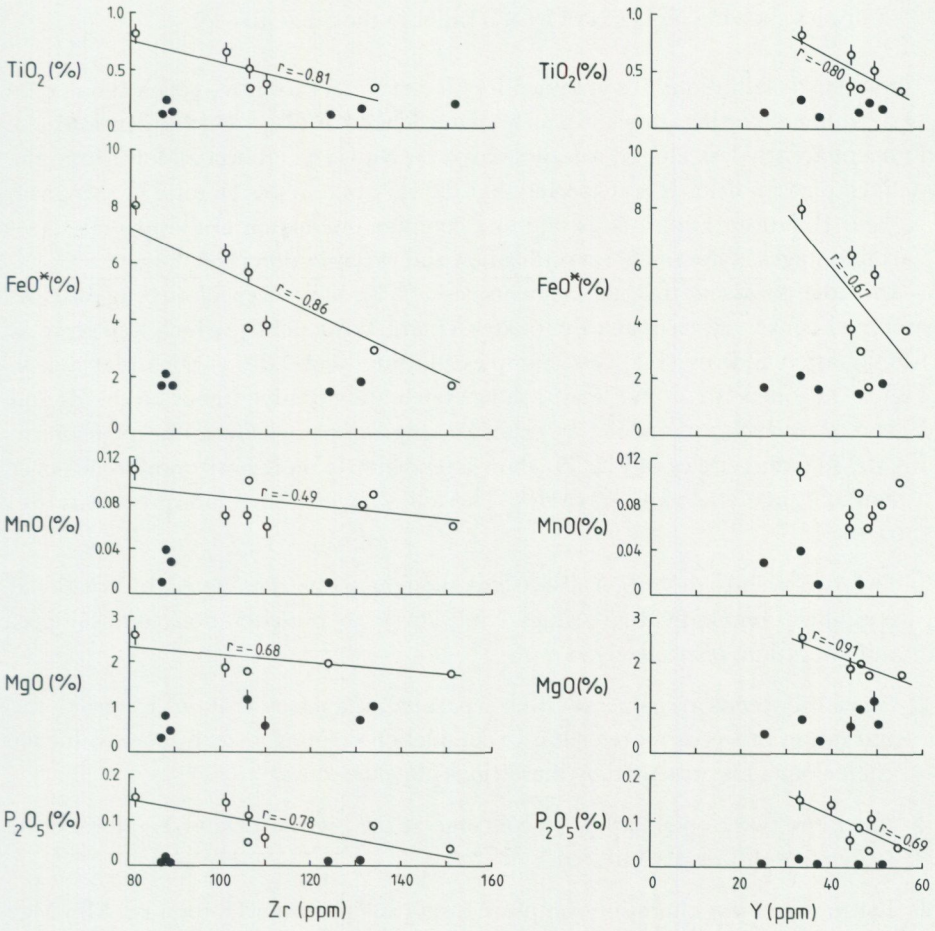

Fig. 39. Plot of elements (except K) showing plateau development (low values) in Fig. 38 against the incompatible elements Zr and Y. Samples plotting above the respective plateaux in Fig. 38 are indicated by open circles, show negative trends — regression lines and correlation coefficients (r) indicated — and are thought to represent pre-alteration compositions; samples defining the respective plateaux in Fig. 38 are indicated by filled circles and are thought to represent altered compositions. The subvolcanic intrusions showing both low Na_2O/CaO ratios and reasonable SiO_2 values when compared with 'normal' felsic rocks (see text) are shown by a vertical line through the symbol.

and fall *consistently* into two groups:

1. Those samples with lower Na_2O/CaO ratios including, in the case of Ti, total Fe, Mn, P (and Mg), the four apparently less altered samples (based on Na-Ca-Si criteria).

2. Samples showing higher Na_2O/CaO ratios in the range 10—20.

Similar distributions are obtained for all elements, except K, which shows only two samples plotting above a poorly defined plateau (Fig. 38); furthermore, the four apparently less altered samples based on Na-Ca-Si criteria all fall within the defined plateau field. It is suspected that the variation in the Ti, total Fe, Mn, Mg, K, and P data in Figure 38 is due to a complex interaction of the two effects — variable stages of fractional crystallization and variable alteration.

In order to assess this, all elements, except K, have been plotted against the assumed conserved elements Zr (model A) and Y (model B), which also serve as fractionation indices (Fig. 39). Samples plotting above the various plateaux in Figure 38 (open circles in Fig. 39) show systematic negative trends on the Zr and Y variation diagrams, while, as expected, the samples defining the plateaux in Figure 38 (solid circles in Fig. 39) show a tendency to more horizontal trends over a similar range of Zr and Y values. The following tentative interpretations are, thus, made:

1 The two trends described above are thought to be dominated by fractional crystallization, individual values lying closer to pre-alteration compositions, and alteration, respectively.

2. Since the trends are generally well separated, it appears that, once started, the alteration proceeds more or less to completion defining a steady state value for each element represented by the various plateau values.

3. Since the two trends appear to converge at the highest Zr and Y values, open system conditions are inferred.

4. Estimates of pre-alteration compositions for the elements Ti, total Fe, Mn, Mg, and P may be made using the samples falling above the plateaux in Figure 38; the mean and standard deviation values for this data take into account primary magmatic fractionation variation. Estimates of altered compositions may be made using the samples defining the plateau values in Figure 38.

The element K is more difficult to assess due to the poor definition of a plateau and the scarcity of samples plotting above it. Based on the discussion above, however, it is considered likely that the samples lying above the plateau in Figure 38 are more representative of the pre-alteration compositions, while those defining the plateau are more representative of altered compositions.

Comparison of the fractionation trends for TiO_2, FeO*, MgO, and P_2O_5 (Fig. 39) with the Group 1A mafic rocks (Fig. 24) again highlights the 'Zr gap' and shows also a clear 'MgO gap'. Furthermore, the P_2O_5 fractionation trend on both Zr and Y diagrams (Fig. 39) is not compatible with the fractionation trend for the

Group 1A mafic rocks (Fig. 24). Thus, the data here support the conclusion drawn from the Zr-Y relationships that the main group of felsic rocks does not belong to the same fractionation series as the Group 1A mafic rocks.

PRE-ALTERATION CHARACTER OF THE FELSIC ROCKS AND RELATION TO THE MAFIC ROCKS

Using the methods of calculation discussed in the previous section, an estimate of the average pre-alteration and altered compositions for the main group of felsic rocks are presented in Table 5. Most elements show lower standard deviation values for the altered compared with the pre-alteration compositions, reflecting again how effective the alteration process was, once initiated. Irrespective of whether an alteration model based on conserved Zr (model A) or conserved Y (model B) is chosen, substantial loss of Ti, total Fe, Mn, Mg, Ca, P, and probably K is indicated; less significant loss of Al is also implied. As argued earlier, the alteration also involved real addition of Na_2O. The question of SiO_2 addition is uncertain as it depends on the choice of model. The volume loss implicit in model A (10—15 %) would effectively increase an initial mean SiO_2 value of 69.2 % (Table 5) to between 76.9 and 81.4 % (see Table 4), thus accounting for the apparent increase; choice of model B involving Y conservation implies a small addition of SiO_2 (10—15 %) together with Zr. As far as the pervasiveness of the alteration process is concerned, its effects are most marked with respect to Na, somewhat less marked with respect to Si, Al, Ca, and K and least effective with respect to Ti, total Fe, Mn, Mg, and P. However, once the alteration initiated, the chemical reactions appear to have been efficient in removing even the more resilient species. The chemical changes noted above are consistent with pervasive breakdown of more calcic plagioclase to albite, loss of K-feldspar and less pervasive breakdown of primary ferromagnesian minerals (*e.g.* biotite, hornblende?) to chlorite. The chemical changes are quantified and the implications both of this alteration and the chemical changes apparent during the spilitization of the Group 1B basalts are discussed in Stephens (1980b).

In summary, the bulk of the felsic rocks (18 of 20 samples), containing albite-quartz-chlorite±epidote±mica±calcite mineral assemblages, are thought to represent original, variably differentiated, dacite—rhyodacite compositions, probably of the low-Al_2O_3 (Barker 1979), low-K (Peccerillo and Taylor 1976) type, which have undergone substantial alteration to quartz keratophyre. On the basis of textures represented, both volcanites and subvolcanic high-level intrusions are present. The average pre-alteration composition estimate is most readily comparable to Tertiary-Recent, low-K island arc felsic volcanites (Ewart 1979, see Table 5, column 5). The presence of SiO_2, Zr and MgO 'gaps' between the main group of felsic rocks and the Group 1A mafic rock series, and particularly the incompatibility of the respective fractionation trends on Zr *versus* Y and P_2O_5 *versus* both Zr and

TABLE 5. Mean and standard deviation of pre-alteration and altered composition estimates for the main group of felsic rocks (x = mean, s = standard deviation, number of analyses shown in brackets, volatile-free basis) and comparison with mean values of different types of Tertiary-Recent, silica-saturated, felsic (>63 % SiO_2) rocks from selected orogenic and non-orogenic regions (N = number of analyses, recalculation to 100 % on a volatile-free basis), (after Ewart 1979). The method of calculation of the pre-alteration and altered composition estimates for the main group of felsic volcanites is discussed in the text.

	Altered composition estimate		Pre-alteration composition estimate		Orogenic regions				Non-orogenic regions dacite-rhyolite	
					Mean Low-K dacite-rhyolite	Mean Medium-K dacite-rhyolite		Mean High-K dacite-rhyolite		
					S.W. Pacific and Japan-Kurile-Saipan region	S.W. Pacific and Japan-Kurile-Saipan region	Cascades-Alaska - Aleutians	Western South America	Iceland	W. Scotland-N. Ireland
	$\bar{x}$	s	$\bar{x}$	s	$\bar{x}$ (N=177)	$\bar{x}$ (N=370)	$\bar{x}$ (N=107)	$\bar{x}$ (N=99)	$\bar{x}$ (N=48)	$\bar{x}$ (N=38)
SiO_2 (%)	77.5 (14)	2.4	69.2 (4)	4.7	67.51	69.04	67.60	69.13	72.22	71.97
TiO_2	0.18 (11)	0.06	0.54 (7)	0.20	0.60	0.50	0.53	0.52	0.39	0.58
Al_2O_3	11.5 (14)	1.1	13.0 (4)	1.0	14.97	15.14	15.98	15.25	13.46	12.77
FeO^*	1.9 (9)	0.3	4.4 (9)	1.9	5.28	3.80	3.55	3.08	3.49	4.13
MnO	0.03 (6)	0.02	0.08 (8)	0.02	0.13	0.10	0.09	0.06	0.09	0.15
MgO	0.8 (12)	0.3	2.2 (6)	0.6	1.58	1.35	1.62	1.27	0.46	0.62
CaO	1.0 (14)	1.0	3.2 (4)	0.9	4.87	3.68	3.83	2.94	2.13	1.87
Na_2O	5.5 (14)	0.7	5.0 (4)	0.8	3.75	3.92	4.41	3.57	4.56	3.75
K_2O	0.3 (16)	0.2	1.3 (2)	0.2	0.94	2.15	2.07	3.81	2.93	3.83
P_2O_5	0.01 (6)	0.01	0.09 (8)	0.04	0.16	0.14	0.15	0.16	0.09	0.13
Total	98.7		99.0		99.79	99.82	99.83	99.79	99.82	99.80
Zr (ppm)	114 (8)	25	100 (4)	13	66 (34)	151 (41)	156 (24)	159 (39)	401 (14)	327 (17)
Y	43 (8)	10	43 (4)	7	23 (52)	25 (57)	23 (22)	6 (3)	44 (14)	37 (13)
Cu	5 (10)	2	28 (2)	20	19 (50)	14 (54)	24 (19)	23 (36)	9 (14)	9 (13)
Zn	30 (9)	16	91 (3)	29	92 (39)	64 (16)	67 (2)	105 (23)	125 (14)	76 (10)

Y diagrams suggest that these felsic rocks are not derived by fractional crystallization from the same basaltic parent melt that gave rise to the Group 1A island arc tholeiite series. Furthermore, on the basis of the contents of the incompatible elements P, Zr and Y, the main group of felsic rocks do not belong to either of the other mafic fractionation series (Groups 1B+2A and Group 2B). They, thus, form a separate magma series influenced themselves by fractional crystallization processes (negative trends for TiO_2, FeO*, MgO, and P_2O_5; flat to positive trend for Zr relative to Y). Two of the felsic rock samples (Analyses 59 and 66), both interpreted as volcanites and showing the same mineral assemblages as the main group, show low Zr, Y and Zr/Y values and plot along the Group 1A Zr-Y fractionation trend together with the basaltic andesites; they are tentatively suggested to represent variably altered fractionation products of the Group 1A island arc tholeiite series.

PETROGENESIS AND EVOLUTION OF MAGMAS

GENERAL REMARKS

The apparently bimodal nature of the Stekenjokk volcanites in the field is supported by the petrochemical analysis. Furthermore, it appears that the absence of silicic andesite compositions is an inherited primary feature and cannot be explained by alteration. The petrochemical analysis exposes not only the important alteration (spilitization) that both the mafic and particularly the felsic rocks have suffered but also the pre-alteration chemical inhomogeneity of the Stekenjokk volcanites, three different mafic fractionation series and a separate felsic series being proposed. Fractional crystallization appears, however, to have played an important role in each of the series, primitive magmas being only recognized with any confidence in the Groups 1B+2A mafic fractionation series.

Both the major and trace element discriminant diagrams illustrate well the different groups of mafic rocks. As indicated earlier, this data, together with the general consideration of their petrochemistry, has provided an assessment of the affinity of the three different mafic fractionation series to basaltic rocks from modern tectonic settings, *i.e.* island arc tholeiite (1A), mid-ocean ridge basalt (1B+2A) and within-plate basalt (2B), respectively. At first sight, such a mixing of 'tectonic settings' in one single formation seems difficult to understand but this clearly has much to do with the interpretation of such discriminant diagrams. It can be stated that basaltic rocks showing different major and trace element geochemistries reflect different mantle source characteristics and/or different physical conditions (P_{load}, P_{H_2O}, T) controlling varying degrees of partial melting at the mantle source site. Accepting this premise, it is likely that the various discriminant diagrams reflect variations in such parameters rather than tectonic environments

in a strict sense (Stephens 1981b). For example, affinity to mid-ocean ridge basalt does not necessarily imply basalt generation in such an environment but may imply generation under similar conditions as are found along modern mid-ocean ridge systems. Such basalts are known to form today not only along mid-ocean ridges in a truly oceanic setting but also in continental situations during *early* rifting stages and, perhaps of more relevance to the present study, at the opening and during the spreading of back-arc and inter-arc basins in volcanic arc situations.

Before assessing the tectonic significance of the magma evolution in the Stekenjokk volcanites, some constraints on the petrogenesis of the different fractionation series are presented. The discussion relies heavily on present ideas regarding the origin of equivalent modern basalts, basaltic andesites and dacite—rhyodacites.

GROUP 1A MAFIC FRACTIONATION SERIES

The Group 1A basalts and basaltic andesites, showing an IAT affinity, are both highly fractionated and depleted in the more incompatible elements (*e.g.* Zr) and the Zr/Y ratio relative to MORB.

The Group 1A rocks pose the same petrochemical enigma as more recent island arc tholeiites (Ringwood 1974). As emphasized by Pearce and Norry (1979), the low Zr in these types of magmas cannot be *solely* explained by a higher degree of partial melting or lower degree of fractional crystallization compared to MORB, since Ni and Cr should also be higher than MORB in both of these cases. Furthermore, the intimate spatial relationship between active orogenic-type volcanism and depth to Benioff Zone suggests magma generation at great depths under high P_{load}; this raises problems regarding basalt genesis due to limitations on the primary field of crystallization of olivine with P_{load} (Ringwood 1974).

A solution to these problems was suggested by Nicholls and Ringwood (1973) by invoking direct partial melting of mantle pyrolite (unfractionated primary mantle, Green and Ringwood 1967) above the Benioff Zone, under conditions of high load pressure and *high water pressure*, the latter effectively extending the pressure at which olivine remains on the liquidus (for an olivine tholeiite composition, for example, olivine remains on the liquidus up to 27 kb at $P_{H_2O} = P_{load}$ compared with 13 kb under anhydrous conditions). Their results indicate that generation of an olivine tholeiite melt is possible down to a depth of 100 km by partial melting of mantle under water-saturated conditions. A high degree of partial melting of unfractionated primary mantle, related to high P_{H_2O} (Green 1973), will give rise to basalts with low Zr content and low Zr/Y ratio (Pearce and Norry 1979). Due to the decreasing solubility of water in the melt at decreasing pressure, rise of these magmas to shallower depths (P_{load} and P_{H_2O} decreasing) causes olivine and Cr-spinel precipitation (Nicholls and Ringwood 1973). Such crystallization explains the generation of basaltic andesite from basalt and the

highly fractionated character of the IAT series. Ringwood (1974) emphasized the role of amphibolite in the subducting oceanic slab and its dehydration to eclogite + H_2O (Lambert and Wyllie 1968) in the depth interval 80—100 km as a means of providing the necessary water to the mantle immediately overlying the Benioff Zone.

Based on the above, the peculiar highly fractionated yet depleted minor and trace element characteristics of the Group 1A series may be explained by a high degree of partial melting of upwelling mantle material immediately overlying a Benioff Zone combined with a high degree of fractional crystallization (olivine+Cr-spinel±pyroxene), both related to an initially high P_{H_2O} at the partial melting site; basaltic magma generation down to depths of approximately 80—100 km is suggested. Consideration of the content of TiO_2 in the least fractionated of the Group 1A samples (0.31%) suggests that the mantle source was more depleted, at least with respect to this element, than the pyrolite composition (0.7 % TiO_2) of Green and Ringwood (1967).

GROUPS 1B+2A MAFIC FRACTIONATION SERIES

The tholeiitic 1B+2A basalts, displaying both more primitive and more differentiated magmas in a proposed single fractionation series, show an affinity to MORB. Higher values of both the more incompatible (*e.g.* Zr) and compatible (*e.g.* Ni, Cr) elements and the Zr/Y ratio relative to the 1A series characterize these basalts. All the 2A and some of the 1B rocks are high-level intrusions, the more differentiated 2A rocks belonging to the latest phase of magmatic activity in the Stekenjokk volcanites.

The similarity to MORB suggests that these basalts were generated under similar mantle melting conditions as basalts at mid-ocean ridge settings. Thus, partial melting of unfractionated primary mantle under relatively shallow, dry conditions during upwelling of mantle material from a low-velocity layer is inferred (Green 1971, 1972). An important consequence of drier partial melting conditions is to reduce the degree of partial melting (Green 1973). Pearce and Norry (1979) have shown that variation in the degree of partial melting of mantle material, in particular progressive partial melting, affects, for example, Zr contents and Zr/Y ratios of the resultant basaltic melts. In particular, lower degrees of partial melting leads to increased Zr content and Zr/Y ratio.

Such a low-velocity layer, usually extending between 50 and 250 km depth, probably existed in the upper mantle wedge above the Benioff Zone and, in part, above the site of Group 1A magma generation proposed in the previous section. It is suggested that generation of the 1B+2A series occurred at shallower depths than the 1A series, further away from the Benioff Zone, thus fulfilling the necessary conditions of magma generation under both lower P_{load} and P_{H_2O}. Lower degrees

both of partial melting and olivine+Cr-spinel±pyroxene crystallization related to lower P_{H_2O} are thought to account for the different minor and trace element characteristics of these basalts compared with the Group 1A basalts and basaltic andesites; significant plagioclase separation is also suggested from the composition of the 2A rocks.

GROUP 2B MAFIC FRACTIONATION SERIES

The strongly fractionated, mildly alkalic Group 2B basalts, showing a WPB affinity, are notably enriched in P and K and probably Zr and Y in more parental magmas compared to the other groups of mafic rocks. Furthermore, Ti shows a more compatible behaviour than in the other groups. The Group 2B rocks, together with the more differentiated basaltic rocks of the 1B+2A series, define the latest phase of magmatic activity in the Stekenjokk volcanites.

Mantle source heterogeneity with respect to moderately and strongly incompatible minor and trace elements (*e.g.* Ti, K, P, Zr, Y which are of interest in this study) has been invoked as an explanation for the peculiar enrichment of these elements in WPB magmas (see, for example, Green 1968; Schilling 1973; Hart *et al.* 1973; Frey *et al.* 1978). Migration within the upper mantle (low-velocity layer or lower) of either a melt or a H_2O/CO_2-enriched supercritical fluid depleting certain mantle regions and enriching others is one mechanism which has been invoked to explain the creation of such heterogeneities (*e.g.* Lloyd and Bailey 1975, Frey *et al.* 1978). Frey *et al.* (1978) have also demonstrated how a single mantle source can give rise to a variety of within-plate basaltic compositions ranging from strongly silica-undersaturated basalt to olivine tholeiite by varying degrees of partial melting, more alkalic and more tholeiitic types forming at lower and higher degrees of partial melting respectively (note also Gast 1968; Green 1973). The lower degrees of partial melting associated with the generation of more alkalic basalts may be a result of magma generation at a relatively deeper site (Green and Ringwood 1967).

The above considerations suggest that the Group 2B magmas were generated by a relatively low degree of partial melting (<15—20 %, see Frey *et al.* 1978) of a mantle source enriched in at least the minor and trace elements P, K, Zr, and Y. Subsequent olivine+Cr-spinel±pyroxene crystallization together with significant removal of plagioclase and a Ti-rich phase would explain the highly fractionated character of these basaltic rocks. It is emphasized that the Group 2B rocks show closest temporal affinity to the emplacement of the more differentiated basaltic rocks of the 1B+2A series, and accordingly their generation is thought to be more closely related to the MORB-affinity 1B+2A rather than IAT-affinity 1A magmatism. It is suggested that the source of the heterogeneity postulated above may arise from the previous melting history of the mantle wedge above the Benioff

Zone, some earlier 1A or even 1B melts not being able to escape from the mantle and, thus, giving rise to pockets locally enriched in the more incompatible elements P, K, Zr, and Y.

FELSIC FRACTIONATION SERIES

The intense alteration which the felsic rocks have suffered leads to difficulties in assessing pre-alteration compositions and, thus, speculations on petrogenesis. However, although it is possible that the two samples with very low Zr and Y contents and Zr/Y values represent highly altered fractionation products of the 1A mafic rock series, the bulk of the felsic rocks appear to form a separate fractionation series unrelated to any of the mafic series represented in the Stekenjokk volcanites. It is tentatively suggested that the main group of felsic rocks represents a fractionation series ranging from dacite to rhyodacite, probably of the low-Al_2O_3, low-K type, and most readily comparable to Tertiary-Recent, low-K island arc felsic volcanites. However, it is noteworthy that, although these felsic rocks occur in intimate spatial and temporal association with mafic island arc tholeiites (1A mafic series), the proportion of felsic rocks is much greater in the Stekenjokk volcanites than in Tertiary-Recent island arcs where the mafic volcanism is tholeiitic rather than calc-alkalic.

Generation of such dacitic melts by either low pressure fractional crystallization from or partial melting of a mafic rock parent under both relatively dry and relatively wet conditions has been summarized by Barker and Arth (1976). Various fractionation/residue models have been invoked to explain major and trace element distributions involving eclogite (Hanson and Goldich 1972; Arth and Hanson 1972), amphibole (Arth and Barker 1976), plagioclase (Barker *et al.* 1976) or some combination, the experimental works of Green and Ringwood (1968, 1972), Holloway and Burnham (1972) and Helz (1973, 1976), for example, providing a basis for these ideas. The dominance of felsic rocks in the Stekenjokk volcanites and, more significantly, the independence of the main group from the different mafic fractionation series argue strongly for a model or models for this group based on partial melting of a mafic parent. Based on the discussion in Ringwood (1974), the low K_2O and Zr values of the Stekenjokk felsic rocks are more compatible with amphibole as a residual product, thus restricting the generation of these melts to depths of less than 90—100 km. Separation of plagioclase is suggested from the occurrence of plagioclase (together with quartz) phenocrysts and this may well be controlling the low-Al_2O_3 nature of the Stekenjokk felsic rocks. The location of the partial melting event is more controversial; two models consistent with the above, the magmatic history in the Stekenjokk volcanites and the island arc setting indicated by the spatially and temporally related 1A mafic series are suggested below:

1. Partial melting of low-K_2O basalt at the root of an island arc, *i.e.* a crustal location under conditions of low P_{load}. Even at high P_{H_2O}, temperatures just under or greater than 700°C are required (Helz 1976).

2. Partial melting of the upper basaltic part of the downgoing lithospheric slab along a Benioff Zone, *i.e.* a sub-crustal location at higher P_{load} than the crustal model above but nevertheless at depths of less than 90—100 km. Conditions of high P_{H_2O} and temperatures just under or greater than 700°C are required (Green and Ringwood 1968, 1972; Green 1972; Helz 1976).

The first model, by definition, allows for the intimate spatial and temporal association of the felsic and 1A mafic rocks but requires very high geothermal gradients. If the Stekenjokk volcanites formed on the flank of an arc which was as much as 10 km thick prior to deformation, geothermal gradients at least in the order of 70°C/km would be necessary.

The high P_{H_2O} conditions required in the second model would be attained at the depths mentioned, since hydrous phases in the subducting slab only start to break down at depths greater than 100 km (Ringwood 1974, note earlier discussion). From the various models presented for the temperature distribution in a downgoing slab of lithosphere (see, for example, Oxburgh and Turcotte 1970; Toksöz *et al.* 1971; Griggs 1972), it appears possible that temperatures near to or greater than 700°C may be attained in the upper part of the subducting plate at depths of around 100 km; thus, the temperature conditions required by the second model may be fulfilled. It is noteworthy that similar depth and P_{H_2O} conditions are indicated for generation of the felsic rocks using the second model and for the 1A mafic series. Thus, the second model also allows for the intimate spatial and temporal association of the Stekenjokk felsic rocks and the 1A mafic series.

WORKING MODEL

Based on the discussion above, a two-stage model, relying heavily on modern petrogenetic thinking as applied to Tertiary-Recent magmas, is suggested for the magmatic evolution of the Stekenjokk volcanites (Fig.40). Processes of spilitization converting the more mafic rocks into spilites and the felsic rocks into quartz keratophyres are ignored here (note, however, Stephens 1980b).

The first stage, giving rise to the Group 1A mafic series and the felsic rocks, is dictated by subduction of a downgoing lithospheric slab in a convergent plate margin situation and development of an island arc.

The direction and amount of dip of the Benioff Zone shown in Figure 40 (45°E) is chosen arbitrarily. Since the felsic rocks are probably of the low-K type, it is inferred that there was no contribution by continental crust to the magmas; this

may well imply that the Stekenjokk arc was founded on either oceanic or very thin continental crust. At 80—100 km depth and at temperatures near to or greater than 700°C, dehydration and possibly partial melting of the amphibolitic (variably spilitic) oceanic crust would occur. Fluids released during the dehydration reactions would rise into the immediately overlying mantle wedge and initiate mantle diapirism and generation of tholeiitic basaltic melts under high P_{load} and high P_{H_2O} conditions. At shallower levels, these melts would undergo severe fractional crystallization (olivine+Cr-spinel±pyroxene) giving rise to basalts with very low compatible element contents and basaltic andesites (1A mafic series with IAT affinity). Partial melting of the upper part of the downgoing slab with amphibole as a residual phase, again under high P_{load} and high P_{H_2O} conditions, and subsequent fractional crystallization of plagioclase may account for the main group of felsic rocks. Alternatively, without partial melting of the downgoing slab, they may have formed by partial melting of basalt at the root of the island arc, *i.e.* a crustal location under conditions of low P_{load}, combined with fractional crystallization of plagioclase at shallower levels.

The second stage, giving rise to the Groups 1B+2A and 2B mafic series, is dictated by upwelling of mantle material from the low-velocity layer lying above the Benioff Zone established during stage 1. Since several of the Group 1B mafic rocks are inferred to be volcanic and intimately interlayered with 1A mafic rocks and the felsic rocks, it is emphasized that stage 2 overlapped temporally with stage 1. However, since the more differentiated members (Group 2A) of the 1B+2A series and all Group 2B rocks appear to be intrusive into the total Stekenjokk pile, even the stratigraphically youngest(?) tuffite—phyllite complex, it is inferred that stage 2 continued after the cessation of stage 1. Magma generation during stage 2 occurred under both lower P_{load} and P_{H_2O} than during stage 1, and only basalts were produced. The mantle source appears to have been somewhat heterogeneous, unfractionated primary mantle giving rise to the tholeiitic 1B+2A series and a lower degree of partial melting of a mantle source enriched in at least P, K, Zr, and Y giving rise to the subordinate mildly alkalic 2B series. The source of this heterogeneity is tentatively suggested to be due to the previous melting history of the mantle wedge above the Benioff Zone (stage 1 and early stage 2), resulting in pockets locally enriched in the more incompatible elements P, K, Zr, and Y. Separation of olivine+Cr-spinel±pyroxene, plagioclase and a Ti-rich phase (2B series only) is necessary at higher levels as the magmas approached the surface. The magmas produced during stage 2, showing mixed MORB and WPB affinity, are typical of rifting situations.

It is suggested that the stage 1 magmas represent establishment of an island arc in a probably ensimatic setting, while the stage 2 magmas represent an incipient rifting of the arc. It is uncertain whether the rifting episode attained the advanced stage depicted in Figure 40d (ocean basin opening). Two challenging problems are

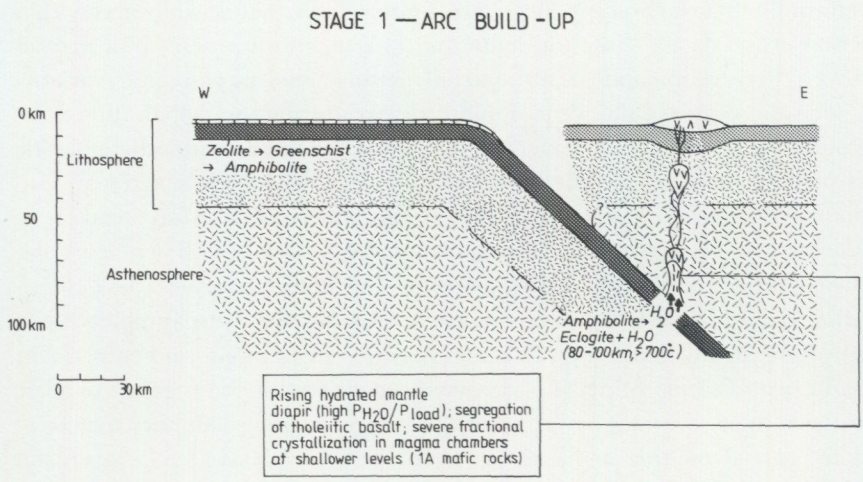

a

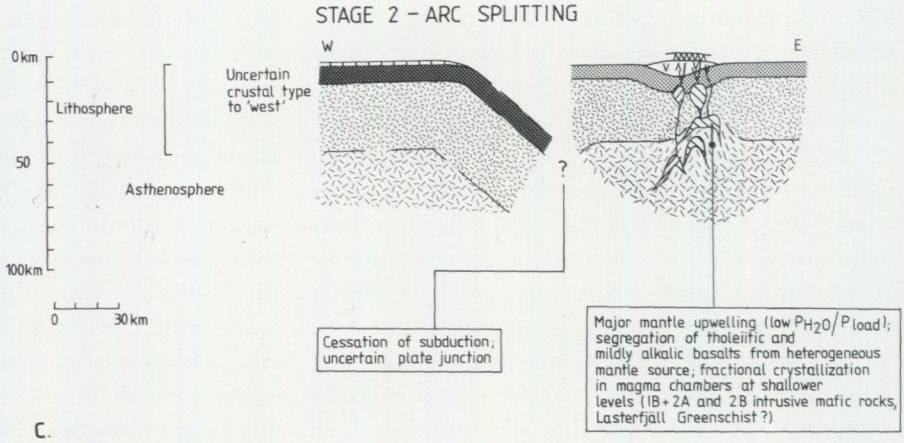

c.

LEGEND

Oceanic sediment

Island arc, part of which — eastern segment in d. — is represented by Stekenjokk volcanites

Lasterfjäll Greenschist, gabbros within Blåsjö Phyllite

Oceanic crust

Crust of uncertain type (oceanic or thin continental?) in overriding plate

Peridotitic lithosphere (Upper Mantle)

Sub-lithosphere mantle

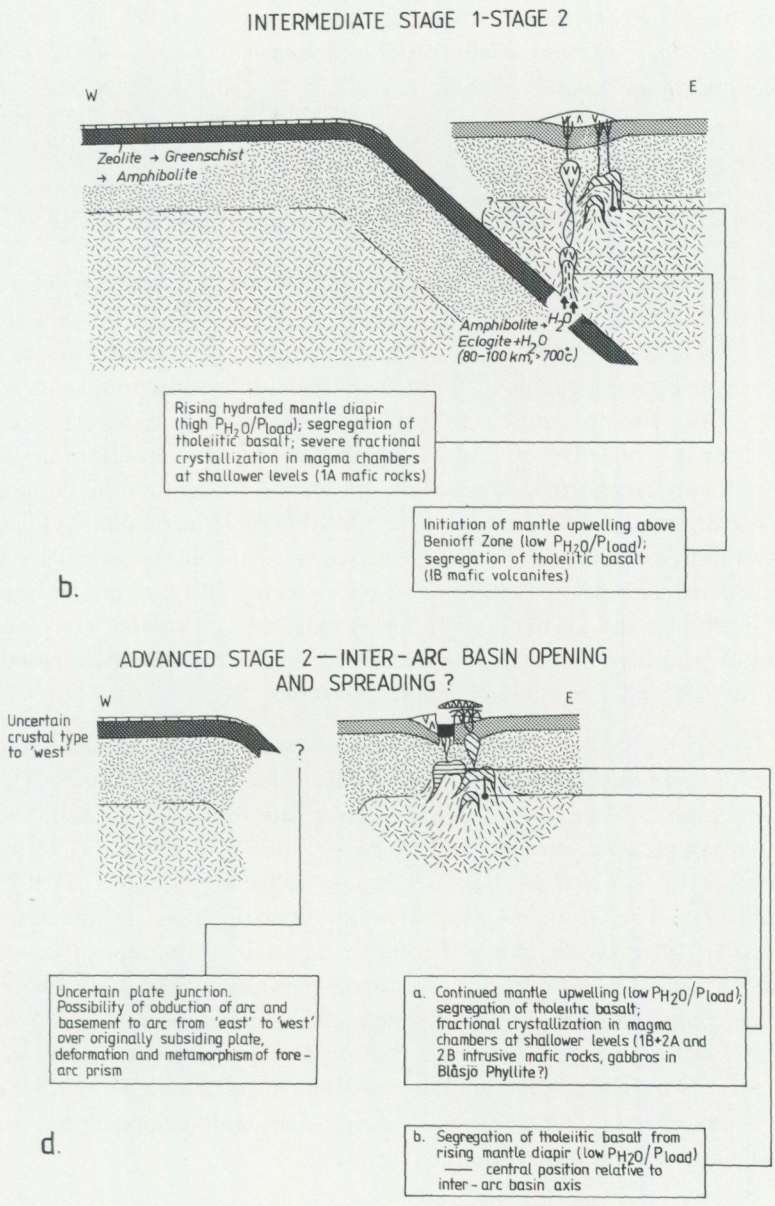

Fig. 40. A working model for the evolution of the Stekenjokk volcanites. Generation of felsic volcanites not represented in this figure. They are thought to have formed during arc build-up (Stage 1 and intermediate Stage 1 — Stage 2) by partial melting of basalt either along the Benioff Zone at depths not greater than 90—100 km or at the root of the island arc itself, *i.e.* crustal depths, and subsequent plagioclase separation at shallower levels. For further details, see discussion in text.

raised by this working model: What caused the arc, to which the Stekenjokk volcanites belong, to rift and to what other tectonic events such a radical change in the Stekenjokk magmatism is related?

SUMMARY OF RESULTS AND CONCLUDING REMARKS

1. Inspection of the chemical data for the mafic rocks, emphasizing particularly the distribution of the elements Ti, Mg, K, P, Zr, Y, Ni, and Cr as well as the ratios FeO*/MgO and Zr/Y, suggests breakdown of each of the field/microscope-distinguishable mafic rock groups into two subgroups (1A and 1B, 2A and 2B). The breakdown of the darker Group 2 mafic rocks corresponds to amphibole-bearing (Group 2A) and amphibole-free (Group 2B) mineralogical types already recognized. Application of Q-mode cluster analysis supports the proposed breakdown. The contents of relatively more incompatible (Ti, P, Zr, Y) and more compatible (Ni, Cr) elements as well as the varying behaviour of the elements Ti, total Fe, P, and Zr with increasing differentiation indicate that the Groups 1A and 2B mafic rocks form separate fractionation series, and that the more primitive 1B basalts may well complement the more differentiated 2A basaltic rocks in a third mafic fractionation series.

2. The Group 1A basalts and basaltic andesites (mineral assemblages = chlorite-albite±amphibole±epidote±calcite±Ti-rich minerals; probably both volcanites and high-level intrusions) are strongly spilitic and show a mildly tholeiitic differentiation trend (strong Mg/Ni/Cr separation from the liquid, initial concentration in followed by later separation from the liquid of Ti/P/Fe and possibly Zr). The Group 1A rocks are both highly fractionated and, relative to mid-ocean ridge basalt (MORB), highly depleted in the more incompatible elements and Zr/Y ratio; they show a strong affinity to island arc tholeiites. It is, thus, suggested that they were generated at depths down to approximately 80—100 km by a high degree of partial melting of upwelling mantle material immediately overlying a Benioff Zone, combined with a high degree of fractional crystallization of olivine+Cr-spinel±pyroxene; both factors are related to an initially high P_{H_2O} at the partial melting site.

3. The Groups 1B+2A basaltic rocks (mineral assemblages=chlorite-albite ±amphibole±epidote±calcite±Ti-rich minerals in the more primitive (1B) samples and amphibole-albite-chlorite-epidote-Ti-rich minerals±calcite in the more differentiated (2A) samples; predominantly high-level intrusions) are variably spilitic and show a strongly tholeiitic differentiation trend (mild to moderate Mg/Ni/Cr separation from the liquid, strong Fe-Ti-P-Zr-Y enrichment in residual melts). Allowing for the broad range in degree of fractionation

in the 1B+2A series as well as Cr and minor Zr losses during spilitization of 1B basalts, an affinity to mid-ocean ridge basalt (MORB) is indicated. Thus, it is thought that these basaltic rocks were generated by partial melting of unfractionated primary mantle under relatively shallow, dry conditions during upwelling of mantle material from a low-velocity layer, combined with, in the case of the 2A rocks especially, a moderate degree of fractional crystallization of olivine+Cr-spinel±pyroxene and plagioclase. Lower degrees of both partial melting and olivine+Cr-spinel±pyroxene crystallization related to lower P_{H_2O} are thought to account for the different minor and trace element characteristics of these basaltic rocks compared with the 1A series.

4. The Group 2B basaltic rocks (mineral assemblages = chlorite-albite-calcite-Ti-rich minerals±biotite±epidote±apatite±white mica; high-level intrusions only) are apparently little altered and mildly alkalic and highly differentiated in character. They show a firm within-plate basalt (WPB) affinity, being enriched in P, K and probably Zr and Y in more parental magmas compared with the other mafic rock series. It is suggested that they were generated by a relatively low degree of partial melting of a mantle source enriched in, at least, the minor and trace elements P, K, Zr, and Y, combined with a high degree of crystallization of olivine+Cr-spinel±pyroxene, plagioclase and a Ti-rich phase. It is speculated that partial melting occurred under higher P_{load} conditions than for the 1B+2A series and that the mantle source heterogeneity may be a function of the complex, earlier melting history of the mantle wedge lying above the postulated Benioff Zone.

5. The chemical variation within the Stekenjokk mafic rocks can be largely explained by secondary alteration processes combined with fractional crystallization *within* the three separate fractionation series. Partial melting of a mantle source under varying P_{H_2O} (1A>1B+2A and 2B) and P_{load} (1A>2B>1B+2A) conditions, controlling both varying degrees of partial melting and Mg/Ni/Cr separation from the liquid, together with mantle source heterogeneity are thought to be dictating the chemical variation *between* the different mafic series.

6. The bulk of the felsic rocks investigated petrochemically (mineral assemblages = albite-quartz-chlorite±epidote±mica±calcite±Fe-Ti oxides; both volcanites and high-level intrusions) represent original variably differentiated dacite—rhyodacite compositions, probably of the low-Al_2O_3, low-K type. However, similar to the basalt and basaltic andesite to spilite alteration, the felsic rocks have suffered substantial alteration to quartz keratophyre. On the basis of the contents of the more incompatible elements, P, Zr and Y, the presence of SiO_2, Zr and MgO 'gaps' (silicic andesite compositions absent) and the form of Zr-Y, P_2O_5-Zr and P_2O_5-Y variation trends, it appears that the main group of felsic rocks does not belong to any of the three mafic fractionation series which have

been recognized. Instead, they are thought to have formed by partial melting of a basaltic parent with amphibole as a residual product and subsequent separation of plagioclase from the resultant liquid. Alternative models involving partial melting of either the subducting slab of basaltic oceanic crust along the postulated Benioff Zone (sub-crustal depths, but not greater than 90—100 km) or low-K_2O basaltic material at the root of the island arc (crustal depths) are suggested.

7. Two felsic rock samples investigated, both interpreted as volcanic and showing the same mineral assemblages as the main group, show low Zr, Y and Zr/Y values and plot along the Group 1A Zr-Y variation trend together with basaltic andesites. They are possibly altered fractionated products of the Group 1A island arc tholeiite series.

8. A two-stage working model is suggested for the Stekenjokk volcanites involving firstly build-up of an island arc in a probably ensimatic setting (generation of felsic rocks and 1A mafic series) passing progressively over to a rifted arc situation (generation of 1B+2A and 2B mafic series).

ACKNOWLEDGEMENT

This paper is a contribution to the IGCP Project No. 60 "Correlation of Caledonian Stratabound Sulphides". Discussions and critical remarks by T. Sjöstrand, K. Sundblad och E. Zachrisson (all at SGU) are gratefully acknowledged. It is also with pleasure that I thank G. Kautsky (SGU) for his support and interest in the IGCP-CCSS project.

REFERENCES

AMSTUTZ, G.C., 1968: Spilites and spilitic rocks. — *In* H.H. Hess and A. Poldervaart (edits.): The Poldervaart Treatise on Rocks of Basaltic Composition, Wiley-Interscience, London and New York, p. 737—753.

— 1974: Spilites and spilitic rocks. — Springer-Verlag, Berlin, Heidelberg and New York, 482 pp.

ARTH, J.G., and BARKER, F., 1976: Rare-earth partitioning between hornblende and dacitic liquids and implications for the genesis of trondhjemitic-tonalitic magmas. — Geology, v. 4, p. 534—536.

ARTH, J.G., and HANSEN, G.N., 1972: Quartz diorites derived by partial melting of eclogite or amphibolite at mantle depths. — Contr. Mineral. Petrol., v. 37, p. 161—174.

ASKLUND, A-M., GRUNDULIS, V., and RÖNNHOLM, B., 1966: Våtkemisk analys av silikatbergarter. — Sveriges Geol. Unders. C 616, 55 pp.

AUMENTO, F., MITCHELL, W.S., and FRATTA, M., 1976: Interaction between sea-water and oceanic layer two as a function of time and depth. — 1. Field evidence. — Can. Mineral., v. 14, p.269—290.

BAKER, P.E., 1968: Comparative volcanology and petrology of the Atlantic island-arcs. — Bull. Volcanol., v. 32, p. 189—206.

BARKER, F., 1979: Trondhjemite: definition, environment and hypotheses of origin. — *In* F. Barker (edit.): Trondhjemites, Dacites and Related Rocks, Developments in Petrology 6, Elsevier, Amsterdam, Oxford and New York, p. 1—12.

BARKER, F., and ARTH, J.G., 1976: Generation of trondhjemitic-tonalitic liquids and Archean bimodal trondhjemite-basalt suites. — Geology, v. 4, p. 596—600.

BARKER, F., ARTH, J.G., PETERSEN, Z.G., and FRIEDMAN, I., 1976: The 1.7—1.8 b.y.-old trondhjemites of southwestern Colorado and northern New Mexico: Geochemistry and depth of genesis. — Bull. Geol. Soc. Am., v. 87, p. 189—198.

BATTEY, M.H., 1955: Alkali metasomatism and the petrology of some keratophyres. — Geol. Mag., v. 92, p. 104—126.

BEACH, A., 1974: A geochemical investigation of pressure solution and the formation of veins in a deformed greywacke. — Contr. Mineral. Petrol., v. 46, p. 61—68.

BECKHOLMEN, M., 1980: Geology of the Nordhallen-Duved-Greningen area in Jämtland, central Swedish Caledonides, — Geol. Fören. Stockh. Förh., v. 100, p. 335—347.

BLOXAM, J.W., and LEWIS, A.D., 1972: Ti, Zr and Cr in some British pillow lavas and their petrogenetic affinities. — Nature Phys. Sci., v. 237, p. 134—136.

BONATTI, E., HONNOREZ, J., KIRST, P., and RADICATI, F., 1975: Metagabbros from the mid-Atlantic ridge at 06°N : Contact-hydrothermal-dynamic metamorphism beneath the axial valley. — J. Geol., v. 83, p. 61—78.

BROOKS, C.K., and JAKOBSSON, S.P., 1974: Petrochemistry of volcanic rocks of the North Atlantic ridge system. — *In* L. Kristjansson (edit.): Geodynamics of Iceland and the North Atlantic Areas, Reidel, Dordrecht, p. 139—154.

BRYAN, W.B., STICE, G.D., and EWART, A., 1972: Geology, petrography and geochemistry of the volcanic island of Tonga. — J. Geophys. Res., v. 77, p. 1566—1587.

CANN, J.R., 1969: Spilites from the Carlsberg Ridge, Indian Ocean. — J. Petrol., v. 10, p. 1—19.

— 1971: Major element variations in ocean-floor basalts. — Phil. Trans. Roy. Soc. Lond., v. A268, p. 495—505.

CHALOUPSKY, J., and FEDIUK, F., 1967: Geology of the western and north-eastern part of the Meråker area. — Norges Geol. Unders., v. 245, p. 9—21.

CHAYES, F., 1964: A petrographic distinction between Cenozoic volcanics in and around the open oceans. — J. Geophys. Res., v. 69, p. 1573—1588.

CHURKIN, M., CARTER, C., and JOHNSON, B.R., 1977: Subdivision of Ordovician and Silurian time scale using accumulation rates of graptolitic shale. — Geology, v. 5, p. 452—456.

DANIELSSON, A., 1967: Spectrochemical analysis for geochemical purposes. — Colloq. Spec. Int. XIII, Ottawa, p. 311—323.

DAVIS, J.C., 1973: Statistics and Data Analysis in Geology. — John Wiley and Sons Inc., London and New York, 550 pp.

DICKINSON, W.R., 1962: Metasomatic quartz keratophyre in Central Oregon. — Am. J. Sci., v. 260, p. 249—266.

DONNELLY, T.W., 1966: Geology of St. Thomas and St. John, U.S. Virgin Islands. — Mem. Geol. Soc. Am., v. 98, p. 85—176.

DU RIETZ, T., 1941: Nyare undersökningar inom Remdalens malmtrakt och dess omgivningar. — Sveriges Geol. Unders. C439, 85 pp.

ELLIOTT, R.B., 1973: The chemistry of gabbro/amphibolite transitions in South Norway. — Contr. Mineral. Petrol., v. 38, p. 71—79.

ENGEL, A.E.J., and ENGEL, C.G., 1970: Mafic and ultramafic rocks. — *In* A.E. Maxwell (edit.), The Sea, v. 4, Interscience (Wiley), London and New York, p. 465—519.

ENGEL, A.E.J., ENGEL, C.G., and HAVENS, R.G., 1965: Chemical characteristics of oceanic basalts and the upper mantle. — Bull. Geol. Soc. Am., v. 76, p. 719—734.

EWART, A., 1979: A review of the mineralogy and chemistry of Tertiary-Recent dacitic, latitic, rhyolitic and related salic volcanic rocks. — *In* F. Barker, (edit.), Trondhjemites, Dacites and Related Rocks, Developments in Petrology 6, Elsevier, Amsterdam, Oxford and New York, p. 13—121.

EWART, A., BROTHERS, R.N., and MATEEN, A., 1977: An outline of the geology and geochemistry, and the possible petrogenetic evolution of the volcanic rocks of the Tonga-Kermadec-New Zealand island arc. — J. Volcanol. Geotherm. Res., v. 2, p. 205—250.

EWART, A., BRYAN, W.B., and GILL, J.B., 1973: Mineralogy and geochemistry of the younger volcanic islands of Tonga, Southwest Pacific. — J.Petrol., v. 14, p. 429—465.

FAYE, G.C., and ØDEGÅRD, M., 1975: Determination of major and trace elements in rocks employing optical emission spectroscopy and X-ray fluorescence. — Norges Geol. Unders., v. 322, p. 35—53.

FIELD, D., and ELLIOT, R.B., 1974: The chemistry of gabbro/amphibolite transitions in South Norway: trace elements. — Contr. Mineral. Petrol., v. 47, p. 63—76.

FLANAGAN, F.J., 1973: 1972 values for international geochemical reference samples. — Geochim. Cosmochim. Acta, v. 37, p. 1189—1200.

FLOYD, P.A., and WINCHESTER, J.A., 1975: Magma type and tectonic setting discrimination using immobile elements. — Earth Planet. Sci. Lett., v. 27, p. 211—218.

FREY, F.A., GREEN, D.H., and ROY, S.D., 1978: Integrated models of basalt petrogenesis : a study of quartz tholeiites to olivine melilitites from South Eastern Australia utilizing geochemical and experimental petrological data. — J. Petrol., v. 19, p. 463—513.

GAST, P.W., 1968: Trace element fractionation and the origin of tholeiitic and alkaline magma types. — Geochim. Cosmochim. Acta, v. 32, p. 1057—1086.

GEE, D.G., 1968: The structure of Arefjället, Västerbottens län. — Abstract, 8th Nord. Geol. Vintermötet 1968, Geol. Fören. Stockh. Förh., v. 90, p. 458.

GEE, D.G., and ZACHRISSON, E., 1979: The Caledonides in Sweden. — Sveriges Geol. Unders. C769, 48 pp.

GETZ, A., 1890: Graptolitførende skiferzoner i det trondhjemske. — Nyt. Mag. Naturv., v. 3, p. 31—42.

GILL, J.B., 1970: Geochemistry of Viti Levu, Fiji, and its evolution as an island arc. — Contr. Mineral. Petrol., v. 27, p. 179—203.

GRAHAM, C.M., 1976: Petrochemistry and tectonic significance of Dalradian metabasaltic rocks of the SW Scottish Highlands. — Jl. Geol. Soc. London, v. 132, p. 61—84.

GRAY, D.R., 1977: Differentiation associated with discrete crenulation cleavages. — Lithos, v. 10, p. 89—101.

GREEN, D.H., 1968: Origin of basaltic magmas. — *In* H.H. Hess and A. Poldervaart (edits.): The Poldervaart Treatise on Rocks of Basaltic Composition, Wiley-Interscience, London and New York, p. 835—862.

— 1971: Compositions of basaltic magmas as indicators of conditions of origin : application to oceanic volcanism. — Phil. Trans. Roy. Soc. Lond., v. A268, p. 707—725.

— 1972: Magmatic activity as the major process in the chemical evolution of the Earth's crust and mantle. — *In* A.R. Ritsema, (edit.): The Upper Mantle, Tectonophysics, v. 13, p. 47—71.

— 1973: Contrasted melting relations in a pyrolite upper mantle under mid-oceanic ridge, stable crust and island arc environments. — *In* P.J. Wyllie, (edit.): Experimental Petrology and Global Tectonics, Tectonophysics, v. 17, p. 285—297.

GREEN, D.H., and RINGWOOD, A.E., 1967: The genesis of basaltic magmas. — Contr. Mineral. Petrol., v. 15, p. 103—190.

GREEN, T.H., and RINGWOOD, A.E., 1968: Genesis of the calc-alkaline igneous rock suite. — Contr. Mineral. Petrol., v. 18, p. 105—162.

GREEN, T.H., and RINGWOOD, A.E., 1972: Crystallization of garnet-bearing rhyodacite under high pressure hydrous conditions. — Jl. Geol. Soc. Aust., v. 19, p. 203—212.

GRENNE, T., GRAMMELTVEDT, G., and VOKES, F.M., 1980: Cyprus-type sulphide deposits in the western Trondheim district, central Norwegian Caledonides. — *In* A. Panayiotou (edit.): Ophiolites. Proceedings International Ophiolite Symposium Cyprus 1979, Geol. Survey Cyprus, p. 727—743.

GRIGGS, D.T., 1972: The sinking lithosphere and the focal mechanism of deep earthquakes. — *In* E.C. Robertson, (edit.): The Nature of the Solid Earth. McGraw-Hill, New York, 677 pp.

GUNN, B.M., and ROOBOL, M.J., 1976: Metasomatic alteration of the predominantly island arc igneous suite of the limestone Caribees (E.Caribbean). — Geol. Rundschau, v. 65, p. 1078—1108.

HANSEN, G.N., and GOLDICH, S.S., 1972: Early Precambrian rocks of the Saganaga Lake — Northern Light Lake Area, Minnesota-Ontario: Part II : Petrogenesis. — Mem. Geol. Soc. Am., v. 135, p. 179—192.

HARDENBY, C., 1980: Geology of the Kjølhaugan area, eastern Trøndelag, central Scandinavian Caledonides. — Geol. Fören. Stockh. Förh., v. 102, p. 475—492.
HART, R.A., 1970: Chemical exchange between sea water and deep ocean basalt. — Earth Planet. Sci. Lett., v. 9, p. 269—279.
HART, S.R., 1969: K, Rb, Cs contents and K/Rb, K/Cs ratios of fresh and altered submarine basalts. — Earth Planet. Sci. Lett., v. 6, p. 295—303.
— 1971: K, Rb, Cs, Sr and Ba contents and Sr isotope ratios of ocean floor basalts. — Phil. Trans. Roy. Soc. Lond., v. A268, p. 573—587.
HART, S.R., ERLANK, A.J., and KABLE, E.J.D., 1974: Sea-floor basalt alteration : some chemical and Sr isotope effects. — Contr. Mineral. Petrol., v. 44, p. 219—230.
HART, S.R., SCHILLING, J-G., and POWELL, J.L., 1973: Basalts from Iceland and along the Reykjanes Ridge : Sr isotope geochemistry. — Nature Phys. Sci., v. 246, p. 104—107.
HAWKINS, J.W.Jr., 1976: Petrology and geochemistry of basaltic rocks of the Lau Basin. — Earth Planet. Sci. Lett., v. 28, p. 283—297.
HEKINIAN, R., 1971: Chemical and mineralogical differences between abyssal hill basalts and ridge tholeiites in the Eastern Pacific Ocean. — Marine Geol., v. 11, p. 77—91.
HELLMAN, P.L., and HENDERSON, P., 1977: Are rare earth elements mobile during spilitization? — Nature, v. 267, p. 38—40.
HELZ, R.T., 1973: Phase relations of basalts in their melting range at P_{H_2O} = 5 kb as a function of oxygen fugacity. Part I Mafic phases. — J. Petrol., v. 14, p. 249—302.
— 1976: Phase relations of basalts in their melting ranges at P_{H_2O} = 5 kb. Part II, Melt compositions. — J. Petrol., v. 17, p. 139—193.
HERRMANN, A.G., POTTS, M.J., and KNAKE, D., 1974: Geochemistry of the rare earth elements in spilites from the oceanic and continental crust. — Contr. Mineral. Petrol., v. 44, p. 1—16.
HOLLOWAY, J.R., and BURNHAM, C.W., 1972: Melting relations of basalt with equilibrium water pressure less than total pressure. — J. Petrol., v. 13, p. 1—29.
HUGHES, C.J., 1973: Spilites, keratophyres and the igneous spectrum. — Geol. Mag., v. 109, p. 513—527.
HUTCHISON, M.N., and SCOTT, S.D., 1980: Sphalerite geobarometer applied to metamorphosed sulfide ores of the Swedish Caledonides and U.S. Appalachians. — Norges Geol. Unders., v. 360, p. 59—71.
HÄGGBOM, O., 1972: Aspects on the Fjällfjäll Antiform. — Unpublished diss., Univ. Lund, 38 pp.
— 1980: Polyphase deformation of a discontinuous nappe in the central Scandinavian Caledonides. — Geol. Fören. Stockh. Förh., v. 100, p. 349—354.
HÖGBOM, A., 1925: De geologiska förhållandena inom Stekenjokk-Remdalens malmtrakt. — Sveriges Geol. Unders. C 329, 96 pp.
IRVINE, T.N., and BARAGAR, W.R.A., 1971: A guide to the classification of the common volcanic rocks. — Can. J. Earth Sci., v. 8, p. 523—549.
JACKSON, T.A., and SMITH, T.E., 1978: Metasomatism in the Tertiary volcanics of the Wagwater belt, Jamaica, W.I. — Geol. en Mijnb., v. 57, p. 213—220.
JUVE, G., 1977: Metal distribution at Stekenjokk : primary and metamorphic patterns. — Geol. Fören. Stockh. Förh., v. 99, p. 149—158.
KERRICH, R., FYFE, W.S., GORMAN, B.E., and ALLISON, I., 1977: Local modification of rock chemistry by deformation. — Contr. Mineral. Petrol., v. 65, p. 183—190.
KOLLUNG, S., 1979: Stratigraphy and major structures of the Grong District, Nord-Trøndelag. — Norges Geol. Unders., v. 354, p. 1—51.
KULLING, O., 1933: Bergbyggnaden inom Björkvattnet-Virisen-området i Västerbottensfjällens centrala del. — Geol. Fören. Stockh. Förh., v. 55, p. 167—422.
KUNO, H., 1959: Origin of the Cainozoic petrographic provinces of Japan and surrounding areas. — Bull. Volc., v. 20, p. 37—76.
LAMBERT, I.B., and WYLLIE, P.J., 1968: Stability of hornblende and a model for the low velocity zone. — Nature, v. 219, p. 1240—1241.
LeMAITRE, R.W., 1976: The chemical variability of some common igneous rocks. — J. Petrol., v. 17, p. 589—637.
LLOYD, F.E., and BAILEY, D.K., 1975: Light element metasomatism of the continental mantle : The evidence and the consequences. — Phys. Chem. Earth, v. 9, p. 389—416.
LOESCHKE, J., 1976: Major element variations in Ordovician pillow lavas of the Støren Group, Trondheim region, Norway. — Norsk Geol. Tidsskr., v. 56, p. 141—159.
MACDONALD, G.A., and KATSURA, T., 1964: Chemical composition of Hawaiian lavas. — J. Petrol., v. 5, p. 82—133.
MACGEEHAN, P.J., 1978: The geochemistry of altered volcanic rocks at Matagami, Quebec : a geothermal model for massive sulphide genesis. — Can. J. Earth Sci., v. 15, p. 551—570.

MATTHEWS, D.H., 1971: Altered basalts from Swallow Bank, an abyssal hill in the NE Atlantic, and from a nearby seamount. — Phil. Trans. Roy. Soc. Lond., v. A268, p. 551—571.
MCKERROW, W.S., LAMBERT, R.St.J. and CHAMBERLAIN, V.E., 1980: The Ordovician, Silurian and Devonian time scales. — Earth Planet. Sci. Lett., v. 51, p. 1—8.
MELSON, W.G., and van ANDEL, J.H., 1966: Metamorphism in the Mid-Atlantic Ridge, 22°N latitude. — Marine Geol., v. 4, p. 165—186.
MIYASHIRO, A., 1974: Volcanic rock series in island arcs and active continental margins. — Am. J. Sci., v. 274, p. 321—355.
— 1975: Classification, characteristics, and origin of ophiolites. — J. Geol., v. 83, p. 249—281.
MIYASHIRO, A., and SHIDO, F., 1975: Tholeiitic and calc-alkalic series in relation to the behaviours of titanium, vanadium, chromium, and nickel. — Am. J. Sci., v. 275, p. 265—277.
MIYASHIRO, A., SHIDO, F., and EWING, M., 1971: Metamorphism in the Mid-Atlantic Ridge near 24° and 30°N. — Phil. Trans. Roy. Soc. Lond., v. A268, p. 589—603.
NICHOLLS, I.A., and RINGWOOD, A.E., 1973: Effect of water on olivine stability in tholeiites and the production of silica-saturated magmas in the island-arc environment. — J. Geol., v. 81, p. 285—300.
NIELSEN, T.F.D., 1978: The Tertiary dike swarms of the Kangerdlugssuaq area, East Greenland. An example of magmatic development during continental break-up. — Contr. Mineral. Petrol., v. 67., p. 63—78.
NILSSON, G., 1964: Berggrunden inom Blåsjöområdet i nordvästra Jämtlandsfjällen. — Sveriges Geol. Unders. C 595, 70 pp.
OSBORN, E.F., 1962: Reaction series for subalkaline igneous rocks based on different oxygen pressure conditions. — Am. Mineral., v. 47, p. 211—226.
OXBURGH, E.R., and TURCOTTE, D.L., 1970: The thermal structure of island arcs. —Bull. Geol. Soc. Am., v. 81, p. 1665—1688.
PEARCE, J.A., 1975: Basalt geochemistry used to investigate past tectonic environments on Cyprus. — Tectonophysics, v. 25, p. 41—68.
— 1976: Statistical analysis of major element patterns in basalts. — J. Petrol., v. 17, p. 15—43.
PEARCE, J.A., and CANN, J.R., 1971: Ophiolite origin investigated by discriminant analysis using Ti, Zr and Y. — Earth Planet. Sci. Lett., v. 12, p. 339—349.
PEARCE, J.A., and CANN, J.R., 1973: Tectonic setting of basic volcanic rocks determined using trace element analyses. — Earth Planet. Sci. Lett., v. 19, p. 290—300.
PEARCE, J.A., and NORRY, M.J., 1979: Petrogenetic implications of Ti, Zr, Y and Nb variations in volcanic rocks. — Contr. Mineral. Petrol., v. 69, p. 33—47.
PEARCE, T.H., GORMAN, B.E., and BIRKETT, T.C., 1975: The TiO_2-K_2O-P_2O_5 diagram: a method of discriminating between oceanic and non-oceanic basalts. — Earth Planet. Sci. Lett., v. 24, p. 419—426.
PEARCE, T.H., GORMAN, B.E., and BIRKETT, T.C., 1977: The relationship between major element chemistry and tectonic environment of basic and intermediate volcanic rocks. — Earth Planet. Sci. Lett., v. 36, p. 121—132.
PECCERILLO, A., and TAYLOR, S.R., 1976: Geochemistry of Eocene calc-alkaline volcanic rocks from the Kastamonu area, northern Turkey. — Contr. Mineral. Petrol., v. 58, p. 63—81.
RINGWOOD, A.E., 1974: The petrological evolution of island arc systems. — Jl. Geol. Soc. Lond., v. 130, p. 183—204.
ROBERTS, D., 1978: Caledonides of south central Norway. — *In* IGCP Project 27, Caledonian-Appalachian Orogen of the North Atlantic Region, Geol. Surv. Canada, Paper 78—13, p. 31—37.
ROSS, C.S., and SMITH, R.L., 1961: Ash-flow tuffs : their origin, geologic relations and identification. — U.S. Geol. Survey Prof. Paper 366, 81 pp.
SANDWALL, J., 1981: Caledonian geology of the Jofjället area, Västerbotten, Sweden : Stratigraphy, metamorphism, deformation. — Sveries Geol. Unders. C 778, 105 pp.
SCEAL, J.S.C., and WEAVER, S.D., 1971: Trace element data bearing on the origin of salic rocks from the Quaternary volcano Paka, Gregory Rift, Kenya. — Earth Planet. Sci. Lett., v. 12, p. 327—331.
SCHERMERHORN, L.J.G., 1973: What is keratophyre? — Lithos, v. 6, p. 1—11.
SCHILLING, J-G., 1973: Iceland mantle plume: Geochemical study of the Reykjanes Ridge. — Nature, v. 242, p. 565—571.
SHIDO, F., MIYASHIRO, A., and EWING, M., 1971: Crystallization of abyssal tholeiites. — Contr. Mineral. Petrol., v. 31, p. 251—266.
SIEDLECKA, A., 1967: Geology of the eastern part of the Meråker area. — Norges Geol. Unders., v. 245, p. 22—58.
SJÖSTRAND, T., 1978: Caledonian geology of the Kvarnbergsvattnet area, northern Jämtland, central Sweden. — Sveriges Geol. Unders. C 735, 107 pp.

SMITH, R.E., 1968: Redistribution of major elements in the alteration of some basic lavas during burial metamorphism. — J. Petrol., v. 9, p. 191—219.

SPOONER, E.T.C., and FYFE, W.S., 1973: Sub-sea-floor metamorphism, heat and mass transfer. — Contr. Mineral. Petrol., v. 42, p. 287—304.

SPOONER, E.T.C., CHAPMAN, H.J., and SMEWING, J.D., 1977: Strontium isotopic contamination and oxidation during ocean floor hydrothermal metamorphism of the ophiolitic rocks of the Troodos Massif, Cyprus. — Geochim. Cosmochim. Acta, v. 41, p. 873—890.

SPOONER, E.T.C., BECKINSALE, R.D., FYFE, W.S., and SMEWING, J.D., 1974: O^{18} enriched ophiolitic metabasic rocks from E. Liguria (Italy), Pindos (Greece) and Troodos (Cyprus). — Contr. Mineral. Petrol., v. 47, p. 41—62.

STARK, J.T., 1963: Petrology of the volcanic rocks of Guam. — U.S. Geol. Survey Prof. Paper 403-C, 32 pp.

STEPHENS, M.B., 1977: Stratigraphy and relationship between folding, metamorphism and thrusting in the Tärna-Björkvattnet area, northern Swedish Caledonides. — Sveriges Geol. Unders. C 726, 146 pp.

— 1980a: Occurrence, nature and tectonic significance of volcanic and high-level intrusive rocks within the Swedish Caledonides. — *In* D.R. Wones, (edit.): The Caledonides in the USA, Virginia Polytechnic Inst. and State Univ., Dept. Geol. Sci. Mem. 2, p. 289—298.

— 1980b: Spilitization, element release and formation of massive sulphides in the Stekenjokk volcanites, central Swedish Caledonides. — Norges Geol. Unders., v. 360, p. 159—193.

— 1981a: Evidence for arc build-up and arc splitting in the Upper Allochthon of central Scandinavia. — Abstract in Terra Cognita, v. 1, p. 75—76.

— 1981b: The use of less mobile elements in elucidating palaeotectonic environments — a critical review. — Abstract in Geol. Fören. Stockh. Förh., v. 103, p. 139—140.

STEPHENS, M.B., THELANDER, T., and ZACHRISSON, E., 1979a: Compilation and bibliography of stratabound sulphide deposits in the Swedish Caledonides. — Unpublished report, Sveriges Geol. Unders. 22.51.2, 36 pp.

STEPHENS, M.B., GLASSON, M.J., and KEAYS, R.R., 1979b: Structural and chemical aspects of metamorphic layering development in metasediments from Clunes, Australia. — Am. J. Sci., v. 279, p. 129—160.

STERN, C., deWIT, M.J., and LAWRENCE, J.R., 1976: Igneous and metamorphic processes associated with the formation of Chilean ophiolites and their implication for ocean floor metamorphism, seismic layering, and magnetism. — J. Geophys Res., v. 81, p. 4370—4380.

STRAND, T., and KULLING, O., 1972: Scandinavian Caledonides. — Wiley Interscience, London and New York, 302 pp.

SUNDBLAD, K., 1980: A tentative "volcanogenic" formation model for the sediment-hosted Ankarvattnet Zn-Cu-Pb massive sulphide deposit, central Swedish Caledonides. — Norges Geol. Unders., v. 360, 211—227.

TEGENGREN, F.R., *et al.*, 1924: Sveriges ädlare malmer och bergverk. — Sveriges Geol. Unders. Ca 17, 406 pp.

THOMPSON, G., 1973: A geochemical study of the low-temperature interaction of sea-water and oceanic igneous rocks. — Trans, Am. Geophys. Union, v. 54, p. 1015—1019.

THOMPSON, G., SHIDO, F., and MIYASHIRO, A., 1972: Trace element distribution in fractionated oceanic basalts. — Chem. Geol., v. 9, p. 89—98.

TOKSÖZ, M.N., MINEAR, J.W., and JULIEN, B.R., 1971: Temperature field and geophysical effects of a downgoing slab. — J. Geophys. Res., v. 76, p. 1113—1138.

TROUW, R.A.J., 1973: Structural geology of the Marsfjällen area, Caledonides of Västerbotten, Sweden. — Sveriges Geol. Unders. C 689, 115 pp.

VALLANCE, T.G., 1965: On the chemistry of pillow lavas and the origin of spilites. — Min. Mag., v. 34, p. 471—481.

— 1969: Spilites again: some consequences of the degradation of basalts. — Proc. Linn. Soc. N.S. Wales, v. 94, p. 8—53.

— 1974: Spilitic degradation of a tholeiitic basalt. — J. Petrol., v. 15, p. 79—96.

VALLIER, T.L., and BATIZA, R., 1978: Petrogenesis of spilite and keratophyre from a Permian and Triassic volcanic arc terrane, eastern Oregon and western Idaho, U.S.A. — Can. J. Earth Sci., v. 15, p. 1356—1369.

WATERS, A.C., 1961: Stratigraphic and lithologic variation in the Columbia River basalt. — Am. J. Sci., v. 259, p. 583—611.

WILLIAMS, P.F., 1972: Development of metamorphic layering and cleavage in low grade metamorphic rocks at Bermagui, Australia. — Am. J. Sci., v. 272, p. 1—47.

WINCHESTER, J.A., and FLOYD, P.A., 1976: Geochemical magma type discrimination : application to altered and metamorphosed basic igneous rocks. — Earth Planet. Sci. Lett., v. 28, p. 459—469.

WOLFF, F.C., 1967: Geology of the Meråker area as a key to the eastern part of the Trondheim region. — Norges Geol. Unders., v. 245, p. 123—142.
— 1976: Geologisk kart over Norge, berggrunnskart Trondheim 1:250 000. — Norges Geol. Unders.
ZACHRISSON, E., 1964: The Remdalen Syncline. — Sveriges Geol. Unders. C 596, 53 pp.
— 1969: Caledonian geology of Northern Jämtland — Southern Västerbotten. — Sveriges Geol. Unders. C 644, 33 pp.
— 1973: The westerly extension of Seve rocks within the Seve-Köli Nappe Complex in the Scandinavian Caledonides. — Geol. Fören. Stockh. Förh., v. 95, p. 243—251.
— 1977: Stratigraphic position and base metal proportions of stratabound Köli sulphide deposits, central Swedish Caledonides. — *In* A., Bjørlykke, I. Lindahl and F.M. Vokes, (edits.): Kaledonske Malmforekomster, BVLI'S Tekniske Virksomhet, Trondheim, p. 8—16.
— 1980: Aspects of stratabound base metal mineralization in the Swedish Caledonides. — Geol. Surv. Irl. Special Paper No 5, p. 47—61.

APPENDIX

Listing of whole rock chemical analyses from the Stekenjokk volcanites
(Volatile-free basis)

Key:

Analyses 1- 9 = Mafic Group 1A
Analyses 10-24 = Mafic Group 1B
Analyses 25-41 = Mafic Group 2A
Analyses 42-49 = Mafic Group 2B
Analyses 50-69 = Felsic rocks

Sample location:

Field samples are located by reference to a 1:100 000 topographic map-sheet and coordinates in the National Grid System displayed on the map.

Borehole samples are located by reference to a 1:100 000 topographic map-sheet and depth in the respective borehole

BH 70001/2/4-Bj = Borehole sample, Björkvattnet
BH 70710-S = Borehole sample, Stekenjokk (Duoranåjje)
BH 69111/8-R = Borehole sample, Remdalen (Beitsetjenjunje)

Type:

1. Lithology
   Gr = Greenschist or greenstone
   Ga = Gabbro
   Qk = Quartz keratophyre

2. Extrusive/intrusive origin

   Factors, such as grain size, texture, presence of chilled margins, have been employed to assess extrusive (E) or intrusive (I) origin. Interpretation for the gabbros and quartz keratophyres is more confident than for the greenschists, greenstones.

3. Mineralogy
   1 = Chlorite - albite $\pm$ amphibole $\pm$ epidote $\pm$ calcite $\pm$ Ti-rich minerals
   2 = Amphibole - albite - chlorite - epidote - Ti-rich minerals $\pm$ calcite
   3 = Chlorite - albite - calcite - Ti-rich minerals $\pm$ epidote $\pm$ biotite $\pm$ apatite $\pm$ white mica
   4 = Albite - quartz - chlorite $\pm$ epidote $\pm$ calcite $\pm$ biotite $\pm$ white mica $\pm$ Fe-Ti oxides

Analyses:
– = not determined
n.d. = not detected
† = Analysis first recalculated to 100 %, then recalculated on a volatile-free basis

Analysis No.	1	2	3	4	5
Laboratory No.	011-0139	011-0141	011-1000	050-7525	011-0679
Specimen No.	Z75-48	T75-119	M77-11	T70-106	M76-31
Map-sheet	22D, 3j	22E, 3a	22E, 3a	22D, 3j	22D, 3j
Coordinate	140000: 716860	140035: 716885	140035: 716885	139895: 716890	139900: 716890
Type	GrEl	GrEl	Gr	Gr	GrIl
Oxides (Wt.%)					
SiO_2	52.7	51.3	51.7	53.5	53.0
TiO_2	0.48	0.77	0.67	0.75	0.64
Al_2O_3	16.6	16.7	16.9	16.6	16.4
Fe_2O_3	2.5	5.0	2.9	4.0	5.5
FeO	5.9	6.7	8.3	6.3	7.4
MnO	0.25	0.18	0.19	0.17	0.20
MgO	7.6	5.9	5.9	6.7	6.4
CaO	5.9	6.7	6.2	6.8	6.6
Na_2O	5.5	4.8	6.0	4.6	4.9
K_2O	0.1	0.1	0.1	0.2	0.2
P_2O_5	0.05	0.08	0.06	0.05	0.06
Total	97.6	98.2	98.9	99.7	101.3
$H_2O > 105^o$	2.0	1.2	3.4	3.1	3.2
$H_2O < 105^o$	0.5	0.3	0.1	0.3	0.3
CO_2	4.1	0.86	0.92	0.07	0.86
FeO^*	8.2	11.2	10.9	9.9	12.4
FeO^*/MgO	1.08	1.90	1.85	1.48	1.94
Trace elements ppm					
Zr	18	30	39	38	33
Y	11	15	16	20	24
Cu	55	22	36	24	115
Zn	81	91	84	-	60
Ni	29	19	21	-	28
Cr	40	11	25	25	18
Zr/Y	1.64	2.00	2.44	1.90	1.38

Analysis No.	6	7†	8	9†	10
Laboratory No.	011-0681	12408-82	011-0685	12408-74	011-0677
Specimen No.	M76-77	Z174	M76-124	S7	M76-28
Map-sheet	23E, 1e	23E, 6i	23E, 7h	23E, 8i	22D, 3j
Coordinate	142405: 720745	144130: 723200	143860: 723870	144225: 724025	139980: 716865
Type	GrEl	Gr	GrEl	Gr	GrEl
Oxides (Wt.%)					
SiO_2	52.0	55.6	50.6	56.0	51.1
TiO_2	0.49	0.6	0.55	0.3	0.60
Al_2O_3	16.5	17.3	16.3	14.7	14.6
Fe_2O_3	3.3	3.0	3.3	1.9	3.9
FeO	9.9	8.7	8.1	8.6	8.1
MnO	0.22	-	0.19	-	0.15
MgO	8.5	6.3	8.3	7.7	10.9
CaO	5.7	4.5	9.7	5.7	10.1
Na_2O	4.5	4.0	2.7	5.1	2.3
K_2O	0.1	0.1	0.7	0.1	0.1
P_2O_5	0.05	-	0.07	-	0.07
Total	101.3	100.1	100.5	100.1	101.9
$H_2O > 105^o$	4.6	3.7	4.3	2.2	4.0
$H_2O < 105^o$	0.4	0.3	0.5	0.2	0.2
CO_2	4.1	0.1	5.5	1.0	1.9
FeO^*	12.9	11.4	11.1	10.3	11.6
FeO^*/MgO	1.52	1.81	1.34	1.34	1.06
Trace elements (ppm)					
Zr	18	35	27	13	38
Y	11	20	13	9	17
Cu	16	60	34	24	70
Zn	73	-	65	-	59
Ni	23	-	35	-	190
Cr	45	50	79	86	644
Zr/Y	1.64	1.75	2.08	1.44	2.24

Analysis No.	11	12	13	14	15
Laboratory No.	011-0678	050-7524	011-0999	011-0675	011-0674
Specimen No.	M76-29	T70-80	M77-8	M76-18	M76-17
Map-sheet	22D, 3j	22E, 3a	22E, 3a	22D, 4j	22D, 4j
Coordinate	139965: 716875	140045: 716930	140025: 716940	139935: 717095	139940: 717110
Type	GrIl	Gr	GaI	GrEl	GrEl
Oxides (Wt.%)					
SiO_2	47.3	50.9	51.1	49.3	53.5
TiO_2	1.26	0.72	0.42	0.65	0.56
Al_2O_3	16.4	15.4	13.3	18.3	15.4
Fe_2O_3	2.7	2.5	1.4	4.0	4.7
FeO	7.3	7.0	8.2	6.3	6.0
MnO	0.19	0.16	0.31	0.13	0.20
MgO	5.7	10.5	7.0	6.3	7.2
CaO	12.8	7.7	12.2	11.3	7.5
Na_2O	6.2	4.0	4.1	4.4	5.3
K_2O	0.1	0.2	0.1	0.1	0.1
P_2O_5	0.16	0.08	0.04	0.06	0.08
Total	100.1	99.2	98.2	100.8	100.5
$H_2O > 105^o$	2.8	3.6	2.8	2.9	2.5
$H_2O < 105^o$	0.3	0.3	0.1	0.2	0.2
CO_2	8.0	<0.01	4.0	1.6	0.48
FeO^*	9.7	9.3	9.5	9.9	10.2
FeO^*/MgO	1.70	0.89	1.36	1.57	1.42
Trace elements (ppm)					
Zr	64	43	25	32	49
Y	28	14	12	15	20
Cu	37	1	5	72	6
Zn	68	33	61	50	86
Ni	67	-	180	47	54
Cr	174	600	449	143	101
Zr/Y	2.29	3.07	2.08	2.13	2.45

Analysis No.	16	17	18	19	20
Laboratory No.	011-1003	011-1002	011-1005	011-1004	011-0683
Specimen No.	M77-16	M77-14	M77-49	M77-48	M76-88
Map-sheet	22E, 6c	22E, 6c	22E, 8d	22E, 8d	23E, 0d
Coordinate	140000: 718175	141005: 718180	141595: 719190	141595: 719205	141860: 720335
Type	Gr	Gr	Gr	Gr	GrEl
Oxides (Wt.%)					
SiO_2	49.8	49.2	48.9	51.3	48.1
TiO_2	0.64	0.66	0.71	0.64	0.98
Al_2O_3	16.9	14.6	17.0	15.6	15.5
Fe_2O_3	3.8	2.5	2.6	2.2	3.8
FeO	7.2	7.9	7.5	7.4	8.6
MnO	0.20	0.22	0.18	0.18	0.17
MgO	7.0	8.8	8.8	8.3	8.5
CaO	10.5	13.1	11.8	12.0	10.1
Na_2O	4.3	3.7	2.0	2.9	4.5
K_2O	0.1	0.2	0.7	0.5	0.1
P_2O_5	0.06	0.05	0.08	0.06	0.09
Total	100.5	100.9	100.3	101.1	100.4
$H_2O > 105^o$	3.2	3.2	3.5	1.5	3.9
$H_2O < 105^o$	0.1	0.2	0.2	0.2	0.3
CO_2	1.1	3.4	0.08	1.8	2.6
FeO^*	10.6	10.2	9.8	9.4	12.0
FeO^*/MgO	1.51	1.16	1.11	1.13	1.41
Trace elements (ppm)					
Zr	35	33	55	50	40
Y	15	17	18	17	22
Cu	74	52	34	68	66
Zn	34	67	74	66	65
Ni	80	161	85	82	99
Cr	251	517	419	406	281
Zr/Y	2.33	1.94	3.06	2.94	1.82

Analysis No.	21	22	23†	24	25
Laboratory No.	011-0684	011-1006	12408-85	011-1008	011-0099
Specimen No.	M76-94	M77-72	Z319	M77-74	M70002(2-3)
Map-sheet	23E, 2f	23E, 5h	23E, 5h	23E, 5h	22E, 3a
Coordinate	142685: 721245	143865: 722700	143845: 722720	143770: 772820	BH70002-Bj (3.00-3.89m)
Type	GrEl	Gr	Gr	GaI	GrI2
Oxides (Wt.%)					
SiO_2	50.7	48.9	50.3	52.2	50.5
TiO_2	1.02	1.28	0.6	0.54	2.62
Al_2O_3	16.4	14.8	17.1	15.4	13.8
Fe_2O_3	3.6	2.4	2.1	2.3	4.6
FeO	6.7	7.3	6.8	7.2	7.3
MnO	0.14	0.20	-	0.19	0.21
MgO	8.6	7.7	7.1	8.0	6.1
CaO	10.0	12.8	13.0	9.5	12.1
Na_2O	3.0	2.7	3.0	3.5	2.5
K_2O	0.2	0.2	0.1	0.6	0.1
P_2O_5	0.15	0.1	-	0.07	0.23
Total	100.5	98.4	100.1	99.5	100.1
$H_2O > 105^o$	3.0	2.7	2.6	2.5	2.9
$H_2O < 105^o$	0.3	0.2	0.1	0.2	0.3
CO_2	3.0	0.21	2.3	< 0.01	1.4
FeO^*	9.9	9.5	8.7	9.3	11.4
FeO^*/MgO	1.15	1.23	1.23	1.16	1.87
Trace elements (ppm)					
Zr	93	91	-	52	167
Y	29	31	-	15	47
Cu	47	5	-	5	44
Zn	61	75	-	70	109
Ni	160	69	-	108	63
Cr	331	374	-	424	196
Zr/Y	3.21	2.94	-	3.47	3.55

Analysis No.	26	27	28	29	30
Laboratory No.	011-0100	011-0102	011-0103	011-1001	-
Specimen No.	M70002(4)	M70004(1-2)	M70004(3)	M77-12	-
Map-sheet	22E, 3a	22E, 3a	22E, 3a	22D, 4j	23E, 4h
Coordinate	BH70002-Bj (4.99-5.73m)	BH70004-Bj (14.72-15.62m)	BH70004-Bj (16.56-17.04m)	139910: 717030	from Juve (1974)
Type	GrI2	GrI2	GrI2	GrI	GaI
Oxides (Wt.%)					
SiO_2	48.8	48.2	47.5	44.7	48.0
TiO_2	2.62	2.63	2.75	2.92	3.92
Al_2O_3	14.5	15.1	15.2	14.1	14.9
Fe_2O_3	5.3	5.4	5.9	7.4	3.3
FeO	7.3	7.3	7.1	8.9	12.9
MnO	0.22	0.21	0.21	0.28	0.28
MgO	6.7	6.4	6.4	6.3	5.8
CaO	11.2	11.2	10.8	11.1	9.2
Na_2O	2.2	2.3	3.0	2.6	2.7
K_2O	0.1	0.1	0.1	0.2	0.3
P_2O_5	0.23	0.23	0.23	0.48	-
Total	99.2	99.1	99.2	99.0	101.3
$H_2O > 105^o$	3.4	3.6	3.7	3.7	4.8
$H_2O < 105^o$	0.3	0.5	0.6	0.6	0.29
CO_2	0.72	0.88	1.3	0.25	3.04
FeO^*	12.1	12.2	12.4	15.6	15.9
FeO^*/MgO	1.81	1.91	1.94	2.48	2.74
Trace elements (ppm)					
Zr	164	169	173	-	-
Y	50	47	51	-	-
Cu	47	42	41	-	28
Zn	108	107	114	-	146
Ni	72	69	61	-	12
Cr	203	190	195	-	-
Zr/Y	3.28	3.60	3.39	-	-

Analysis No.	31	32	33	34	35
Laboratory No.	011-0109	011-0110	011-0111	011-0112	011-0113
Specimen No.	M70710(5)	M70710(6-7)	M70710(8-9)	M70710(10-11)	M70710(12)
Map-sheet	23E, 5h	23E, 5h	23E, 5h	23E, 5h	23E, 5h
Coordinate	BH70710-S (4.40-5.04m)	BH70710-S (6.77-7.67m)	BH70710-S (11.03-11.98m)	BH70710-S (50.76-51.84m)	BH70710-S (72.94-73.65m)
Type	GrI2	GrI2	GrI2	GrI2	GaI2
Oxides (Wt.%)					
SiO_2	49.3	50.0	51.0	49.3	49.7
TiO_2	3.80	3.32	3.02	2.90	2.30
Al_2O_3	13.8	13.9	14.5	14.2	13.3
Fe_2O_3	5.0	4.7	4.8	5.0	3.9
FeO	10.5	10.1	9.3	9.0	8.2
MnO	0.28	0.28	0.27	0.24	0.21
MgO	5.1	5.0	5.8	6.2	6.7
CaO	8.9	7.9	7.3	9.5	12.1
Na_2O	3.5	4.4	3.8	3.1	2.4
K_2O	0.2	0.5	0.1	0.2	0.1
P_2O_5	0.35	0.44	0.39	0.36	0.24
Total	100.7	100.5	100.3	100.0	99.2
$H_2O > 105^o$	2.6	2.6	3.2	2.9	3.1
$H_2O < 105^o$	0.1	0.3	0.4	0.5	0.3
CO_2	0.05	0.86	0.42	0.20	0.72
FeO^*	15.0	14.3	13.6	13.5	11.7
FeO^*/MgO	2.94	2.86	2.34	2.18	1.75
Trace elements (ppm)					
Zr	313	359	368	253	141
Y	81	93	87	65	43
Cu	34	42	42	41	56
Zn	140	142	173	183	106
Ni	27	23	29	42	90
Cr	n.d.	11	18	74	201
Zr/Y	3.86	3.86	4.23	3.89	3.28

Analysis No.	36	37	38	39	40
Laboratory No.	011-0114	011-0115	011-0116	011-0-117	011-1009
Specimen No.	M70710(13)	M70710(14)	M70710(15)	M70710(16-18)	M77-77
Map-sheet	23E, 5h	23E, 5h	23E, 5h	23E, 5h	23E, 5R
Coordinate	BH70710-S (76.26-77.28m)	BH70710-S (79.95-80.90m)	BH70710-S (92.10-93.66m)	BH70710-S (101.56-102.93m)	143695: 742895
Type	GaI2	GaI2	GaI2	Gr2	GaI
Oxides (Wt.%)					
SiO_2	50.5	50.2	49.4	51.2	48.4
TiO_2	2.37	2.26	2.27	2.83	2.17
Al_2O_3	13.2	13.5	14.2	13.6	14.4
Fe_2O_3	3.9	4.4	5.1	5.3	2.6
FeO	8.4	7.8	7.1	8.1	9.9
MnO	0.21	0.21	0.41	0.27	0.31
MgO	6.1	6.6	6.6	7.0	6.8
CaO	11.6	11.6	12.4	8.6	11.3
Na_2O	2.3	2.3	2.1	2.5	2.8
K_2O	0.1	0.1	0.1	0.1	0.1
P_2O_5	0.24	0.25	0.25	0.27	0.21
Total	98.9	99.2	99.9	99.8	99.0
$H_2O > 105^o$	2.4	2.3	2.8	4.0	2.8
$H_2O < 105^o$	0.3	0.2	0.4	0.3	0.1
CO_2	0.04	0.12	0.06	0.22	0.04
FeO^*	11.9	11.8	11.7	12.9	12.2
FeO^*/MgO	1.95	1.79	1.77	1.84	1.79
Trace elements (ppm)					
Zr	152	141	183	214	-
Y	50	46	45	57	-
Cu	63	53	21	79	-
Zn	105	105	236	381	-
Ni	55	82	93	66	-
Cr	137	204	242	142	-
Zr/Y	3.04	3.07	4.07	3.75	-

Analysis No.	41	42	43	44	45
Laboratory No.	011-0121	011-0097	011-0098	011-0101	011-0680
Specimen No.	M69111(7-9)	M70001(2-4)	M70001(5-7)	M70002(5-6)	M76-39
Map-sheet	23E, 7i	22E, 3a	22E, 3a	22E, 3a	22D, 4j
Coordinate	BH69111-R (44.87-46.01m)	BH70001-Bj (26.10-27.87m)	BH70001-Bj (28.71-29.50m)	BH70001-Bj (23.69-24.89m)	139870: 717085
Type	Gr2	GrI3	GrI3	GrI3	GrI3
Oxides (Wt.%)					
SiO_2	50.2	47.1	50.9	47.6	51.3
TiO_2	1.79	3.68	2.91	4.11	2.88
Al_2O_3	15.7	15.9	14.6	15.3	13.3
Fe_2O_3	3.2	2.5	3.4	4.0	5.6
FeO	5.6	10.9	9.5	10.2	9.3
MnO	0.15	0.23	0.22	0.24	0.27
MgO	6.2	4.3	5.4	4.7	3.5
CaO	12.2	8.8	8.4	9.1	7.0
Na_2O	3.7	3.9	3.1	3.3	5.0
K_2O	0.2	0.9	1.2	1.0	0.3
P_2O_5	0.17	0.67	0.79	0.82	1.17
Total	99.1	98.9	100.4	100.4	99.6
$H_2O > 105^o$	3.3	3.5	3.6	4.0	1.9
$H_2O < 105^o$	0.4	0.5	0.7	0.4	0.3
CO_2	1.4	3.5	3.1	3.3	3.9
FeO^*	8.5	13.2	12.6	13.8	14.3
FeO^*/MgO	1.37	3.07	2.33	2.94	4.09
Trace elements (ppm)					
Zr	140	237	210	206	236
Y	29	33	45	33	56
Cu	49	60	43	50	11
Zn	70	60	104	60	109
Ni	74	15	21	12	8
Cr	257	n.d.	89	n.d.	<5
Zr/Y	4.83	7.18	4.67	6.24	4.21

Analysis No.	46	47	48	49	50
Laboratory No.	011-0142	011-0143	011-1007	011-0124	050-7526
Specimen No.	T75-121	T75-122	M77-73	M69118(6-7)	T70-110
Map-sheet	22D, 4j	22D, 4j	23E, 5h	23E, 7i	22D, 3j
Coordinate	139870: 717085	139915: 717165	143785: 722815	BH69118-R (110.74-111.90m)	139890: 716855
Type	GrI3	GrI3	Gr	Gr3	Qk
Oxides (Wt.%)					
SiO_2	51.5	50.7	48.8	49.4	63.0
TiO_2	3.60	3.37	3.91	3.15	0.83
Al_2O_3	14.4	14.3	12.8	15.0	14.3
Fe_2O_3	7.8	5.9	3.5	6.5	3.8
FeO	6.9	8.2	11.8	8.0	4.6
MnO	0.25	0.26	0.24	0.23	0.11
MgO	3.8	3.4	4.4	4.8	2.6
CaO	7.3	6.5	8.9	6.9	4.4
Na_2O	4.5	4.4	3.2	3.6	5.4
K_2O	0.1	1.9	0.7	0.5	0.2
P_2O_5	1.54	1.34	0.45	0.48	0.15
Total	101.7	100.3	98.7	98.6	99.4
$H_2O > 105^o$	3.6	1.9	2.4	3.5	1.9
$H_2O < 105^o$	0.5	0.9	0.4	0.4	0.2
CO_2	1.5	2.3	0.01	0.66	1.73
FeO^*	13.9	13.5	15.0	13.9	8.0
FeO^*/MgO	3.66	3.97	3.41	2.90	3.08
Trace elements (ppm)					
Zr	249	252	-	153	81
Y	50	48	-	33	33
Cu	2	1	-	45	42
Zn	122	116	-	107	47
Ni	1	n.d.	-	19	< 5
Cr	n.d.	n.d.	-	26	< 5
Zr/Y	4.98	5.25	-	4.64	2.45

Analysis No.	51	52	53	54	55
Laboratory No.	011-0138	011-0179	011-0747	011-0748	050-7533
Specimen No.	Z75-46	Z75-47	M76-24	M76-32	T70-35
Map-sheet	22D, 3j	22D, 3j	22E, 3a	22D, 3j	22D, 3j
Coordinate	140000: 716860	140000: 716860	140025: 716875	139915: 716890	139985: 716910
Type	QkE4	QkE4	QkE4	QkI4	Qk
Oxides (Wt.%)					
SiO_2	78.6	78.0	73.8	70.0	74.3
TiO_2	0.23	0.36	0.34	0.51	0.38
Al_2O_3	11.2	12.1	11.8	12.6	12.0
Fe_2O_3	1.0	1.3	1.2	3.5	1.9
FeO	1.9	1.9	2.7	2.7	2.1
MnO	0.06	0.09	0.10	0.07	0.06
MgO	1.8	1.0	1.8	1.2	0.6
CaO	0.4	0.5	0.4	2.2	3.0
Na_2O	4.3	6.5	5.7	5.9	4.2
K_2O	1.1	0.2	0.3	0.1	0.4
P_2O_5	0.04	0.09	0.05	0.11	0.06
Total	100.6	102.0	98.2	98.9	99.0
$H_2O > 105^o$	2.6	4.1	1.3	1.1	1.3
$H_2O < 105^o$	0.3	0.2	0.2	0.2	0.2
CO_2	0.15	0.02	0.54	0.26	0.32
FeO^*	2.8	3.1	3.8	5.9	3.8
FeO^*/MgO	1.56	3.10	2.11	4.92	6.33
Trace elements (ppm)					
Zr	151	134	106	106	110
Y	48	46	55	49	44
Cu	1	2	< 5	< 5	< 5
Zn	68	81	123	35	16
Ni	n.d.	n.d.	< 5	6	< 5
Cr	n.d.	n.d.	< 5	< 5	< 5
Zr/Y	3.15	2.91	1.93	2.16	2.50

Analysis No.	56	57	58	59	60†
Laboratory No.	011-1091	011-0676	011-0751	011-0750	12408-84
Specimen No.	M77-13	M76-21	M76-87	M76-76	Z301
Map-sheet	22D, 4j	22D, 4j	23E, 0d	23E, 1e	23E, 5h
Coordinate	139910: 717025	139870: 717080	141870: 720320	142385: 720730	143665: 722745
Type	Qk	QkI4	QkE4	QkE4	Qk
Oxides (Wt.%)					
SiO_2	75.9	69.3	81.3	78.8	77.4
TiO_2	0.29	0.66	0.11	0.31	0.1
Al_2O_3	12.2	13.1	9.2	9.0	12.6
Fe_2O_3	1.1	3.0	0.9	1.8	0.4
FeO	1.9	3.8	0.8	2.3	1.8
MnO	0.05	0.07	0.01	0.05	-
MgO	0.6	1.9	0.3	0.6	0.9
CaO	2.5	3.0	0.1	0.4	0.7
Na_2O	5.3	4.5	5.4	4.6	5.6
K_2O	0.2	0.3	0.1	0.1	0.6
P_2O_5	0.05	0.14	0.01	0.06	-
Total	100.1	99.7	98.2	98.0	100.1
$H_2O > 105^o$	0.9	1.6	0.2	0.9	0.4
$H_2O < 105^o$	0.2	0.2	0.1	0.1	0.1
CO_2	0.16	0.04	0.04	0.02	0.1
FeO^*	1.7	6.5	1.6	3.9	2.2
FeO^*/MgO	2.83	3.42	5.33	6.5	2.44
Trace elements (ppm)					
Zr	-	101	87	24	-
Y	-	44	37	17	-
Cu	-	< 5	< 5	18	-
Zn	-	12	< 5	50	-
Ni	-	< 5	< 5	< 5	-
Cr	-	< 5	< 5	< 5	-
Zr/Y	-	2.30	2.35	1.41	-

Analysis No.	61	62†	63	64†	65
Laboratory No.	011-1092	12408-81	011-0755	12408-6	011-0122
Specimen No.	M77-75	Z174	M76-130	Z389	M69118(4)
Map-sheet	23E, 5h	23E, 6i	23E, 6h	23E, 7h	23E, 7i
Coordinate	143760: 722840	144130: 723200	143810: 723415	143790: 723520	BH69118-R (18.36-19.34m)
Type	Qk	Qk	QkI4	Qk	QkI4
Oxides (Wt.%)					
SiO_2	76.0	78.1	76.4	75.3	75.5
TiO_2	0.18	0.2	0.13	0.7	0.18
Al_2O_3	12.9	10.6	12.1	11.5	11.9
Fe_2O_3	0.7	1.1	0.8	0.5	1.1
FeO	1.1	1.3	1.1	2.7	0.9
MnO	0.05	-	0.03	-	0.08
MgO	0.6	0.9	0.5	3.2	0.7
CaO	1.2	2.3	0.7	0.5	2.8
Na_2O	5.8	5.4	5.9	5.6	6.6
K_2O	0.7	0.1	0.5	0.1	0.2
P_2O_5	0.02	-	0.01	-	0.01
Total	99.3	100.0	98.2	100.1	100.0
$H_2O > 105^o$	0.9	0.9	0.8	2.2	0.9
$H_2O < 105^o$	0.2	0.2	< 0.1	0.1	0.3
CO_2	0.02	1.3	0.06	0.1	0.84
FeO^*	1.7	2.3	1.8	3.2	1.9
FeO^*/MgO	2.83	2.56	3.6	1.0	2.71
Trace elements (ppm)					
Zr	-	-	89	-	131
Y	-	-	25	-	51
Cu	-	-	< 5	-	7
Zn	-	-	26	-	40
Ni	-	-	< 5	-	1
Cr	-	-	< 5	-	n.d.
Zr/Y	-	-	3.56	-	2.57

Analysis No.	66	67	68	69†
Laboratory No.	011-0123	011-0125	011-0754	12408-24
Specimen No.	M69118(5)	M69118(8)	M76-129	Z354
Map-sheet	23E, 7i	23E, 7i	23E, 7h	23E, 7h
Coordinate	BH69118-R (26.12-26.83m)	BH69118-R (125.24-126.02m)	143880: 723860	143840: 723920
Type	QkE4	QkE4	QkE4	Qk
Oxides (Wt.%)				
SiO_2	63.7	77.9	77.4	83.0
TiO_2	0.74	0.25	0.13	0.2
Al_2O_3	14.1	11.5	12.2	9.1
Fe_2O_3	5.3	0.6	0.5	0.6
FeO	3.9	1.6	1.1	1.4
MnO	0.17	0.04	0.01	-
MgO	2.9	0.8	2.0	1.2
CaO	5.8	2.1	0.3	0.1
Na_2O	3.3	4.5	5.7	4.7
K_2O	0.2	1.4	0.1	0.1
P_2O_5	0.05	0.02	0.01	-
Total	100.2	100.7	99.5	100.4
$H_2O > 105^o$	2.5	0.8	1.4	1.1
$H_2O < 105^o$	0.5	0.5	0.1	0.2
CO_2	0.06	0.64	0.02	0.1
FeO^*	8.7	2.1	1.6	1.9
FeO^*/MgO	3.0	2.63	0.8	1.58
Trace elements (ppm)				
Zr	29	88	124	-
Y	23	33	46	-
Cu	22	14	< 5	-
Zn	99	46	45	-
Ni	n.d.	n.d.	< 5	-
Cr	n.d.	n.d.	< 5	-
Zr/Y	1.26	2.67	2.70	-

GEOLOGICAL SETTING OF THE STEKENJOKK VOLCANITES, N. JÄMTLAND - S. VÄSTERBOTTEN CALEDONIDES, SWEDEN

Compositional variation of the Stekenjokk volcanites and location of samples chemically analyzed

Michael B. Stephens, 1981

1:250 000 (0 – 10 km)

LEGEND:

- Ultramafite
- Metagabbro
- 'Quartz keratophyre'-intrusive in Blåsjö Phyllite
- Remdalen Group (Stikke, Gelvenåkko Nappes). Bjurälv Lst, Røyrvik Group (Leipikvattnet Nappe)
- Stekenjokk Quartz-Keratophyre (Stekenjokk volcanites) in Stikke and Gelvenåkko Nappes:
  - Felsic rocks (quartz keratophyre – volc./subvolc. intrusive) dominant
  - Mixed mafic/felsic rocks
  - Mafic rocks (greenschist, greenstone, metagabbro, volcanic breccia) dominant
  - Tuffite, phyllite
- Lasterfjäll Greenschist/ (Stikke, Gelvenåkko Nappes)
- Blåsjö Phyllite, Haraön Phyllites near Kvarnbergsvattnet (Stikke, Gelvenåkko Nappes). Brakkfjället Phyllite (Leipikvattnet Nappe)

  (Stikke, Gelvenåkko and Leipikvattnet Nappes)
- Lövfjäll, Vesken and Viris Fms. (Eastern Synform), equivalents on eastern limb of Western Synform
- Bellovare Formation (Western Synform), Broken, Vojtja and Slätdal Fms. (Eastern Synform)
- Tjopasi Group (Western Synform), Seima and Gilliks Formations (Eastern Synform)

  (Björkvattnet Nappe)
- Garnet-mica, quartz-rich and quartzo-feldspathic schist/gneiss, amphibolite
- Migmatitic gneiss, amphibolite

  (Seve Nappes)

  (Köli Nappes)

  (SEVE-KÖLI NAPPE COMPLEX)
- LOWER NAPPES including quartzites and phyllites around Børgefjell Window, Fjällfjäll Arkose and Särv Nappe equivalents (?) east of Saxnäs
- PRECAMBRIAN CRYSTALLINE BASEMENT (Børgefjell Window)

- Normal lithological contact
- Fault (undifferentiated)
- Thrust fault
- Thrust fault separating major tectonic units within Seve-Köli Nappe Complex
- Thrust fault at base of Seve-Köli Nappe Complex
- Thrust fault between Precambrian crystalline basement of Børgefjell Window and Lower Nappes

(Tentative tectonic boundaries are indicated by a widely spaced dashed line)

- ● 8 — Location of chemically analyzed sample from Stekenjokk volcanites. Number refers to listing in Appendix I in text.
- A — A‴ — Line of section

Map compilation with minor modification after:

22D-E Nilsson 1964; Sjöstrand 1978; Geological Survey of Sweden (SGU) unpublished 1:50 000 map (Sjöstrand, T.)

23E Nilsson 1964; Zachrisson 1964, 1969; SGU unpublished 1:50 000 map (Zachrisson, E.)

23F Trouw 1973; SGU unpublished 1:50 000 map (compiled by Stephens, M.B. after Gee, D.G., Häggbom, O., Stigh, J., Zachrisson, E., and University of Leiden preliminary map over Seve rocks)

24E-F SGU unpublished map (compiled by Stephens, M.B. after Gee, D.G. and Stigh, J.)

Sections modified after Zachrisson (1969) and Häggbom (Unpublished diss., 1972)

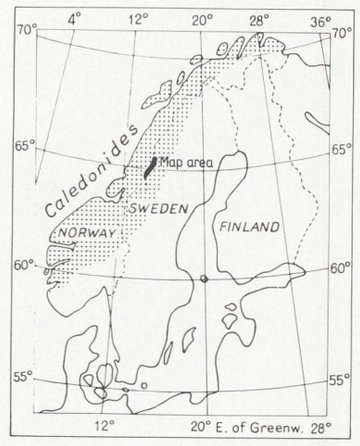

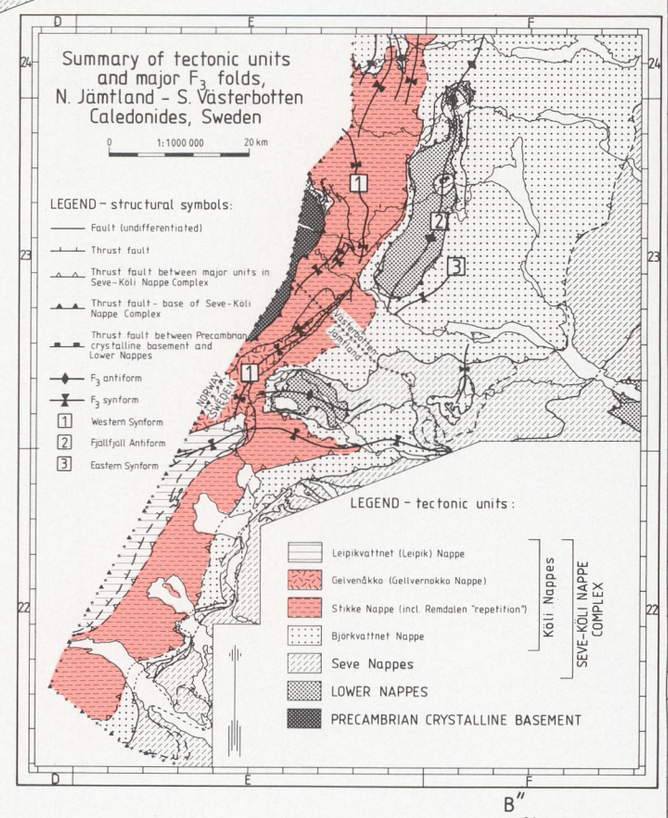

SCHEMATIC SECTIONS

Vertical and horizontal scales 1:250 000

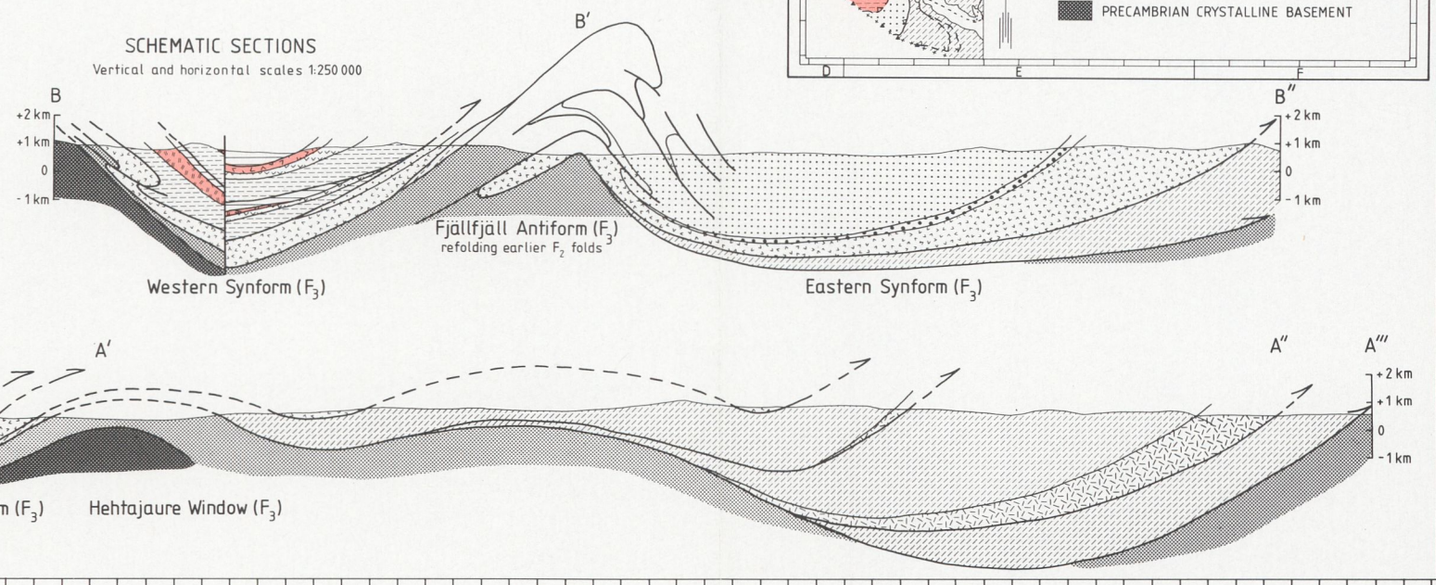

Godkänd ur sekretessynpunkt för spridning. Statens lantmäteriverk 1982-09-27.

PRISKLASS G
Distribution
LiberKartor
162 89 STOCKHOLM

ISBN 91-7158-240-1
ISSN 0082-0024